**The novel mechanism by which proteasome inhibitors induce apoptosis in triple-negative breast cancer**

by

Sriraja Srinivasa

A dissertation submitted to the Graduate Faculty of
Auburn University
in partial fulfillment of the
requirements for the Degree of
Doctor of Philosophy

Auburn, Alabama
May 2, 2026

Keywords: Proteasome, Proteasome inhibitor, Triple-negative Breast Cancer, eIF2α, C-myc, NOXA



Approved by

Dr. Alexei Kisselev, Chair, Professor of Drug Discovery and Development
Dr. Amit Mitra, Associate Professor of Drug Discovery and Development
Dr. Jianzhong Shen, Professor of Drug Discovery and Development
Dr. Robert D. Arnold, Professor of Drug Discovery and Development

Abstract

Triple-negative breast cancer (TNBC) is a challenging malignancy due to a lack of targeted therapeutic options. Genomic studies have found that the proteasome may be a viable therapeutic target in TNBC, suggesting that proteasome inhibitors (PIs) could be a potential therapeutic option. In this dissertation, I wanted to find the mechanism by which proteasome inhibitors induce apoptosis in TNBC. Proteasome inhibitors are currently approved for the treatment of multiple myeloma (MM) and mantle cell lymphoma and have been shown to induce proteotoxic stress due to a buildup of misfolded proteins in MM cells. However, the exact mechanism by which proteasome inhibitors induce apoptosis is debated. In this dissertation, I demonstrate that, in response to PIs, TNBC cells have a comparable sensitivity profile to MM. Although the mechanism of action in TNBC is distinct from the proposed mechanisms in MM, there is an increase in proteotoxic stress observed in TNBC cells. Proteotoxic stress can be regulated by changes in protein synthesis and protein breakdown. Given that protein breakdown is impaired due to proteasome inhibition, we investigated the role protein synthesis plays in mediating the effects of PIs. eIF2α (eukaryotic initiation factor 2α) promotes global protein synthesis, and its phosphorylation inhibits it. I show that eIF2α does not get phosphorylated in response to PIs and thereby does not decrease protein synthesis rates. In some cases, we observed a decrease in eIF2α phosphorylation. We investigated the role eIF2α phosphatases play in the response of TNBC cells to PIs and found that they contribute to apoptosis in TNBC cells in an eIF2α-independent manner. This suggests that the eIF2α phosphatases regulate apoptosis through a novel mechanism.

The effector of PI-induced apoptosis in MM cells is NOXA. We found the same in TNBC cells. In MM, upstream regulators of NOXA in response to PIs are debated. In this study, we found that c-myc upregulates NOXA expression, regulating apoptosis in response to PIs in TNBC cells. This has not been previously reported in response to PIs in TNBC cells. The findings in this dissertation establish key mediators involved in PI-induced apoptosis in TNBC cells and lay a foundation for identifying combination therapeutic strategies to translate PIs to TNBC treatment.

Artificial Intelligence (AI) Use Disclosure Statement

In the preparation of this dissertation, no Artificial Intelligence (AI) tools were used.

## Digital Accessibility Use Disclosure Statement

In the preparation of this dissertation, the following digital accessibility tools were used to ensure this document complies with federal requirements: Adobe Acrobat Pro. The author acknowledges full responsibility for the intellectual content of this work and has made a good faith effort to comply with digital accessibility requirements in publishing, wherein the nature of the content does not significantly change in order to do so. Furthermore, all content has been reviewed and revised to meet these requirements prior to final publication.

Acknowledgments

I would like to thank all the people who have supported me and helped me get to this point.

I would like to thank my mentor, Dr. Alexei Kisselev, for his wonderful mentorship and for teaching me what it really means to be a scientist.

I would like to thank my committee members, Dr. Shen, Dr. Mitra, and Dr. Arnold, for their guidance through my PhD journey. I appreciate all the advice I have been given.

I would like to thank Dr. Tao for agreeing to be the University Reader for my dissertation.

I would like to thank my parents for their wonderful support and for believing in me from the beginning. I would not be here without you.

I would like to thank my friends for keeping me company and distracting me when I needed it.

I would like to thank the incredible faculty and staff of Harrison College of Pharmacy for sharing their knowledge and making the classes engaging.

I would like to thank Olasubomi, Tyler, Ibtisam, and Andrey for helping build a wonderful lab environment and helping me fit in when I joined the lab. I could not have made it through this PhD journey without you all. Thank you to Chandler and Ellie for being wonderful members of the lab and for making the lab more enjoyable.

Thank you to my fellow graduate students for listening to me during seminars and symposiums and providing me with valuable feedback.

Thank you everyone for guiding me, listening to me, helping me, and for reading this.

Table of Contents

List of Tables

List of Figures

**List of Abbreviations**

| | |
|---|---|
| 4EBP1 | Eukaryotic translation initiation factor 4E binding protein 1 |
| ATF3 | Activating Transcription Factor 3 |
| ATF4 | Activating Transcription Factor 4 |
| ATF6 | Activating Transcription Factor 6 |
| Btz | Bortezomib |
| CCA | Cholangiocarcinoma |
| CDK | Cyclin-dependent Kinases |
| Cfz | Carfilzomib |
| CHX | Cycloheximide |
| p-eIF2α | Phosphorylated Eukaryotic Initiation Factor 2α |
| eIF2α | Eukaryotic Initiation Factor 2α |
| ER | Endoplasmic Reticulum |
| FBS | Fetal Bovine Serum |
| HGSOC | High-grade Serous Ovarian Carcinoma |
| HRI | Heme-regulated Inhibitor |
| IRE1 | Inositol-requiring Enzyme 1 |
| ISR | Integrated Stress Response |
| LDS buffer | Lithium Dodecyl Sulfate buffer |
| MM | Multiple Myeloma |
| MPM | Malignant Pleural Mesothelioma |
| mTOR | Mammalian Target of Rapamycin |
| mTORC1 | Mammalian Target of Rapamycin Kinase Complex 1 |

| | |
|---|---|
| PDAC | Pancreatic Ductal Adenocarcinoma |
| PDX | Patient derived Xenografts |
| PERK | Protein Kinase R-like ER Kinase |
| PI | Proteasome Inhibitor |
| PP1 | Protein Phosphatase 1 Complex |
| T-IC | Tumor-initiating cells/cancer stem cells |
| TNBC | Triple-negative Breast Cancer |
| UPR | Unfolded Protein Response |

## Introduction

### Overview

The proteasome is a multi-subunit cellular structure in eukaryotic cells that breaks down proteins, including regulatory proteins, into amino acids, which are recycled to produce more proteins(1–3). It is a critical part of the ubiquitin proteasome system, which maintains protein homeostasis in cells. Eukaryotic cells tag proteins that need to be degraded with ubiquitin, which serves as a marker for degradation by the proteasome. The 26S proteasome complex comprises a 20S core and two 19S regulatory complexes. The 20S core is a ring-like structure with three catalytically active subunits: β5, β2, and β1. The β5 active site is chymotrypsin-like because it cleaves after hydrophobic residues, β2 is trypsin-like because it cleaves after basic residues, and β1 is caspase-like because it cleaves after acidic residues. β5 is the main catalytic subunit, with it being considered the rate-limiting step(4,5), though the relative contribution of each site is also mediated by the protein being degraded(6).

Protein homeostasis is regulated by the rate at which proteins are synthesized and metabolized(1,2,7,8). Cells must maintain protein levels under a threshold to prevent elevated stress on the endoplasmic reticulum (ER) and thereby the proteasome(9,10). The proteasome degrades proteins, especially misfolded proteins(9,10). Elevated protein levels result in an increased burden on the proteasome because the proteasome is required to metabolize more proteins to reduce the protein levels rapidly. In addition, the cell will activate a series of protective responses, including the unfolded protein response (UPR), to reduce protein synthesis.

In cases where the proteotoxic stress on the ER cannot be mitigated, the cell will undergo apoptosis. The UPR is a signaling pathway consisting of three ER transmembrane "arms" that induce its effects. The three arms consist of Protein Kinase R-like ER Kinase (PERK), activating transcription factor 6 (ATF6), and inositol-requiring enzyme 1 (IRE1)(7,8). Each arm consists of different signaling pathways, which ultimately help regulate ER stress or induce apoptosis if ER stress is not managed.

The PERK arm of the UPR is activated in response to proteasome inhibitors, which causes the phosphorylation of eIF2α(11). When eIF2α is phosphorylated, it inhibits global protein synthesis while upregulating the translation of specific transcription factors, such as ATF4(12,13). ATF4 upregulates ATF3(14), which can induce NOXA transcription. NOXA is a pro-apoptotic BCL-2 protein that binds to and inhibits MCL1 (which normally acts to sequester apoptosis effectors, BAX and BAK). NOXA binding to MCL1 releases BAX and BAK, which ultimately disrupt the mitochondrial outer membrane and induce apoptosis(15). Figure 1.1 illustrates the activation of this pathway.

ATF6 is an ER transmembrane protein that gets cleaved in response to unfolded/misfolded proteins(16). Cleaved ATF6 releases a transcription factor that increases transcription and expression of select proteins and increases protein-folding capacity to promote cell survival(16). IRE1, when activated, induces the splicing of XBP1 or RIDD, and can activate the JNK pathway(17). The activation of JNK by the UPR can promote apoptosis(18,19). While PERK

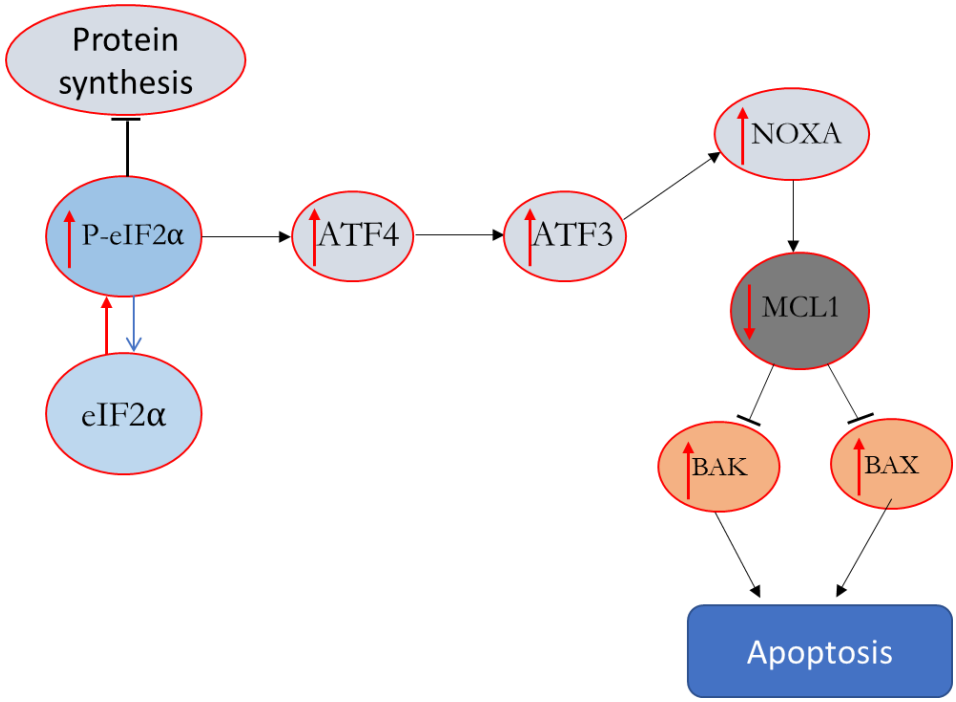


**Figure 1.1 UPR-PERK activation resulting in NOXA upregulation**

signaling persists under prolonged ER stress and leads the cell to undergo apoptosis, IRE1 and ATF6 signaling have been found to be reduced under prolonged stress and do not play a key role in inhibiting apoptosis(17,20).

Due to the proteasome's role in protein homeostasis, it is an enticing therapeutic target for diseases that heavily depend on it. Cancer cells tend to produce more misfolded proteins than normal cells. Thus, the proteasome is pivotal to break down these misfolded proteins to recycle amino acids and prevent amino acid starvation(1,2). Cancer cells also need to rapidly break down misfolded proteins to reduce protein levels within cells and avoid ER stress-induced apoptosis. This reliance on the proteasome makes cancer cells susceptible to proteasome inhibitors (PIs). Proteasome inhibitors function by binding to and inhibiting one or two catalytically active sites of the proteasome to slow down the breakdown of misfolded proteins. Of the three catalytically

active proteasome subunits, most proteasome inhibitors target the β5 site because it is the primary mediator of proteasome activity. Currently, three proteasome inhibitors are FDA-approved: Bortezomib (Btz), Carfilzomib (Cfz), and Ixazomib. They are approved for Multiple Myeloma (MM) and mantle cell lymphoma. While these FDA-approved PIs primarily target the β5 site, they can inhibit the other catalytically active sites at higher concentrations.

Proteasome inhibitors are effective in cancer cells due to the cells' increased dependence on the proteasome. Additionally, proteasome inhibitors have been found to inhibit cell proliferation in sensitive and resistant multiple myeloma cell lines. Proteasome inhibitors can cause cell cycle arrest through various mechanisms. Cyclin-dependent kinases (CDKs) and CDK inhibitors play a crucial role in controlling cell division(21). CDK inhibitors primarily function by inhibiting CDK enzyme activity resulting in the blocking of cell cycle and inhibiting cell proliferation(21,22), and proteasomal degradation of CDK inhibitors leads to uncontrolled cell division in cancer cells. By inhibiting the proteasome, PIs disrupt uncontrolled cell division in cancer cells by preventing the rapid metabolism of CDK inhibitors(21). Proteasome inhibition leads to an increase in the expression of p21 and p27(21). CDK inhibitors p21 and p27 are well-known inhibitors of the cell cycle(21,23). Additionally, PIs have been found to inhibit the NF-κB signaling pathway by preventing the degradation of IκB. NF-κB is a transcription factor with anti-apoptotic properties that regulates apoptosis, cell proliferation, and differentiation, as well as other functions(24). Normally, NF-κB is sequestered in the cytoplasm by IκB(24,25), however, when IκB is degraded by the proteasome, NF-κB can enter the nucleus and induce its effects(24).

Proteasome inhibitors were first identified in the mid-1990s, and Bortezomib was the first proteasome inhibitor approved by the FDA, initially for the treatment of MM. Bortezomib is also approved in the treatment of relapsed patients with mantle cell lymphoma. While effective for the treatment of MM, patients treated with Btz often relapse and develop resistance to Btz. In addition, Btz is associated with peripheral neuropathy. Carfilzomib, a second-generation proteasome inhibitor, was approved by the FDA in 2012 for the treatment of relapsed and refractory MM. Cfz, unlike Btz, irreversibly binds to the proteasome, leading to a longer-lasting effect. Cfz was found to be more effective in patients who developed resistance to Btz. In addition, Cfz, compared to Btz, had better progression-free survival and overall survival(26,27). And while Cfz greatly reduced the risk of peripheral neuropathy, it was associated with greater cardiovascular risk(26). Ixazomib was the first oral proteasome inhibitor approved by the FDA. Ixazomib is also associated with a lower risk of peripheral neuropathy. However, it has a faster proteasome dissociation half-life rate than Btz(28), which results in faster recovery of proteasome activity. Despite various cancers having a reliance on the ubiquitin-proteasome system, Btz, Cfz, and Ixazomib are all ineffective clinically in patients with solid tumors.

Proteasome inhibitors have also been found to be a potential therapeutic approach for the treatment of various cancers in the brain, such as glioblastoma and medulloblastoma, but the current FDA-approved PIs have poor blood-brain barrier penetration, resulting in them not being viable treatments for brain cancers. Marizomib is a proteasome inhibitor that has been found to cross the blood-brain barrier. Phase I/II trials were conducted to test Marizomib in newly diagnosed glioblastoma patients(29). The clinical trial found that adding marizomib did not improve survival in patients and increased toxicity when marizomib was added to standard

temozolomide-based radiochemotherapy(30). Delanzomib was tested in combination with lenalidomide and dexamethasone for relapsed or refractory multiple myeloma patients(31). The development of Delanzomib for myeloma was discontinued(32), because meaningful myeloma responses were not observed in patients in a phase I/II clinical trial(32).

Cancer cells produce more misfolded proteins than normal cells due to various stresses, gene mutations, or proteolysis(33), and need the proteasome to rapidly break down the misfolded proteins to reduce cell stress and to recycle amino acids to produce more proteins. By inhibiting the proteasome, cancer cells are unable to rapidly metabolize proteins, which causes a buildup of proteins, ultimately resulting in elevated ER stress and amino acid shortage. MM cells also produce and secrete large amounts of misfolded(34) monoclonal immunoglobulins, a great proportion of which are misfolded and must be degraded(35). This additional protein synthesis requirement makes MM cells highly dependent on the proteasome to regulate protein homeostasis by breaking down unnecessary proteins to avoid ER stress and to provide amino acids for immunoglobulin synthesis. Therefore, inhibiting the proteasome in MM cells rapidly exacerbates ER stress and induces apoptosis.

While PIs are currently only approved for selected hematologic malignancies, their therapeutic potential has been shown in various disease models, including solid tumors, such as triple-negative breast cancer, colon cancer, pancreatic cancer, and autoimmune diseases(30,36–68). However, the specific mechanisms of action by which PIs induce apoptosis are not clearly defined. There are several proposed mechanisms regarding how PIs induce apoptosis in MM, and these mechanisms and signaling pathways differ in different disease models. This review will

focus on the various pathways that can sensitize cancer cells to proteasome inhibitors and the pathways proposed by which proteasome inhibitors induce apoptosis.

**Adverse Load vs Proteasome Capacity**

In a cell, the balance between the proteasomal capacity and the proteasomal workload must be maintained to prevent proteotoxic stress and apoptosis. The proteasomal capacity is the number of active proteasomes, while the workload is the number of proteins that the proteasome is required to break down. When there is an increase in misfolded and ubiquitinated proteins, there is an elevated load on the proteasome. And when the proteasome is inhibited, such as through proteasome inhibitors, the proteasomal capacity is reduced. As mentioned earlier, the cell can activate various stress responses if the ratio between load and capacity is not controlled to restore balance. Continuously being in a state of elevated proteotoxic stress will lead the cell to undergo apoptosis. The load vs capacity model suggests that cells with higher proteasomal workload, through elevated protein synthesis, or lower proteasomal capacity, by having fewer functional proteasomes, are sensitive to proteasome inhibitor-induced apoptosis(69).

Cancer cells rapidly produce more proteins, especially misfolded proteins, than normal cells(70). This suggests that cancer cells have a higher proteasomal workload compared to normal cells. Multiple myeloma cells have even higher load on the proteasome because they produce and secrete large amounts of monoclonal immunoglobulins. Because multiple myeloma cells have such an elevated load on the proteasome, they are extremely dependent on the proteasomal capacity to keep up with the workload to prevent the buildup of proteins. This potentially makes

multiple myeloma cells extremely susceptible to modulations to this system. Sensitivity of multiple myeloma cells to proteasome inhibitors is thought to be due to an increase in proteasomal workload and/or a decrease in proteasomal capacity(69). Various studies have tried to exploit this in multiple myeloma and other cancers(42,69,71,72), believing that it is the regulator of proteasome inhibitor sensitivity. Let's first look at the effect of proteasomal capacity affecting sensitivity to proteasome inhibitors.

Decreasing proteasome capacity would increase sensitivity to proteasome inhibitors. A study in neurons found that there is an abundance of free proteasomes that are not actively processing substrates. Approximately 20% of proteasomes were found to be in the substrate processing state, with the rest in an idle state to serve as reserves for situations where there is an increase in protein load(39). Suggesting that cells normally are not near the threshold that will make them sensitive to proteasome inhibitors.

In another study, to mimic antibody secretion in cells, as multiple myeloma cells do, I.29$\mu^+$ cells were selected as an antibody-producing model. These cells, when treated with LPS, start to differentiate, resulting in them producing and secreting IgM(73). Compared to non-differentiated I.29$\mu^+$ cells, differentiating B-lymphocytes have decreased proteasome activity(69), which decreases the rate at which proteins are metabolized, and therefore increases the proteasomal workload. This led to a higher apoptotic sensitivity to proteasome inhibitors(69). KMS-18 and MM.1S cells were used as the sensitive cell lines in this study and were found to have lower chymotrypsin-like and trypsin-like activity compared to the more resistant cell lines. The

sensitive cell lines also had significantly lower immune-catalytic subunits compared to the resistant cell lines(69).

The Sitia group, in their study, also found a decrease in proteasomal levels and activity in differentiating cells that secreted IgM(73). As a decrease in proteasomal levels and activity increases sensitivity to proteasome inhibitors, multiple myeloma cells with increased proteasome expression have been associated with higher resistance to proteasome inhibitors(72). This study used two PI-sensitive MM cell lines and two PI-resistant MM cell lines and found that the more PI-resistant MM cell lines express higher proteasomal enzymatic activity per cell, even though all four cell lines contained similar numbers of constitutive proteasomes(72). Yet another study found that higher levels of PSMD1, PSMD4, and PSMD10-gankyrin are associated with adverse prognosis in patients(74). PSMD1 and PSMD4 are 26S proteasome subunits, while PSMD10 is an 19S assembly chaperone. Though that does not directly translate to more proteasomes in the cell.

Other than cells with lower proteasomal capacity, cells with elevated proteasomal load would also be more sensitive to proteasome inhibitors. An increase in proteasomal load can be due to an elevated rate of protein synthesis. Due to multiple myeloma cells secreting antibodies, they have significantly elevated rates of protein synthesis. In several pulse-chase assays conducted, MM.1S and KMS-18 cells incorporated 3-4 times more radioactive methionine than the resistant RPMI8226 or U266 cells into TCA-insoluble polypeptides, which is an indication of higher protein synthesis(69). In differentiated I.29$\mu^+$ cells, apoptosis correlates with massive IgM

synthesis and secretion. In HeLa cells that were generated to express inducible secretory μ-chains, their sensitivity to PI increased when the HeLa cells were made to secrete the μ-chains(73). Normal Ig-secreting cells were found to be extremely sensitive to PI, like their malignant counterparts(73).

All of those are examples of cells with elevated basal rates of protein synthesis that sensitize those cell lines to proteasome inhibitors. In addition, misfolded proteins induced by ER-stressors also elevated the load on the proteasome and sensitized cells to PIs, showing that elevated load on the proteasome does have a causal effect in inducing apoptosis(69). MM cells were treated with tunicamycin, an ER stressor, at a dose that can induce the UPR, and combined it with a non-toxic dose of bortezomib. This induced apoptosis, suggesting a strong synergism. Additionally, MG-132, another PI, in combination with Thapsigargin, an ER stressor, synergized to induce apoptosis at subtoxic doses of both inhibitors. The combinations of these two classes of drugs caused proteasomal overload in a synergistic manner, suggesting that the workload is causally involved in determining PI sensitivity(69).

Having lower proteasome expression and higher proteasome workload in PI-sensitive MM cells can lead the cell to suffer from proteotoxic stress, which can be assessed via an accumulation of poly-ubiquitinated proteins. Critical levels of proteasome overload were assessed using GFP fused to a mutated, uncleavable ubiquitin moiety, which is an established reporter of proteasome overload(69,73,75). They found, in the sensitive cells, that critical proteasomal overload occurred upon 24-hour treatment, suggesting that the PI-sensitive cell lines have a lower

efficiency of the ubiquitin-proteasome system. This is why critical proteasomal overload levels precede PI-induced death(69).

Accumulation of polyubiquitinated proteins, a proteasome substrate, correlates with proteasome inhibition, and a strong correlation exists between Ig synthesis and accumulation of polyubiquitinated proteins(69). UV treatment induced more apoptosis than MG132; however, UV treatment did not cause an increase in polyubiquitinylated proteins, nor did it cause a decrease in proteasome activity(73), suggesting that apoptosis itself does not cause polyubiquitin buildup(73). To determine if the polyubiquitin accumulation is due to rapidly degraded polypeptides or long-lived proteins, cells were treated with a combination of Btz and CHX, a drug that inhibits protein synthesis. This led to a reduction of polyubiquitin accumulation at all time points, suggesting that a sizeable fraction of the accumulation originates from recently synthesized proteins(72). A similar experiment was conducted to see if attenuating protein synthesis reduces the proteasomal workload and rescues cells from apoptosis. Cells were treated with a low dose of CHX that resulted in a significant decrease in protein synthesis and no CHX-induced toxicity and then treated with PI. Attenuating protein synthesis protects MM and activated B-cells from PI-induced apoptosis. In addition, they found that in highly PI-sensitive MM cells, significant proteasome load comes from newly formed proteins, suggesting that there is a strong relationship between protein synthesis and Btz-induced apoptosis(72).

While proteasome inhibitors are currently approved for multiple myeloma and mantle cell lymphoma, there is evidence that PIs should work for solid tumors, too(37,38,76–79). However,

since solid tumors do not secrete antibodies, the mechanism by which solid tumors upregulate protein load, or downregulate protein capacity, must vary.

In Pancreatic ductal adenocarcinoma (PDAC), a subpopulation of patient-derived xenografts (PDXs) was sensitive to PIs, based on a lower $IC_{50}$(41). The Cfz-sensitive phenotype had a higher level of RNA and protein synthesis in basal conditions compared to the Cfz-resistant phenotype. To study protein synthesis, puromycin incorporation assay was used. Puromycin is a naturally occurring aminonucleoside antibiotic that is used as a probe for protein synthesis because it inserts itself into nascent polypeptide chains and prematurely terminates protein synthesis(80). The study found that the combination of puromycin and Cfz rescued Cfz-sensitive cells from apoptosis, suggesting protein synthesis plays a significant role in sensitizing the sensitive PDAC phenotype to Cfz(41).

While that population of PDAC sensitized itself to PI due to an increase in proteasomal workload, a study on malignant pleural mesothelioma (MPM) found that sensitivity correlated with a decrease in proteasomal capacity(42). They found that PI-sensitive human MPM cell lines had lower proteasomal activity, while more resistant MPM cell lines had higher proteasomal activity (chymotrypsin-like and trypsin-like)(42). In addition, Btz-sensitive MPM cell lines have higher levels of unbound ubiquitin compared to resistant cell lines and have more basal accumulation of polyubiquitinated proteins(42).

**mTORC pathway**

The mammalian target of rapamycin (mTOR) pathway is a signaling pathway that regulates cell growth, proliferation, survival, and metabolism(81), and upregulates protein synthesis. This pathway has been found to play various roles in PI-induced apoptosis, though its role is cancer-dependent. Mammalian target of rapamycin kinase complex 1 (mTORC1/TORC1) is part of a complex of proteins that includes mTOR. This complex regulates protein synthesis(82), and an increase in protein synthesis would result in elevated load on the proteasome, as discussed in the previous section. In multiple myeloma, Btz and Btz-dexamethasone combination treatment induces rapid expression of several stress-related genes, including REDD1(83). Btz-dexamethasone combination was tested due to this combination being proven as an enhancement to Btz efficacy in patients with MM. REDD1 is a novel stress response gene reported to be induced by various stressors, including ER stressors, heat shock, and DNA damage. REDD1 negatively regulates mTORC1 signaling, NF-κB activation, among others, and its role in being protective or inducing apoptosis varies depending on the cell type and stressor(83,84). But NF-κB has been shown not to be responsible for PI-induced effects(85). REDD1 overexpression is associated with the inhibition of mTORC1 activity(83). MM cells treated with rapamycin, a specific inhibitor of mTORC1, reduced p70 phosphorylation induced by Btz and Btz-dexamethasone treatment, suggesting that p70 phosphorylation is mediated by mTORC1 activity. The p70 kinase is a downstream target of the TORC1 pathway and plays a role in mediating TORC1's effects on protein synthesis, cell growth, and cell size(86,87). Cell lines were divided into three groups for this study, based on their sensitivity to the Btz-dexamethasone combination. Since a critical role of mTOR is cell size regulation, cells were treated with the Btz-dexamethasone combination, and changes in their morphology were observed. Cell lines

resistant to the combination treatment had early shrinkage but recovered to control size within 12 hours. Cells with intermediate resistance had early shrinkage as well, but it was not as severe and did not completely recover at 12 or 24 hours. Highly sensitive cell lines had no shrinkage at 2 hours. Other studies have also found that deactivation of the mTOR/p70 pathway reduces cellular size and mass, which translates to protection from apoptosis(88). This suggests that REDD1 overexpression and resulting mTORC1 inhibition and cell shrinkage is a possible mechanism for the resistance of MM cells to Btz(83).

Another protein that could affect the sensitivity of PI in MM cells is the 14-3-3ε chaperone protein. YWHAE, coding gene for the isoform 14-3-3ε, had a positive correlation with Cfz and Btz response, and had high expression in MM cell lines and primary patient MM cells, and low expression in healthy donor B cells(71). KD of the 14-3-3ε protein using shRNA in PI-sensitive MM cell lines resulted in decreased sensitivity to PIs, and a corresponding reduction in the upregulation of NOXA, a pro-apoptotic BCL-2 protein. 14-3-3ε is found to interact with p-mTOR and upstream of the negative regulator TSC2. KD of 14-3-3ε resulted in the activation of TSC2 and subsequent inhibition of mTORC1. KD of 14-3-3ε also affected other pathways, such as UPR-related genes. Depletion of 14-3-3ε inhibits translation initiation complex formation and decreases protein synthesis, and higher 14-3-3ε expression increases sensitivity to PI. This suggests that mTORC signaling is needed for the sensitivity of PIs. 14-3-3ε binds directly to p-eIF2α, an eukaryotic initiation factor, and its depletion causes an increase in phosphorylation of eIF2α(71). 14-3-3ε and mTORC may be playing a key role in PI sensitivity. High expression of 14-3-3ε in patients correlated with enhanced sensitivity to proteasome inhibitors and increased protein load(71).

**PTEN status affects PI sensitivity**

PTEN functions to inhibit PI3K signaling by directly antagonizing PI3K function and blocking the activation of AKT and mTOR, and thereby inhibits cell growth, proliferation, and survival(83,89,90). PI3K is a key upstream negative regulator of mTOR.(89,91,92).

A study in Cholangiocarcinoma (CCA) established 34 PDX models from fresh patient samples. They divided the models into two groups, Btz-sensitive and Btz-resistant. The Btz-sensitive group had higher proteolytic activity and higher expression of genes encoding proteasome subunits. The Btz-sensitive group lacked PTEN gene expression, upregulated MAPK, PI3K/AKT, and UPS, and had higher proteasome activity and rate of protein synthesis((43)). PTEN-deficient cells were sensitive to ER stressors, had decreased ER protein folding capabilities, had poor ability to handle proteotoxic stress, and were addicted to a high rate of protein turnover, due to a higher rate of proliferation(43). PTEN deficiency also increases proteosome proteolytic activity and facilitates the effects of Btz in CCA(43). This translated to in vivo studies, where Btz had an enhanced therapeutic effect on PTEN KD tumors(43). Multiple cell lines from various cancers have shown that PTEN mutation results in increased sensitivity to proteasome inhibitors, such as glioblastoma, pancreatic cancer, ovarian cancer, gallbladder cancer, in addition to CCA(40,43,51,93). Reduced PTEN activity, leading to an increase in protein synthesis(43), places a greater load on the proteasome. As discussed earlier, a higher load on the proteasome makes the cells more sensitive to proteasome inhibitors.

PTEN loss may also play a role in sensitizing patients with high-grade serous ovarian carcinoma (HGSOC) to proteasome inhibitors(40). The model used in this study is associated with proteotoxic stress and confers selective vulnerability to PIs and has elevated protein synthesis due to additional chromosomes. An incorrect number of chromosomes leads to aneuploidy, which results in proteotoxic stress due to the aggregation of endogenous proteins as well as the expression of unfolded proteins(94–96).

PTEN loss in HGSOC has also led to increased p-eIF2α, ATF4, and CHOP. Ultimately, this study indicates that the UPR is activated in fallopian tube secretory epithelial cells with chromosomal instability through an eIF2α-mediated stress response pathway(40). As the ovarian cells grow, they grow as detached spheroids that downregulate mTORC1, attenuate translation, and acquire resistance to Btz; however, PTEN KD in ovarian cancer cells resulted in an increase in protein synthesis, upregulation of BiP, p-eIF2α, and CHOP. BiP is an ER chaperone protein that plays a key role in correct protein folding and degradation of misfolded proteins(97,98). The study confirmed that the effects observed are due to mTORC1 activation. They observe an increase in basal p-eIF2α and find that the loss of PTEN sensitizes cells to Btz in HGSOC models(40). Like what was observed in CCA cells(43).

**Discrepancies in eIF2α phosphorylation**

The role of the unfolded protein response and the changes in protein synthesis via the eIF2α in response to proteasome inhibitors appears to vary. Additionally, discrepancies exist in the role of eIF2α phosphorylation and sensitivity to proteasome inhibitor-induced apoptosis.

p-eIF2α is downstream of the PERK arm of the unfolded protein response. eIF2α regulates protein synthesis. In its phosphorylated state, eIF2α inhibits protein synthesis while upregulating select transcription factors. Downstream of eIF2α are ATF4 and ATF3, which ultimately upregulate NOXA, a pro-apoptotic protein that will induce apoptosis through BAX and BAK(99,100). P-eIF2α is downregulated by the protein phosphatase 1 complex (PP1), which can contain one of two regulatory subunits: GADD34 and CReP. The downregulation of p-eIF2α returns it to the state that upregulates protein synthesis. There is a higher expression of GADD34 in the PI-sensitive phenotype of PDAC cells. This phenotype, as mentioned earlier, has increased levels of protein synthesis at basal conditions, and the elevated protein synthesis plays a significant role in sensitizing that phenotype to PI(41).

In addition to PERK, eIF2α is phosphorylated by PKR, GCN2, and HRI(101). PERK is activated by ER stress (UPR) but can also be activated by hypoxia(102). PKR is activated in response to viral infection, and GCN2 is activated in response to glucose and amino acid starvation, and UV light. HRI is activated in response to heme deficiency, oxidative stress, and accumulation of unfolded proteins in the cytosol(103). The regulation of eIF2α phosphorylation through PERK, PKR, GCN2, and HRI, and the subsequent activation of ATF4, is part of the integrated stress response (ISR)(104).

The phosphorylation of eIF2α in Btz-sensitive cells has been observed in multiple myeloma(105,106) and various other cancers, such as hepatocellular carcinoma(107). While

some studies have found that eIF2α dephosphorylation sensitizes cells to PIs, several studies in pancreatic cancers have shown that induction of eIF2α phosphorylation is associated with resistance to Btz(108,109). In addition to the role of eIF2α phosphorylation and its downstream pathways, the kinases responsible for mediating eIF2α in response to PI also vary. Multiple myeloma cell lines were all sensitive to PIs and responded to PIs by rapidly activating PERK. While varying levels of eIF2α phosphorylation were detected in untreated cells, Btz induced phosphorylation within 24 hours(105). Phosphorylation of eIF2α inhibits global protein synthesis, but selectively upregulates certain transcription factors, such as ATF4. In multiple myeloma cell lines, ATF4 expression was rapidly increased within two hours of Btz treatment, and CHOP, a nuclear transcription regulator that is primarily activated through the PERK pathway and plays a key role in ER stress-related apoptosis(110), was rapidly induced within four hours after Btz treatment through ATF4(105). There are several key discrepancies with the implication of this work. The study found a rapid activation of PERK (within 30 minutes); however, the phosphorylation of eIF2α occurred at 12-24 hours. The study suggested that PERK phosphorylates eIF2α; however, it has not demonstrated that eIF2α phosphorylation is due to PERK, as no PERK inhibitors or knockdown studies were used. Additionally, the study implies that the ATF4 upregulation is due to eIF2α phosphorylation; however, ATF4 upregulation occurs within 2 hours, which is earlier than when eIF2α is shown to be phosphorylated.

This study also found that the efficiency of protein folding within the ER can affect the sensitivity of cell lines to MM(105). Similar results were found in mouse embryonic fibroblasts (MEFs). In response to PI, MEF cells exhibited significant reductions in protein synthesis, accompanied by upregulation of ATF4 and CHOP(111). They also found an upregulation of

ATF3 in response to PI; however, this occurred in MEF cells containing wild-type eIF2α and a cell line that expressed a phsospho-site mutant eIF2α , suggesting that the ATF3 upregulation is independent of eIF2α phosphorylation(111).

Contrary to what was observed in multiple myeloma and MEF cell lines, studies in pancreatic cancers found that the phosphorylation of eIF2α in response to PI was associated with resistance to PI(108,109). The Btz-resistant cell lines phosphorylated eIF2α in response to Btz, while the sensitive cell lines did not. In addition, the resistant cell lines had a lower basal eIF2α phosphorylation level compared to the sensitive cell line, though this was found not to play a role in mediating sensitivity(108). In response to Btz, the resistant cell lines rapidly downregulated translation, while the sensitive cell lines continued to exhibit protein synthesis for a longer duration(108). Contrary to its role in multiple myeloma cells, PERK did not play a significant role in mediating apoptosis in pancreatic cells; however, HRI played a significant role. Heme-regulated inhibitor (HRI) is part of the integrated stress response pathway and is induced by heme depletion and mitochondrial stress(112–114). HRI is a kinase that can phosphorylate eIF2α(112,113). The knockdown of HRI strongly promoted apoptosis in Btz-resistant cells, reduced Btz-induced phosphorylation of eIF2α, and reduced ATF4 accumulation(108).

Another eIF2α kinase that could play a role in regulating proteasome inhibitor effects is GCN2. GCN2 is activated in response to amino acid deprivation and UV irradiation(115,116). A study in MEF cells found that eIF2α phosphorylation is required for reduced translation in response to PIs, and GCN2 is the primary eIF2α kinase activated by proteasome dysfunction, not

PERK(116). They found that ATF4 is upregulated in response to PI, and it is required for full induction of ATF3 and CHOP in response to PI(116). In cells containing a mutant eIF2α that makes them unable to be phosphorylated, PIs still induced apoptosis. This shows that PIs are capable of reducing apoptosis, though peIF2α-independent mechanism. PIs containing mutated eIF2α contained aberrantly high levels of protein synthesis in response to PI. While PIs induced apoptosis in cells containing wild-type or mutant eIF2α, the phosphorylation of eIF2α accelerated apoptosis induced by PIs(116). All of this suggests that the role of eIF2α varies across cancers, and, significantly, the mechanisms by which proteasome inhibitors induce apoptosis in cancers differ.

**Regulators of PI-induced apoptosis**

Up till now, we have mostly been discussing pathways that sensitize the cells to proteasome inhibition. This review will now focus on pathways by which proteasome inhibitors induce apoptosis.

Apoptosis is regulated by the BCL-2 family of proteins which consists of pro- and anti-apoptotic proteins(117). The BCL-2 family of proteins can be divided into three groups: anti-apoptotic proteins, pro-apoptotic BH3-only proteins, and pro-apoptotic pore-forming proteins(117). Normally, the anti-apoptotic proteins, such as BCL-XL, BCL-2, and MCL-1, sequester BAX and BAK, which form pores in the mitochondrial outer membrane, causing mitochondrial outer membrane permeabilization, eventually leading to apoptosis(117–119). Pro-apoptotic BH3-only proteins, such as NOXA, PUMA, BIM, and BAD, function by competing with BAX and BAK to

bind to and inhibit the anti-apoptotic BCL-2 proteins(117,120), freeing BAX and BAK to induce apoptosis. BH3-only protein expression is regulated by the proteasome, and proteasome inhibition has been reported to cause upregulation of these proteins, leading to apoptosis(121–125). Various BH3-only pro-apoptotic proteins have been shown to mediate PI-induced apoptosis in different cancers.

In multiple myeloma cells, Btz induces proapoptotic protein BAX in Ag8uH+ cells, a subclone of murine immunoglobulin-negative mouse plasmocytoma Ag8.653(85). BAX and BAK each play a different role in inducing apoptosis depending on the cell type. In Malignant Pleural Mesothelioma (MPM), BAK is an essential regulator of Btz-induced apoptosis(44), whereas BAX silencing did not reduce sensitivity to Btz, suggesting that it does not play a key role in inducing apoptosis in response to Btz(44). Two MPM cell lines were selected for this study and were treated with increasing doses of Btz. This led to the development of resistant cell lines. NOXA accumulation was observed in the MPM parental cells, and the knockdown of NOXA rescued cells from apoptosis; however, the cells with resistance developed,did not upregulate NOXA in response to Btz(44). NOXA accumulation in response to PIs has also been observed in chronic lymphocytic leukemia cells(126), mantle cell lymphoma(61), cisplatin-resistant squamous cell carcinoma(127), melanoma(128,129), and triple-negative breast cancer(130).

As mentioned earlier, NOXA can be upregulated through the p-eIF2α/ATF4/ATF3 pathway of the UPR. In addition, NOXA can also be upregulated by c-myc(44,131). NOXA was not upregulated in c-myc KD MPM cells, suggesting that c-myc is responsible for NOXA

accumulation in MPM cells(44). C-myc interacts directly with the promoter of NOXA to upregulate NOXA in REN parental cells, which increases after treatment with Btz(44).

In a PDAC study of hyperactive myc, two cell lines were identified that highly expressed myc, and two cell lines that expressed low levels of myc(131). They found that translation is a key process linked to MYC in PDAC, and consistent with translation, they also detected increased PERK and ATF4. NOXA accumulation and PARP cleavage occurred only in cell lines with a high level of MYC(131).

MYC is one of the most frequently activated oncogenes in human tumors(132). MYC pathway and mTOR signaling converge on the eukaryotic translation initiation factor 4E binding protein 1 (4EBP1)(132). 4EBP1-dependent inhibition of eIF4E activity impedes myc-driven tumor survival(132). In addition, the study suggested that crosstalk occurs between myc and mTOR signaling pathways at the 4EBP1 phosphorylation level might be a general feature of myc-driven tumors, and myc-driven myeloma requires mTOR-dependent signaling for tumor survival(132).

Other BH3-only proteins also have their expression altered in response to proteasome inhibitors. BID was degraded in response to Btz-induced activation of the JNK pathway in human hepatoma cells(133). Btz also decreased the expression of BCL-2 and BCL-XL proteins(133). In multiple myeloma and plasma cells, the buildup of protein load results in an accumulation of BAX, a pore-forming BCL-2 protein, and BIM, a BH3-only protein(134), which correlated with an increased sensitivity to proteasome inhibitors(73,134,135). In the colon cancer cell line HCT116,

BAX was required to induce apoptosis to MG132, a proteasome inhibitor. Using cell lines with BAX or PUMA knocked down, they found that BAX activation required PUMA. PUMA was found to be regulated by p53, a tumor suppressor protein that can induce apoptosis, a process also described in other studies(136,137). Unlike in human hepatoma cells, BID was not found to be upregulated in HCT116 cells(138).

Another pathway that could be involved in proteasome inhibitors inducing their effects is the JNK pathway. In multiple myeloma, Btz induced c-Jun upregulation(139). Upregulation of c-Jun expression initiates caspase activation and causes growth inhibition of multiple myeloma cells and ultimately induces apoptosis(139). C-Jun is one of the main substrates of JNK, and JNKs function to phosphorylate and activate c-Jun, a transcription factor(140,141). PIs have been suggested to require JNK1 and protein synthesis to rapidly induce apoptosis(142). The JNK pathway could potentially be activated by proteasome inhibition through several mechanisms that include interactions between p53 and MDM2(143), negative regulation through NF-κB(144), and ROS activation of the MAPK pathway, where ROS oxidizes the cysteine residues of stress kinases, including the MAPK pathway(145).

**Potential Therapeutic relevance of translating PIs to TNBC**

Our goal for this project was to characterize the mechanisms by which proteasome inhibitors induce apoptosis in triple-negative breast cancer. Triple-negative breast cancer is an aggressive subtype of breast cancer that is characterized by a lack of estrogen receptors, progesterone receptors, and HER2 protein expression(146), and has a lack of targeted treatment options,

except for a PD-1 inhibitor pembrolizumab (Keytruda) combination in high-risk early-stage TNBC(147), and two antibody-drug conjugates(148). Pembrolizumab is a PD-1 inhibitor that binds to and inhibits PD-1, preventing PD-L1 from binding to it. PD-1 and PD-L1 are immune checkpoint proteins. The effectiveness of Keytruda in TNBC depends on tumor PD-L1 expression. Studies have found that PD-L1 expression frequency in TNBC patients ranges from 19% to 76.6%(149–153), suggesting that alternative treatment options are needed.

Lieberman's lab conducted a genome-wide siRNA screen to find genes that basal-like TNBC cells are dependent on(154). After identifying dependency genes, they were divided into functional groups, and the proteasome degradation group, specifically, contained all proteasome subunits, thereby connecting all the different groups together. Not only did the proteasome degradation functional group form the core module that linked to the other groups, but it was also the group with the most highly selective hits. They tried to translate the results of their siRNA screen to human breast cancer cell lines by using siRNA pools to target 15 dependency genes and found that most basal-like TNBC cell lines shared dependency on the proteasome(154). Given the prominence of the proteasome in dependency genes, the lab used Btz and Cfz and found that these proteasome inhibitors are selectively active against basal-like cell lines(154). Based on this, we first wanted to identify if the pathway inducing apoptosis was shared between multiple myeloma and triple-negative breast cancer. We observed a difference. Therefore, we investigated how proteasome inhibitors induce apoptosis in triple-negative breast cancer and how that varies from multiple myeloma.

## Chapter 2: Materials and Methods

### Cell Culture

MDA-MB-231 and MDA-MB-468 cells were obtained from ATCC. SUM149 cells were obtained from Asterand. MDA-MB-231 cells were cultured in DMEM/F-12 50:50 base media, with 5% fetal bovine serum (FBS). SUM-149 media was additionally supplemented with 1ug/ml hydrocortisone, 4.8ug/ml human recombinant insulin, 10mM HEPES (pH 7.3), and 4mM L-glutamine. MDA-MB-468 cells were cultured in DMEM media with 10% FBS. Multiple myeloma cells were cultured in RPMI-1640 media and supplemented with 10% FBS. All media, except for the media used for siRNA transfection experiments, were further supplemented with Penicillin Streptomycin solution (diluted to 1X), amphotericin-B (0.25ug/ml), and ciprofloxacin (0.2ug/ml). Cells were grown at 37°C in 5% $CO_2$.

### Viability and Activity Assays

Cell viability was measured using resazurin (Alamar Blue,) after treatment. Apoptosis was measured by flow-cytometry on BD Accuri C6 Plus flow-cytometer using CellEvent Caspase-3/7 Green Detection Reagent, and SYTOX cell viability dye (Thermo). Data was analyzed using BD CSampler Plus software. Caspase-3/7 activity was measured in cell extracts using Ac-DEVD-AMC as described by Britton et al(155).

**Inhibitors**

Btz and Cfz were acquired from LC Laboratories. JNK inhibitor VIII was obtained from Cayman Chemicals (Cat#15946). Salubrinal (Cat#HY-15486) was obtained from MedChemExpress.

**Western Blotting and Antibodies**

Cell pellets were frozen after harvesting. Frozen cell pellets were resuspended in whole cell lysis buffer (50mM Tris-HCl, 5mM $MgCl_2$, 1mM EDTA, 10% glycerol, 0.5% CHAPS, 1X PhosSTOP™ (Roche), incubated on ice for 10 minutes, and centrifuged at 20,000 x g for 15 min. 1X PhosSTOP™ is a mixture of phosphatase inhibitors that was added to prevent dephosphorylation of eIF2α in extracts. Protein concentration was quantified using Bradford assay from VWR (Cat# E530-1L), and 20 µg of total protein per sample was heated with LDS buffer from Thermo Fisher (Cat# NP0007). Samples were fractionated on Bis-Tris gels (Genscript) using MES electrophoresis buffer (Genscript) and transferred to either a 0.22 µM PSq PVDF membrane or a 0.45 µM FL PVDF membrane (Immobilon, ISEQ00010). Blots were blocked with either 5% non-fat milk for ECL imaging or intercept blocking buffer (LI-COR Cat#927-70001) for fluorescent imaging on a shaker at room temperature for one hour. Membranes were then incubated overnight at 4°C with primary antibodies, washed with TBST, and incubated with secondary antibodies for one hour at room temperature. They were then rewashed with TBST. Membranes were imaged on Azure c600, directly if using fluorescently labeled secondary antibodies (Table 1), or after incubation with Pierce SuperSignal West Femto Maximum Sensitivity Substrate if HRP-conjugated secondary antibodies were used. Information about antibodies is provided in Table X.

**Table 1. Key Resources Table**

| Antibody | Vendor | Dilution factor | ECL/Fluorescent imaging | Cat# |
|---|---|---|---|---|
| p-eIF2α | Cell Signaling | 1:1000 | Fluorescent | 3398S |
| eIF2α | Cell Signaling | 1:1000 | Fluorescent | 2103S |
| PARP | Cell Signaling | 1:1000 | Fluorescent | 9542S |
| Cleaved PARP | Cell Signaling | 1:1000 | Fluorescent | 32563S |
| ATF4 | Cell Signaling | 1:1000 | Fluorescent | 11815 |
| ATF3 | Cell Signaling | 1:1000 | Fluorescent/ECL | 33593S |
| NOXA | Cell Signaling | 1:1000 | Fluorescent/ECL | 14766S |
| p-c-jun | Cell Signaling | 1:1000 | Fluorescent | 9164S |
| c-jun | Cell Signaling | 1:1000 | Fluorescent | 2315 |
| CReP | Proteintech | 1:1000 | Fluorescent | 14634-1-AP |
| GADD34 | Proteintech | 1:1000 | Fluorescent | 10449-1-AP |
| K48-linkage specific polyubiquitin | Cell Signaling | 1:1000 | Fluorescent | 8081S |
| Puromycin | Millipore/Sigma | 1:10000 | Fluorescent/ECL | MABE343 |
| α-tubulin | Cell Signaling | 1:1000 | Fluorescent/ECL | 3873S |
| β-actin | Cell Signaling | 1:1000 | Fluorescent/ECL | 3700S |
| GAPDH | Cell Signaling | 1:1000 | Fluorescent/ECL | 2118S |
| HRP-linked Horse anti-mouse secondary AB | Cell Signaling | 1:1000 | | 7076P2 |

| | | | | |
|---|---|---|---|---|
| HRP-linked Goat anti-rabbit secondary AB | Cell Signaling | 1:1000 | | 7074P2 |
| Alexa Fluor 647 Goat anti-rabbit secondary AB | Invitrogen | 1:3500 | | A21245 |
| IRDye 800, Goat anti-mouse | LI-COR | 1:3500 | | 926-32210 |

**siRNA Transfections**

CReP, C-myc, ATF4, ATF3, and GADD34 siRNA were purchased from Horizon Discovery. A set of 4 siRNAs was ordered for each gene, and the two that caused the best knockdowns were used for further studies. The transfections used DharmaFECT 1 Transfection Reagent. The On-TARGETplus Non-targeting siRNA #1 was used as the control siRNA in siRNA experiments. Additional ATF3 and NOXA siRNAs were ordered from Thermo Fisher. SiRNA complexes were stored at -20°C in 20μM stocks. Cells were plated at a density of 25-30% the day before transfection. As suggested by Horizon Discovery, the transfection solution was made in two tubes. Tube 1 contained siRNA (final concentration of 25nM) and Opti-MEM Reduced Serum Medium (Gibco Cat# 31985-070). Tube 2 contained DharmaFECT transfection reagent 1 (3% of Tube 2's volume) and Opti-MEM Reduced Serum Medium. The transfection reagent used was optimized from the Horizon Discovery protocol. After preparing Tubes 1 and 2, they were incubated at room temperature for 5 minutes. Tubes 1 and 2 were carefully mixed by pipetting and then incubated at room temperature for 20 minutes. Finally, antibiotic-free full growth medium (80% of the final volume) was added to the transfection solution before it was added to

the cells. Cells were cultured with siRNA for 72 hours before treatments. Media was then removed, and fresh media was added the night before treatments.

**Treatments**

Cells were plated at a density of 60-70% the day before treatment. Cells are pulse-treated with proteasome inhibitors for one hour. Following pulse treatment, the media containing PI was removed, and fresh media was added. Cells were harvested at the given time point.

When treating cells with a combination of Salubrinal and proteasome inhibitors, we pre-treated cells with Salubrinal for one hour before PI treatment. Following the pre-treatment, PI was added for one hour. After treating cells with PI for one hour, the media containing PI and Salubrinal was removed, and fresh media containing Salubrinal was added to the cells. Cells were then harvested at the given time points. For treatments where cells were treated with the subtoxic dose of cycloheximide for 18 hours before being pulse-treated with PI, we first had to determine the dose at which cycloheximide was subtoxic, while also reducing protein synthesis.

We measured protein synthesis by using puromycin incorporation. Puromycin (2.5 μg/ml) was added before cell harvest. The puromycin incubation time was varied for each cell line and had to be optimized for each cell line.

We used flow cytometry to measure apoptosis to identify the dose at which cycloheximide was subtoxic to each cell line. We then used puromycin incorporation to verify that this concentration inhibits protein synthesis. To determine the effect of cycloheximide on sensitivity to proteasome inhibitors, cells were pretreated with cycloheximide for 18 hours, pulse-treated with PI for one hour, incubated in the media (with or without CHX), and then harvested at the given time point.

**Quantification of blots**

Band intensities on western blot membranes were quantified using Image Studio Lite. Western blot quantification accounted for the loading control. Phosphorylation blots measured phosphorylated protein expression divided by total protein expression. In addition to Western blots, we also used dot blots to measure protein expression via puromycin incorporation. For dot blots, we had 5 technical replicates per biological replicate. We used the average of the 5 technical replicates when measuring quantification.

**Statistics**

Statistical analysis was conducted in GraphPad Prism.

## Chapter 3: Dephosphorylation of eIF2α sensitizes TNBC cells to proteasome inhibitors


### Abstract

It has been shown that protein load plays a key role in regulating PI-induced apoptosis in MM cells. While all cancers have a higher protein load than most normal cells, protein load has not been implicated in TNBC response to PIs. Protein load can be regulated by protein synthesis and protein breakdown. To investigate whether the regulator of protein synthesis, eIF2α, contributes to protein load in response to PIs in TNBC, we assessed its phosphorylation status and examined whether its phosphorylation state is regulated by its phosphatases. We found that both of eIF2α's phosphatases, CReP and GADD34, were upregulated in response to PI, though this increase may be due to increased half-life. The increase in eIF2α phosphatases did play a role in PI-induced apoptosis, though not by regulating protein synthesis. This suggests that CReP and GADD34 play a novel eIF2α-independent role in mediating PI-induced apoptosis in TNBC.


### Introduction

Triple-negative breast cancer (TNBC) is an aggressive form of breast cancer associated with the worst prognosis of any breast cancer subtype. The majority of triple-negative breast cancers are typically found to have an epithelial progenitor (basal-like) phenotype. Lieberman's lab conducted a genome-wide siRNA screen to find genes that basal-like TNBC cells are dependent on(154). After identifying dependency genes, they were divided into functional groups, and the proteasome degradation group, specifically, contained all proteasome subunits, thereby connecting all the different groups together. Not only did the proteasome degradation functional group form the core module that linked to the other groups, but it was also the group with the

most highly selective hits. They tried to translate the results of their siRNA screen to human breast cancer cell lines by using siRNA pools to target 15 dependency genes and found that most basal-like TNBC cell lines shared dependency on the proteasome. In patient breast cancer samples, dependency gene expression correlated with poor prognosis. Given the prominence of the proteasome in dependency genes, the lab used Btz and Cfz and found that these proteasome inhibitors are selectively active against basal-like cell lines. Furthermore, basal-like T-ICs (Tumor-initiating cells/cancer stem cells) are sensitive to proteasome inhibitors. T-ICs are thought to be responsible for metastasis and resistance to chemotherapy, in addition to tumor initiation(154). Notably, proteasome inhibition induced apoptosis by promoting NOXA accumulation, a result also observed in multiple myeloma cells, a disease state for which proteasome inhibitors are currently approved. In addition to the work found by Lieberman's lab, our lab also found that triple-negative breast cancer cells are sensitive to proteasome inhibitors(37). We compared the sensitivity to proteasome inhibitors of several TNBC and multiple myeloma (MM) cell lines and found that TNBC and MM cell lines had IC50 values in a comparable range(37). This suggests that TNBC cells would be a potential therapeutic target for proteasome inhibitors. However, multiple myeloma cells produce antibodies, which play a key role in sensitivity to proteasome inhibitors. Contrarily, TNBC cells do not produce antibodies, suggesting that something else is regulating their sensitivity to proteasome inhibitors. Given evidence that PIs are effective in TNBC cells, we sought to identify the mechanism by which proteasome inhibitors induce apoptosis in TNBC cells.

In multiple myeloma, the canonical mechanism by which proteasome inhibitors are thought to induce apoptosis is through a build-up of proteins within the ER, which causes ER stress and

activates the unfolded protein response (UPR). The UPR consists of 3 arms: IRE1α, PERK, and ATF6(156). Aberrant UPR signaling has been found in TNBC cells, especially the activity of IRE1α and PERK(157). The PERK arm of the UPR is activated in response to proteasome inhibitors, which causes the phosphorylation of eIF2α. eIF2α, along with the mammalian target of rapamycin (mTOR), is responsible for the regulation of protein synthesis(158,159). Cells regulate protein homeostasis through the phosphorylation of eIF2α. When eIF2α is phosphorylated, it inhibits global protein synthesis while upregulating the translation of specific transcription factors, such as ATF4(12,13). ATF4 upregulates ATF3(14), which can induce NOXA transcription. NOXA is a pro-apoptotic BCL-2 protein that binds to and inhibits MCL1 (which normally acts to sequester apoptosis effectors, BAX and BAK). NOXA binding to MCL1 frees BAX and BAK, which ultimately go on to disrupt the mitochondrial outer membrane and induce apoptosis(15). This is the mechanism by which PIs are thought to induce apoptosis in MM cells.

In addition to PERK, eIF2α is phosphorylated by PKR, GCN2, and HRI(101). PERK is activated by ER stress (UPR) but can also be activated by hypoxia(102). PKR is activated in response to viral infection, and GCN2 is activated in response to glucose starvation, amino acid starvation, and UV light. HRI is activated in response to heme deficiency, oxidative stress, and accumulation of unfolded proteins in the cytosol(103). The regulation of eIF2α phosphorylation through PERK, PKR, GCN2, and HRI, and the subsequent activation of ATF4, is part of the integrated stress response (ISR)(104). Other facts regarding eIF2α phosphorylation are discussed in Chapter 1.

As stated earlier, the phosphorylation of eIF2α decreases global protein synthesis, thereby reducing the protein level and alleviating the load on the proteasome. While the phosphorylation of eIF2α is carried out by eIF2α kinases, the dephosphorylation of eIF2α is carried out by the protein phosphatase 1 (PP1) complex. More than 200 phosphatases share the PP1 as a catalytic subunit to form complexes that target and dephosphorylate specific proteins. The regulatory subunits of the complexes restrict PP1's specificity. The regulatory/catalytic subunits involved in the dephosphorylation of eIF2α are GADD34 (inducible, encoded by the PPP1R15A gene) and the constitutive repressor of eIF2α phosphorylation (CReP, encoded by the PPP1R15B gene). Either one of them can form a complex with PP1 to dephosphorylate eIF2α. The dephosphorylation of eIF2α would reduce the ability to decrease global protein synthesis and alleviate ER and other forms of proteotoxic stress. This would place a higher burden on the proteasome. If proteasome inhibitors dephosphorylate eIF2α or prevent its phosphorylation, they would increase the proteasome's workload while reducing its capacity, exacerbating proteotoxic stress in cells.

Given the evidence in the literature, in addition to our lab's prior results, we aimed to identify the mechanism by which proteasome inhibitors induce apoptosis in TNBC cells and whether it is the same mechanism observed in multiple myeloma. If eIF2α is phosphorylated in response to proteasome inhibitors, we would investigate which kinase is responsible for the phosphorylation. If eIF2α is not phosphorylated or dephosphorylated, we would aim to identify which eIF2α phosphatase is responsible and what regulates its activity. Additionally, if eIF2α is not phosphorylated, then the pathway downstream that leads to apoptosis would be altered. In this case, we would also investigate the pathway by which apoptosis is induced.

## Results

### Proteasome inhibitors do not induce robust phosphorylation of eIF2α in triple-negative breast cancer cell lines.

To determine effects of proteasome inhibitors on the phosphorylation status of eIf2α, we pulse-treated cells for one hour with proteasome inhibitors to better mimic clinical exposure to these agents than continuous treatment usually used in the in vitro studies. Clinical studies have shown that Btz and Cfz reach peak plasma concentration within one hour after a bolus dosing(79,160), after which they are rapidly cleared.

Our lab initially tested the sensitivity of several triple-negative breast cancer cell lines and found a similar $IC_{50}$ distribution between multiple myeloma and triple-negative breast cancer cell lines(37). We use a mitochondrial dye conversion assay to confirm these results here (Figure 3.1).

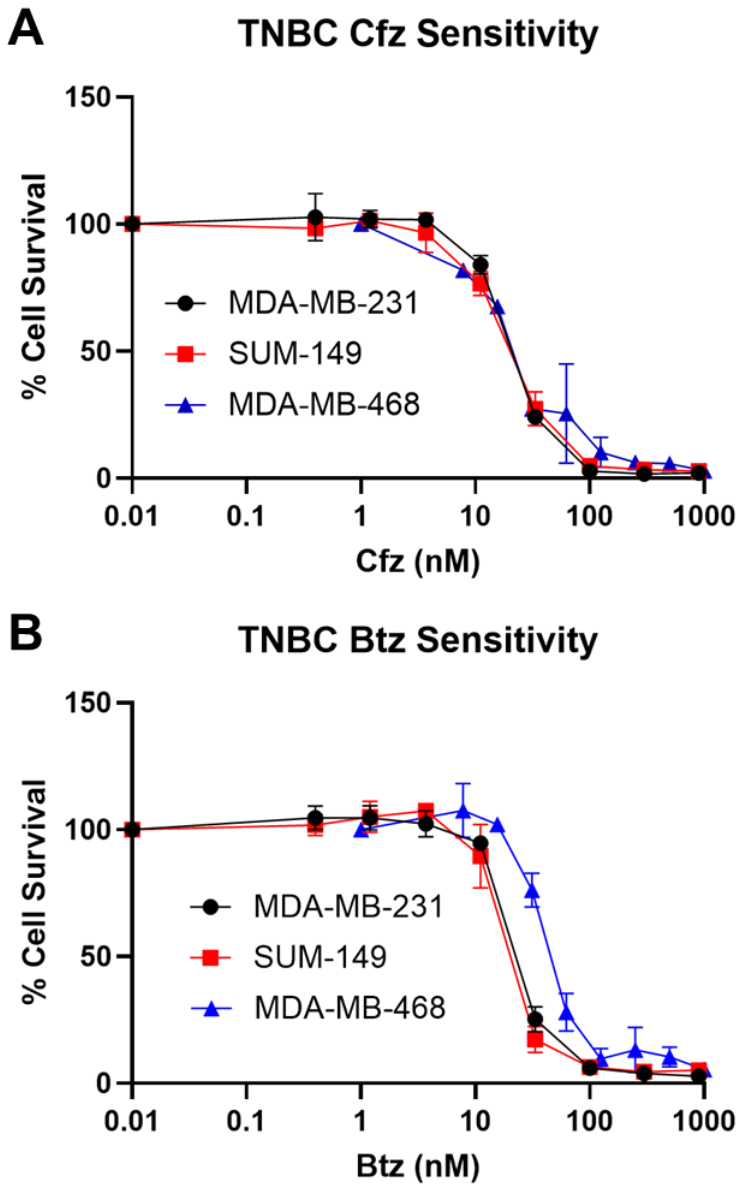


**Figure 3.1 Panel of TNBC cell lines sensitive to Cfz and Btz**

A. TNBC cells were pulse-treated with Cfz for one hour with the indicated dose, and cell survival was measured 48 hours later using the Alamar Blue mitochondrial dye conversion assay (n=2).
B. TNBC cells were pulse-treated with Btz for one hour with the indicated dose, and cell survival was measured 48 hours later with Alamar Blue (n=2).

A comparison of our TNBC cell lines' $IC_{50}$ values with the $IC_{50}$ for btz in MM cell lines is shown in Table below. The MM cell line data is from a previously published work from our lab(161).

**Table 2. Btz $IC_{50}$ values of MM and TNBC cell lines.**

| Cell line | $IC_{50}$ in nM (1hour pulse treatment) |
|---|---|
| **NCI-H929** | 28 |
| **MM1.R** | 68 |
| **MM1.S** | 82 |
| **KMS-18** | 170 |
| **RPMI 8226** | 208 |
| **LR5** | 346 |
| **KMS-12-BM** | 504 |
| **MDA-MB-231** | 22.6 |
| **MDA-MB-468** | 40.8 |
| **SUM 149** | 18.8 |

To determine the eIF2α phosphorylation status, cells were collected at various time points after treatment, and phosphorylated eIF2α levels were measured using Western blots. Thapsigargin was used as a positive control, as it is a known ER stressor that induces the phosphorylation of eIF2α(162,163) (Figure 3.2A).

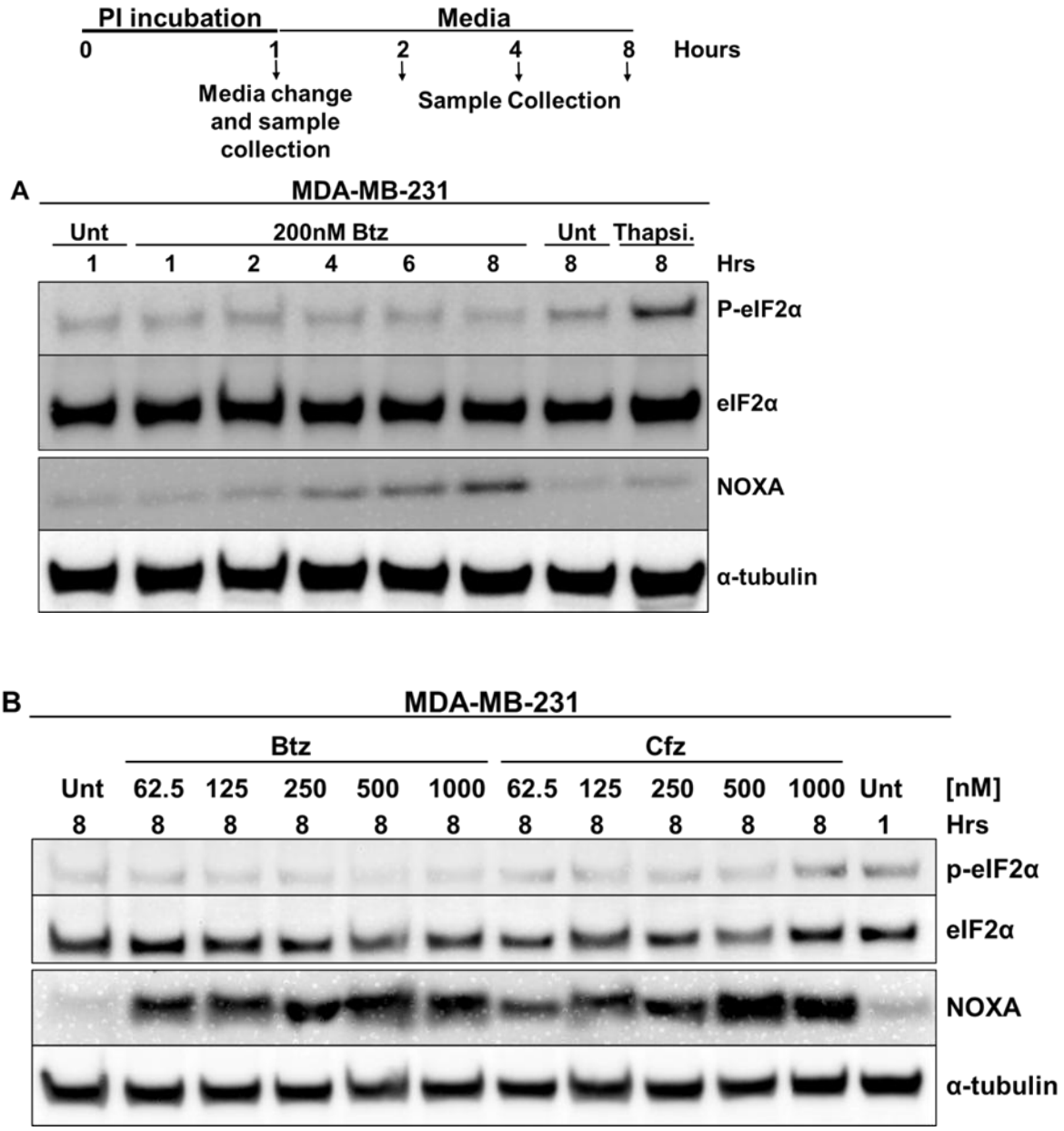
PI incubation
Media
0
1
2
4
8
Hours
Media change and sample collection
Sample Collection
A
MDA-MB-231
Unt
200nM Btz
Unt
Thapsi.
1
1
2
4
6
8
8
8
Hrs
P-eIF2α
eIF2α
NOXA
α-tubulin
B
MDA-MB-231
Btz
Cfz
Unt
62.5
125
250
500
1000
62.5
125
250
500
1000
Unt
[nM]
8
8
8
8
8
8
8
8
8
8
8
1
Hrs
p-eIF2α
eIF2α
NOXA
α-tubulin

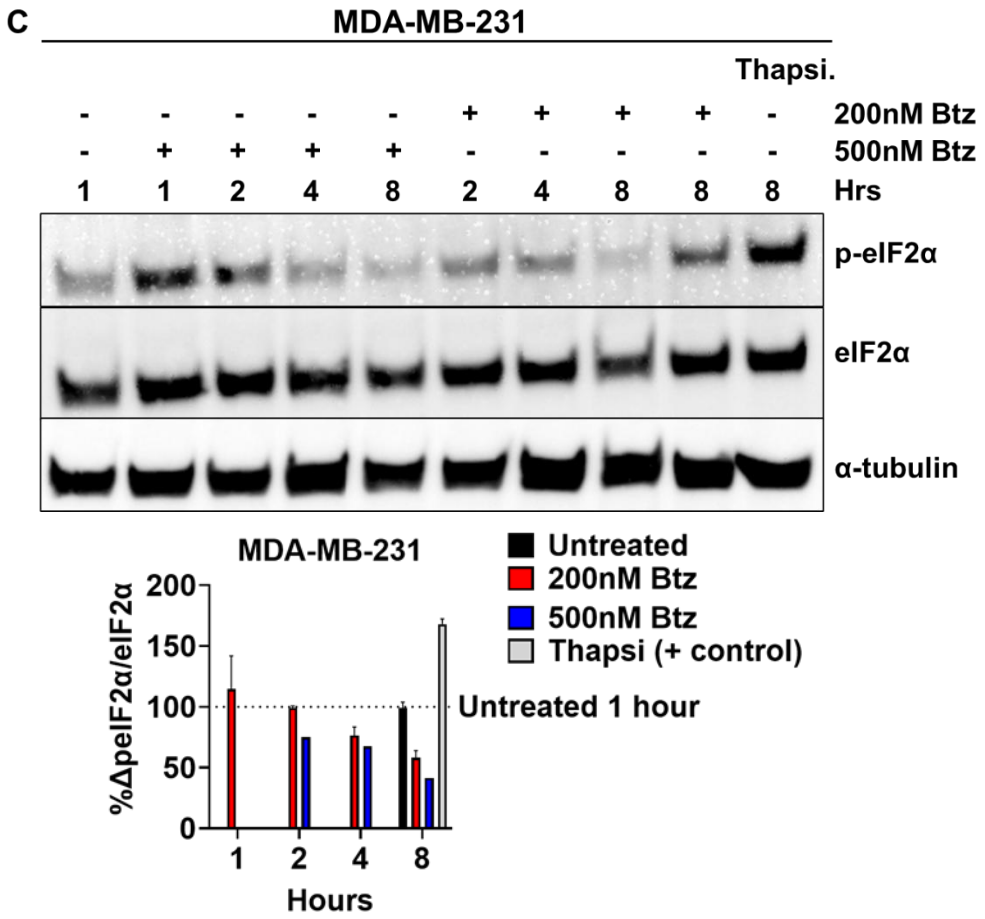


**Figure 3.2 Proteasome inhibition causes the dephosphorylation of eIF2α.**

A. MDA-MB-231 cells were pulse-treated with 200nM Btz for one hour before being collected at the indicated time points. Thapsigargin was used as a positive control for eIF2α phosphorylation.
B. MDA-MB-231 cells were pulse-treated with various doses of Btz or Cfz for one hour and collected 8 hours from the start of treatments.
C. MDA-MB-231 cells were pulse-treated with 200nM Btz or 500nM Btz and collected at the indicated time points. Quantified values are shown on the graph (N=2). Values have been standardized using α-tubulin values.

All samples were analyzed by Western blot, and quantification of blots is represented as bar graphs

We initially treated MDA-MB-231 cells with 200nM Btz, a cytotoxic concentration, for one hour (Figure 3.2A), changed the media, and collected the cells at the indicated time points (treatment scheme shown in Figure 3.2A). We observed no increase in eIF2α phosphorylation at different times varying from 1 to 8 hours after start of the treatment, while Thapsigargin induced a robust phosphorylation. We also probed the blot with antibodies to NOXA, a well-characterized effector of PI-induced apoptosis to prove that Btz did induce apoptosis in this experiment, and observed a time dependent NOXA accumulation, starting at 2 hours. No eIF2α phosphorylation was observed when cells were treated with a range of Btz concentrations at 8 hours (Figure 3.2B). Additionally, the same results were also observed in response to Cfz, another proteasome inhibitor (Figure 3.2B). Robust NOXA accumulation was observed at all concentrations of Btz and Cfz, showing that both PIs induced NOXA accumulation in these experiments. In response to 200nM, there was an initial increase in phosphorylated eIF2α one hour after treatment, though it returned to basal levels at 2 hours and decreased further at later time points (Figure 3.2C). Phosphorylated eIF2α was found to decrease as early as 2 hours from the start of treatment in response to 500nM Btz (Figure 3.2C). The quantification of the Western blot (Figure 3.2C) showed a decrease in eIF2α phosphorylation over time, in response to two different cytotoxic doses of Btz.

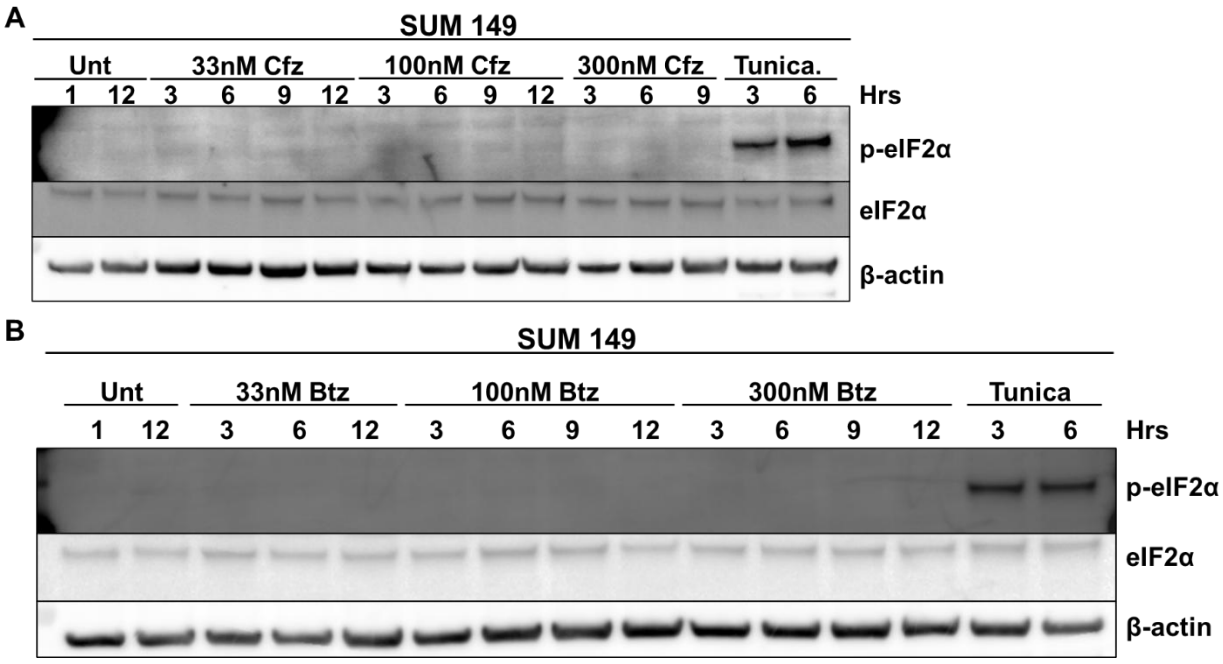


**Figure 3.3 PIs do not cause eIF2α phosphorylation in SUM149 cells**

A. SUM149 cells were pulse-treated with increasing concentrations of Cfz and collected at the indicated time points. 40μg/ml Tunicamycin was used as a positive control for eIF2α phosphorylation.
B. SUM149 cells were pulse-treated with increasing concentrations of Btz and collected at various time points. 40μg/ml Tunicamycin was used as a positive control for eIF2α phosphorylation.

All samples were analyzed by Western blot.

SUM149 cells were pulse-treated with various doses of Cfz, collected at increasing time points, and eIF2α phosphorylation was measured (Figure 3.3A). Tunicamycin was used as a positive control, as it is also a known ER stressor that results in eIF2α phosphorylation(164,165). While eIF2α phosphorylation was observed in response to tunicamycin at both time points, we did not observe phosphorylation in response to any dose of Cfz at any time point. Similar results were observed in response to various doses of Btz (Figure 3.3B).

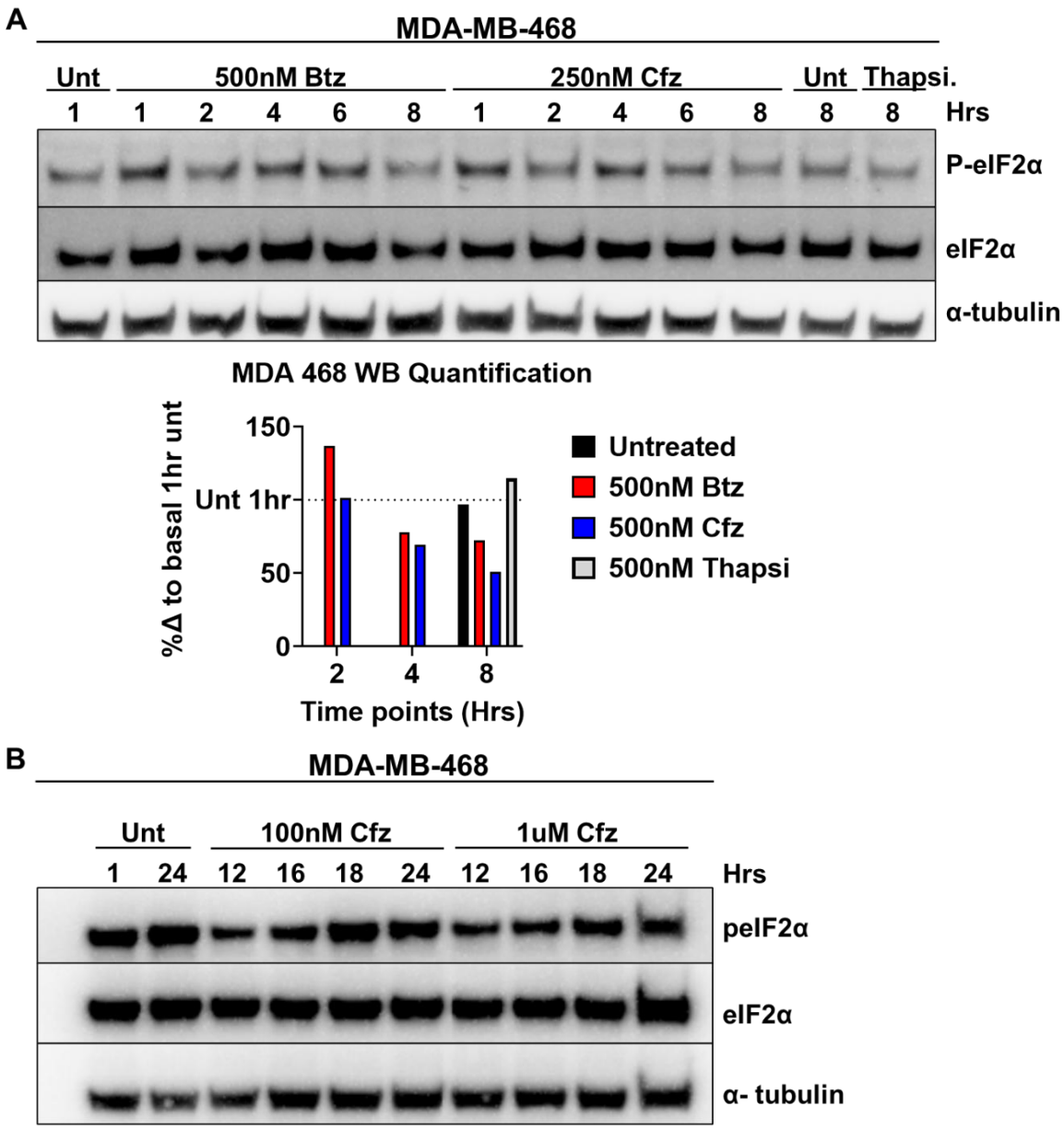


**Figure 3.4 Phosphorylation status of eIF2α in MDA-MB-468 cells in response to PIs**

A. MDA-MB-468 cells were pulse-treated with 500nM Btz or 250nM Cfz and collected at the indicated time points. The graph shows the quantified expression values. 200nM Thapsigargin was used as a positive control.

B. MDA-MB-468 cells were pulse-treated with 100nM or 1μM Cfz and collected at the indicated time points.

All samples were analyzed by Western blot.

MDA-MB-468 cells showed more variance in eIF2α phosphorylation early in response to proteasome inhibitors. An increase in eIF2α phosphorylation in response to Btz and Cfz was observed up to 2 hours (Figure 3.4A), before having a decrease at later time points.

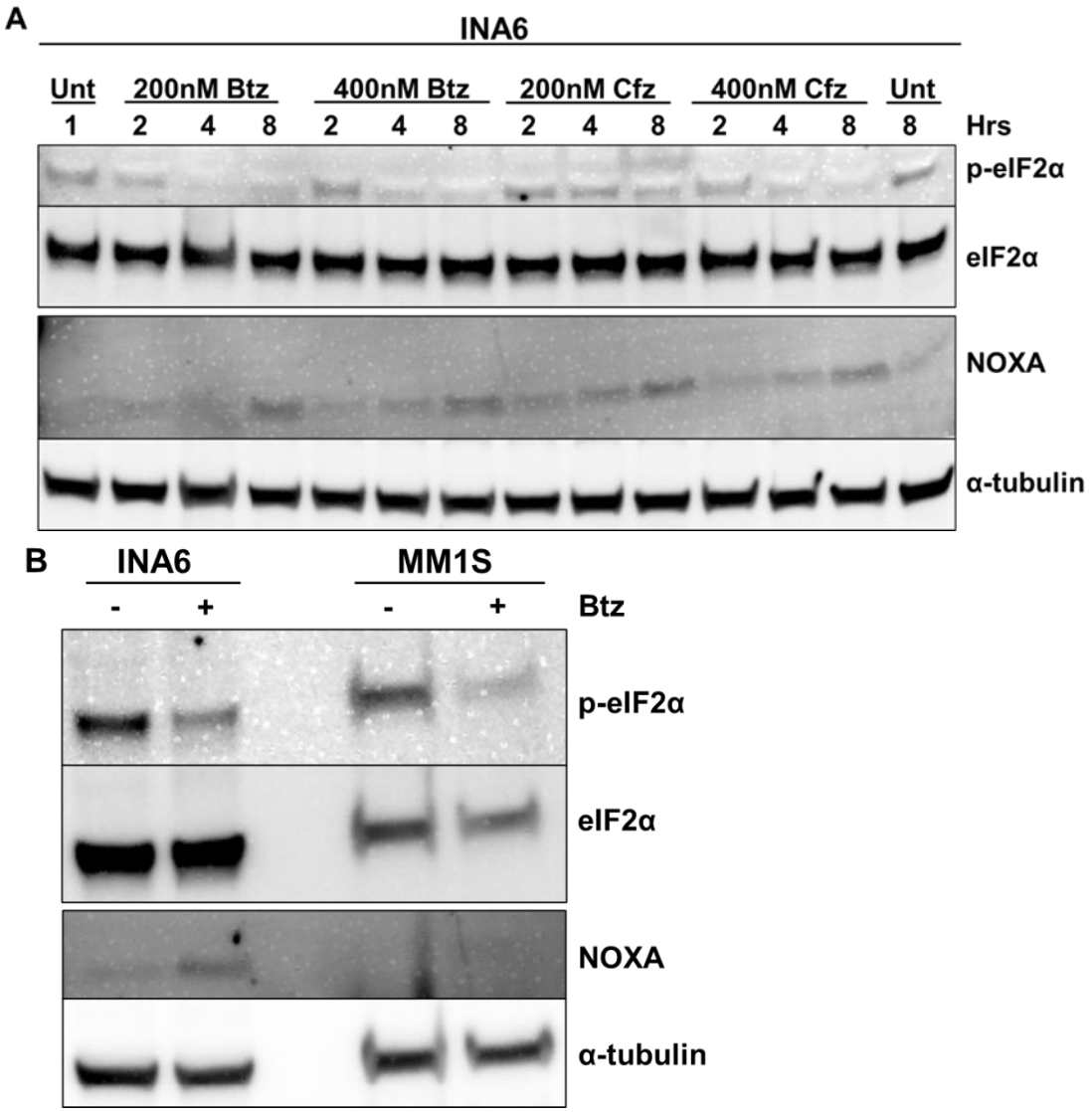


**Figure 3.5 eIF2α phosphorylation in multiple myeloma cell lines**

A. INA6- cells were pulse-treated with various doses of Btz or Cfz for one hour and collected at the indicated time points.
B. INA6 and MM.1S cells were treated with Btz 200nM for one hour and collected 8 hours from the start of treatment.

All samples were analyzed by Western blot.

Given the differences observed in the TNBC cell lines from what was expected based on multiple myeloma cells, we treated multiple myeloma cells with proteasome inhibitors and measured changes in eIF2α phosphorylation. Both lines had detectable levels of basal eIF2α phosphorylation. In response to proteasome inhibitors, we observed dephosphorylation of eIF2α in both INA6 cells and MM.1S cells (Figures 3.5A, B).

**Inhibition of protein synthesis rescues cells from proteasome inhibitor-induced apoptosis.**

The status of eIF2α phosphorylation in cells treated with proteasome inhibitors is inconsistent in the literature(105–109,111), with there being some evidence of eIF2α phosphorylation. We did not detect eIF2α phosphorylation, and in some cases, observed dephosphorylation in response to proteasome inhibitors. Such scenarios would not decrease protein synthesis, preventing cells from alleviating proteotoxic stress and placing a higher burden on the proteasome.

Before identifying the mechanism causing a lack of eIF2α phosphorylation in response to PI, we wanted to verify that a lack of eIF2α phosphorylation translated to a lack of reduction in protein synthesis. We used the puromycin incorporation assay to measure protein synthesis(166). Puromycin is a naturally occurring antibiotic that mimics tyrosyl-tRNA and gets incorporated into nascent protein chains, where it can be detected with a specific antibody. This results in premature termination of protein synthesis, resulting in proteins that are not fully formed. The rate of puromycin incorporation is proportional to the rate of protein synthesis. Therefore, the change in puromycin incorporation between different treatments and times can be used to study the change in the rate of protein synthesis.

Polypeptides, including those with puromycin incorporated, are constantly being synthesized and degraded. Eventually, the rate of synthesis and degradation reaches an equilibrium. We first needed to identify the puromycin incubation time point at which each cell line has increasing puromycin incorporation and has not yet reached equilibrium between synthesis and degradation. To do this, we treated MDA-MB-231, MDA-MB-468, and SUM149 cells with puromycin for 5, 10, 15, 20, 25, 30, 45, and 60 minutes. Puromycin incorporation was measured via western blotting using an anti-puromycin antibody. We imaged puromycin incorporation using western blotting and found that 20- 30 minutes of puromycin incubation was optimal for all three cell lines (MDA-MB-231 and SUM149 results are shown in Figure 3.6).

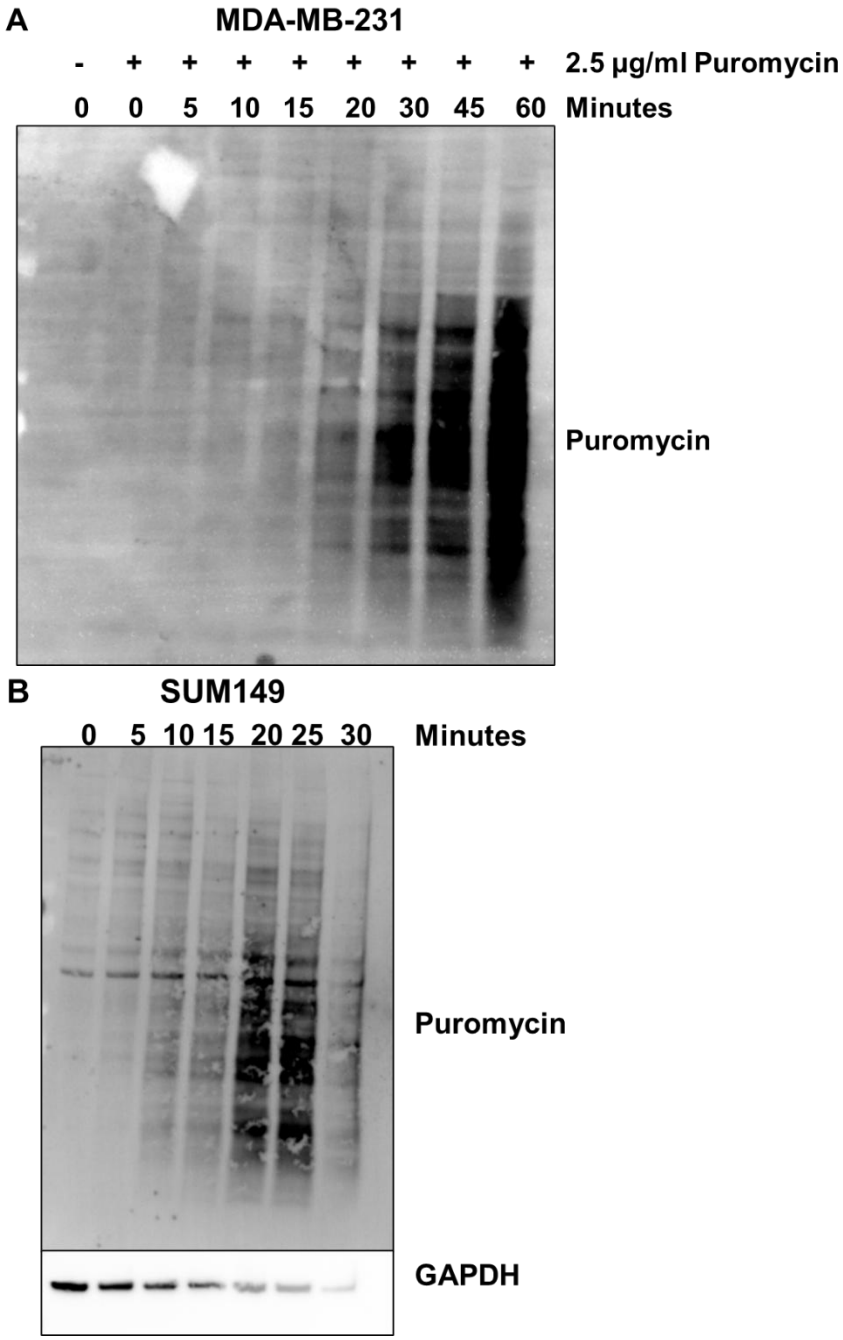


**Figure 3.6 Optimization of puromycin incorporation in TNBC cells**

A. MDA-MB-231 cells were treated with 2.5µg/ml puromycin and collected at the indicated time points.
B. SUM149 cells were treated with 2.5µg/ml puromycin and collected at the indicated time points.

After determining the puromycin incorporation time for each cell line, we treated all three cell lines with PIs and collected them at various time points after the start of treatment (Figure 3.7).

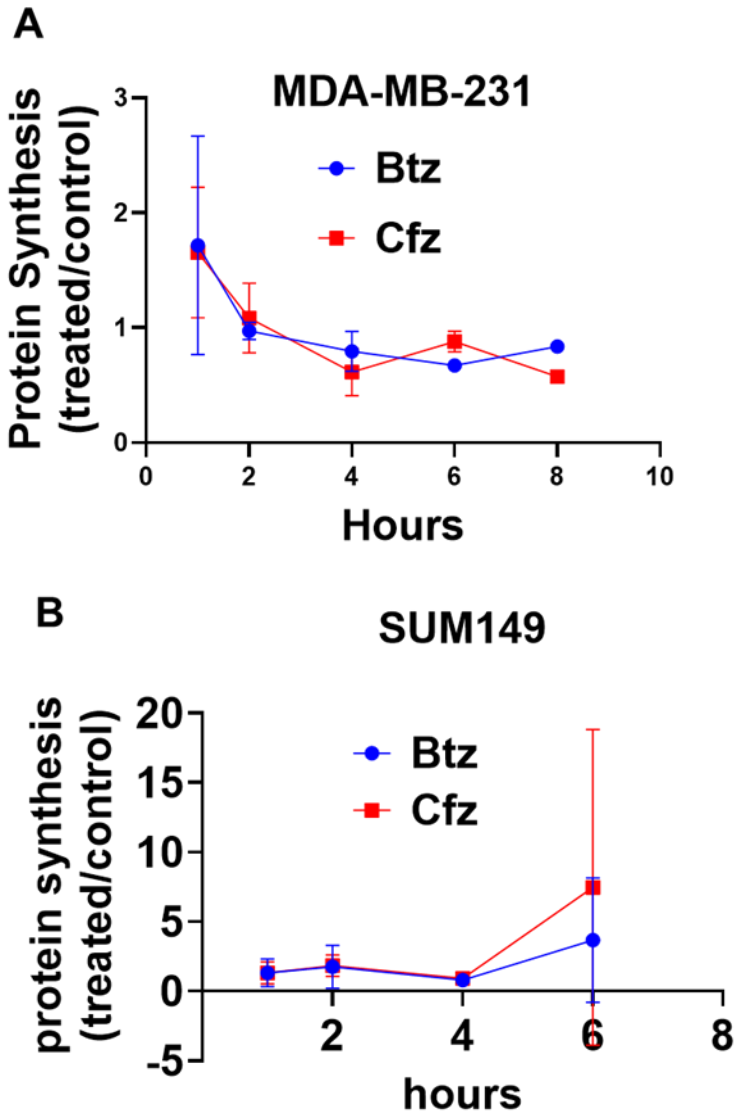


**Figure 3.7 Effect on protein synthesis in response to PIs time course**

MDA-MB-231 (A) or SUM149 (B) cells were pulse-treated with 300 nM Btz or Cfz for 1 hour. Puromycin (2.5 μg/ml and Btz (10 μM, to prevent degradation of puromycylated proteins) were added at the indicated time points. 20 minutes after puromycin addition, cell were harvested using in ice-cold PBS, supplement with CHX (50 μg/ml). Puromycin incorporation was measured by dot blots. Btz N=3 (A,B,C) biological replicates. Cfz N = 2 (A,B) biological replicates.

Quantification of data from experiments performed by other members of the laboratory.

For these experiments, where we studied effects on protein synthesis, we switched from using Western blots to dot blots. We did this because dot blots allow for protein expression to be measured more rapidly than western blotting, allow us to analyze many samples and technical replicates of each sample at the same time to verify the results, and allow us to quantify the results more easily(167,168).

In MDA-MB-231 cells, there was a decrease in protein synthesis in response to Btz and Cfz at two hours, though it stayed steady after that (Figure 3.7A). SUM149 did not show changes in protein synthesis in response to Btz and Cfz (Figure 3.7B). Given that MDA-MB-468 cells initially showed an increase in eIF2α phosphorylation before having dephosphorylation at 4 and 8 hours, we would expect there to be an initial decrease in protein synthesis in response to PIs, with an increase in protein synthesis being observed at 4 hours and later.

Next, we wanted to identify if this reaction was dependent on the PI dose. We did this by pulse-treating cells with various doses of Btz or Cfz for one hour and then collecting them 6 hours later.

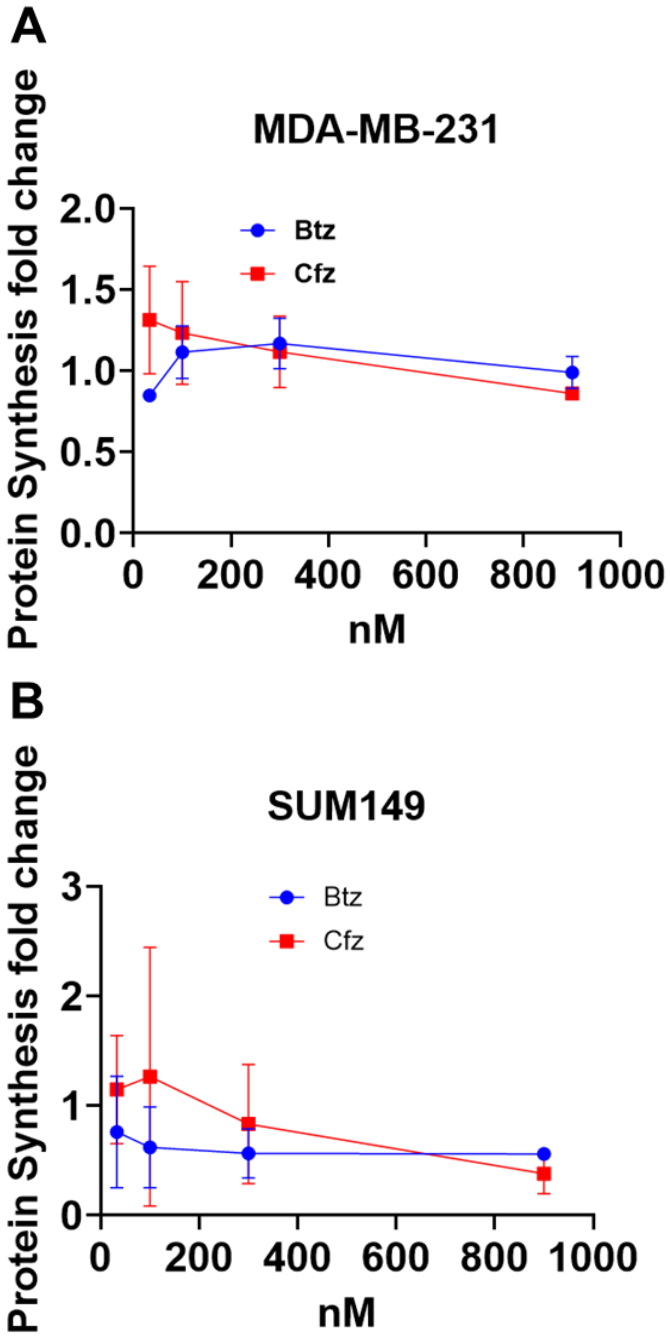


**Figure 3.8 Change in puromycin incorporation in response to Btz**

MDA-MB-231 (A) or SUM149 (B) cells were pulse-treated for 1 hour with increasing concentrations of Btz or Cfz and collected 6 hours from the start of treatments. Puromycin and Btz (10 μM) were added 20 minutes prior to collection. Puromycin incorporation was measured by dot blot. N=2 (A,B) biological replicates

Quantification of data from experiments performed by other members of the laboratory.

In response to Cfz and Btz, MDA-MB-231 cells did not downregulate protein synthesis at 6 hours (Figure 3.8A), compared with untreated levels, which correlated with a lack of eIF2α phosphorylation shown in Figure 3.2. SUM149 cells also did not significantly downregulate protein synthesis at lower concentrations (Figure 3.8B). This decrease at higher concentrations may be due to cells already inducing apoptotic pathways.

The results in Figure 3.8 largely supported the observations presented in Figures 3.2 and 3.3. We did not observe a significant decrease in protein synthesis in response to PIs in MDA-MB-231 and SUM149 cells, which correlated with the lack of eIF2α phosphorylation observed in those cell lines.

We established the lack of phosphorylation of eIF2α in our cell lines and a lack of decrease in protein synthesis in two of our cell lines. We next investigated the role that protein synthesis and the increased load on the proteasome play in inducing PI-dependent apoptosis. By inhibiting protein synthesis, we hypothesized that it would lower the load on the proteasome and thereby rescue cells from PI-induced apoptosis. To investigate the significance of protein load in inducing PI-dependent apoptosis, we inhibited protein synthesis using cycloheximide (CHX) and examined whether it rescued cells from PI-induced apoptosis. Since the production of nascent polypeptides accounts for a significant portion of the load on the proteasome, inhibiting the synthesis of nascent polypeptides with cycloheximide would reduce the load on the proteasome.

We first aimed to identify the time point at which the majority of cells were undergoing apoptosis. We treated cells with 500nM Cfz or 1μM Cfz for one hour, removed the drug-containing media, added fresh media, and collected the cells at 1, 6, 9, and 18 hours from the start of treatment. We measured apoptosis using two different caspase activity assays- flow cytometry caspase probe and enzymatic cleavage of fluorescent caspase substrates. By using the caspase-3/7 Green detection reagent and SYTOX Red dead cells stain, we were able to distinguish between live cells undergoing apoptosis and dead cells that had already undergone apoptosis. We found that 18 hours after proteasome inhibition, cells were undergoing apoptosis or had already died (Figure 3.9A). To verify that the caspase activity observed at 18 hours was not due to the use of high doses of Cfz, we treated cells with various doses of Cfz, starting with 100nM, and measured apoptosis using flow cytometry with a Caspase-3/7 detection dye (Figure 3.9B). We found apoptosis occurring at all doses of Cfz.

Therefore, we wanted to see if we could rescue apoptosis at 18 hours by inhibiting protein synthesis.

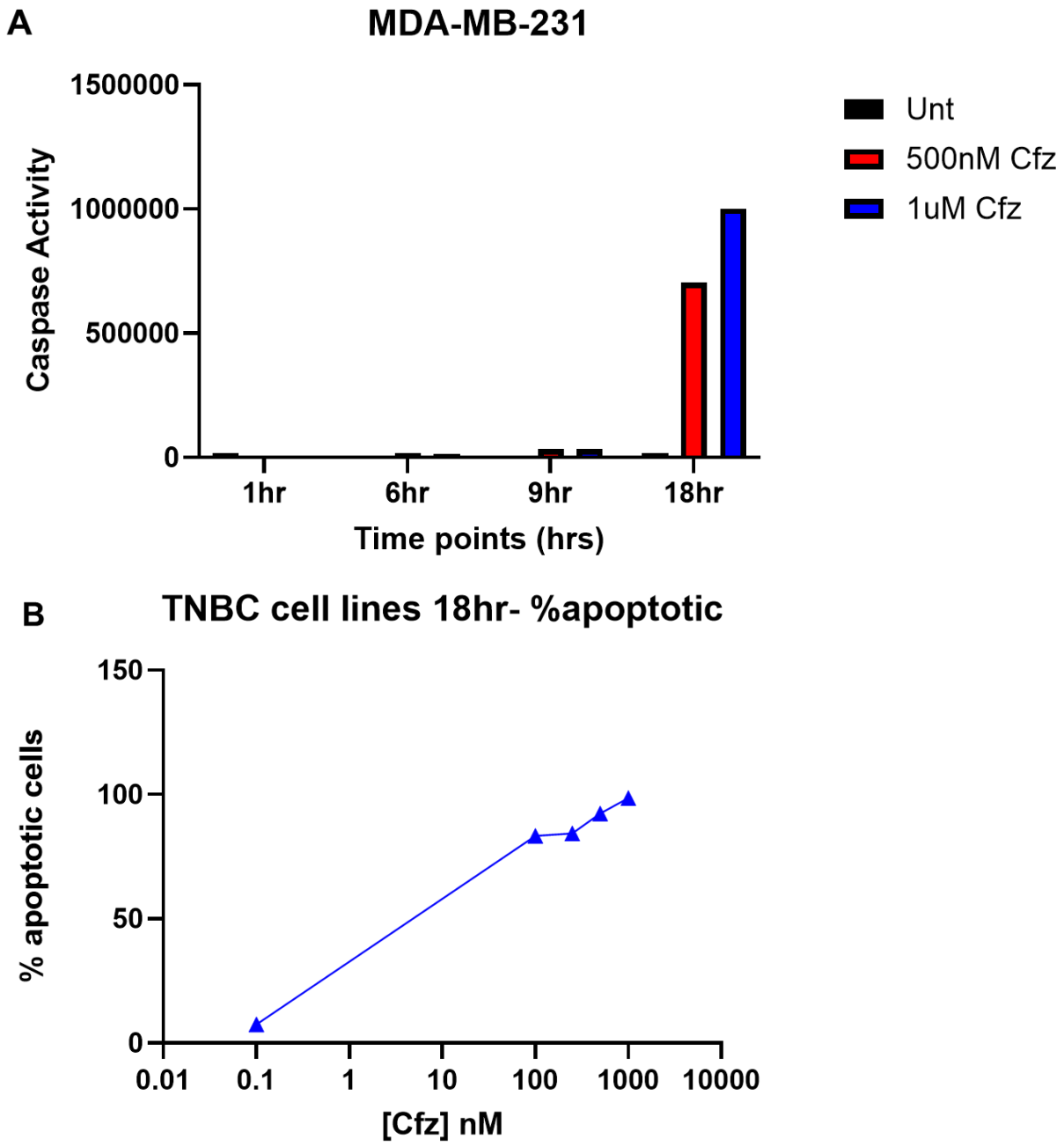


**Figure 3.9 Apoptosis occurring at 18 hours in MDA-MB-231 cells**

A. MDA-MB-231 cells were treated with 500nM Cfz or 1μM Cfz for one hour, and cells were collected at the indicated time points. The figure shows the results of the caspase activity assay measurement.
B. MDA-MB-231 cells were treated with increasing doses of Cfz for one hour and collected at 18 hours from the start of the treatments. Apoptosis was measured using flow cytometry.
C. MDA-MB-231 cells were treated with increasing doses of Cfz for one hour and collected at 18 hours from the start of the treatments. Apoptosis was measured using flow cytometry.

We used cycloheximide (CHX) to inhibit protein synthesis. Cycloheximide, on its own, is toxic to cells; therefore, we first needed to determine a cycloheximide dose range that was not toxic to the cells after 18 hours of incubation but still inhibited protein synthesis. We treated MDA-MB-231 and MDA-MB-468 cells with a range of 0.2μg/ml to 20μg/ml of CHX for 18 hours continuously and measured apoptosis using a caspase probe via flow cytometry. We determined that 0.8, 0.4, and 0.2 μg/ml of CHX were subtoxic for MDA-MB-231 cells (Figure 3.10A), and 10, 5, 1, and 0.5μg/ml of CHX were subtoxic for MDA-MB-468 cells (Figure 3.10B). To verify that the subtoxic doses were inhibiting protein synthesis, we treated cells with the subtoxic doses of CHX for 18 hours and added 2.5μg/ml puromycin 30 minutes prior to collecting. We then measured puromycin incorporation using western blotting. We found that the lowest dose of CHX that reduced/inhibited protein synthesis in MDA-MB-231 cells is 0.4μg/ml, and used 5μg/ml CHX for MDA-MB-468 cells, as it resulted in minimal protein synthesis and maintained the percentage of apoptotic cells below 20% (Figure 3.10C).

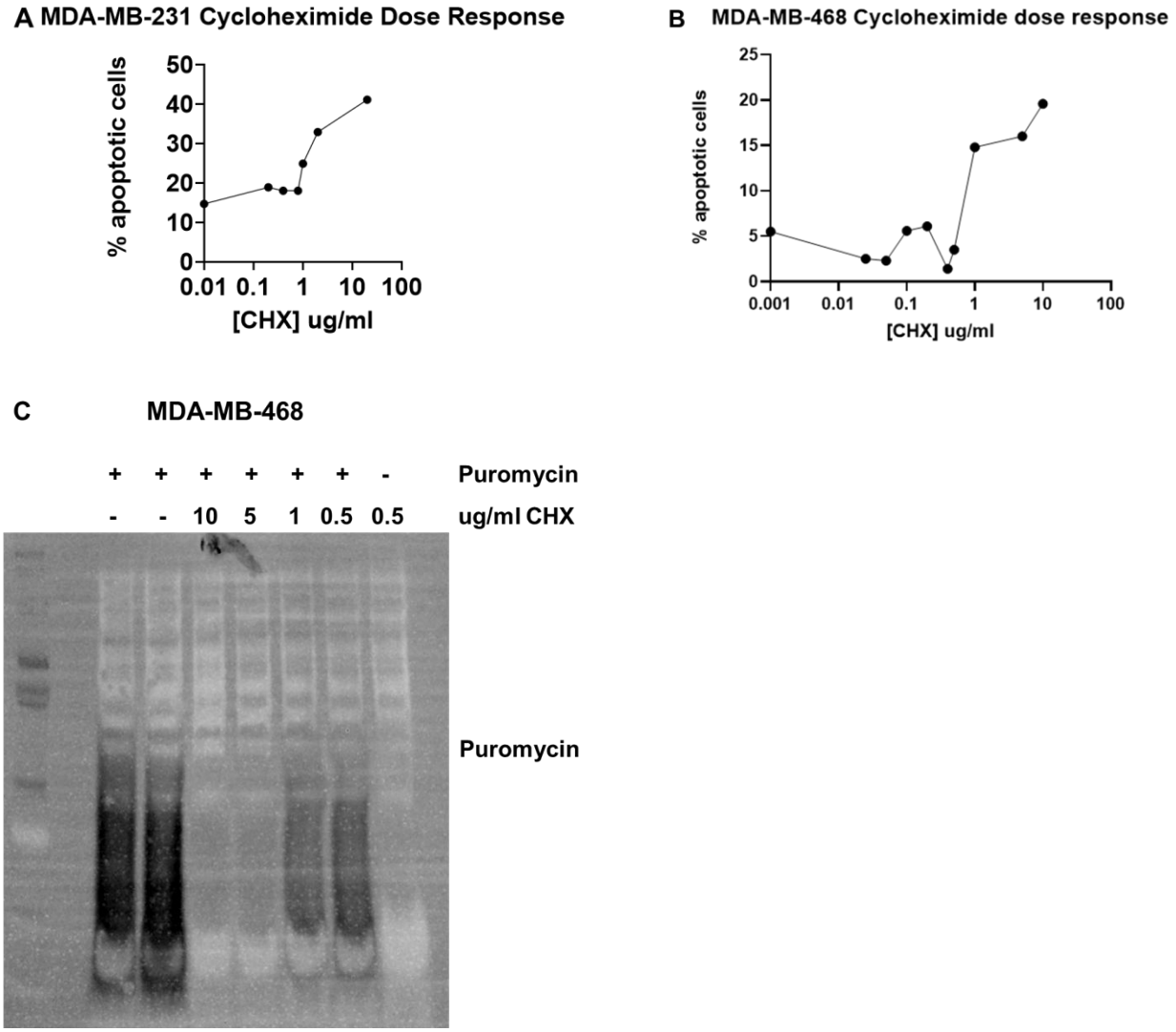


**Figure 3.10 Inhibiting protein synthesis without inducing cell toxicity with cycloheximide**

A. MDA-MB-231 cells were treated with varying doses of cycloheximide for 18 hours. Apoptosis was measured via flow cytometry using caspase-3/7 Green Detection reagent and SYTOX Red dead cells stain.
B. MDA-MB-468 cells were treated with varying doses of cycloheximide for 18 hours. Apoptosis was measured via flow cytometry using caspase-3/7 Green Detection reagent and SYTOX Red dead cells stain.
C. MDA-MB-468 cells were treated with the indicated doses of CHX for 18 hours. Puromycin was added 30 minutes prior to collection.

After establishing the condition at which CHX is subtoxic and reduces protein synthesis, we next tested whether CHX reduces PI-induced apoptosis. We pulse-treated cells with proteasome inhibitors for 1 hour and then incubated them with the subtoxic dose of cycloheximide for 18 hours. MDA-MB-231 cells were treated with 0.4μg/ml of CHX, and MDA-MB-468 cells were treated with 5μg/ml of CHX. We measured apoptosis using the enzymatic caspase activity assay and flow cytometry caspase detection reagent.

MDA-MB-231 cells had a significant increase in caspase activity in response to Btz and Cfz alone (Figure 3.11A). However, in combination with CHX, PI did not induce caspase activity. Similar results were observed when measuring for apoptosis using flow cytometry in MDA-MB-231 cells (Figure 3.11B). In MDA-MB-468 cells, Cfz alone significantly increased caspase activity (Figure 3.11C). This reduction was observed when Cfz was combined with CHX, although the reduction was not as significant as that observed in MDA-MB-231 cells. Similar results were observed using a caspase detection reagent through flow cytometry (Figure 3.11D).

This data suggested that protein synthesis and, thereby, the load on the proteasome played a significant role in PI-induced apoptosis. Based on our observations, we hypothesized that because eIF2α was not being phosphorylated in response to PI, there was no decrease in protein synthesis to reduce the load on the proteasome, and that was how PI-induced apoptosis occurs. Given the role of the UPR and what is known in the literature, we had expected to observe eIF2α phosphorylation. Given the lack of eIF2α phosphorylation, we expected the eIF2α phosphatases, rather than the eIF2α kinases, to play a role in mediating PI-induced apoptosis. Especially given

our observation of eIF2α dephosphorylation occurring in MDA-MB-231 cells (Figure 3.2) and later time points of MDA-MB-468 cells (Figure 3.4).

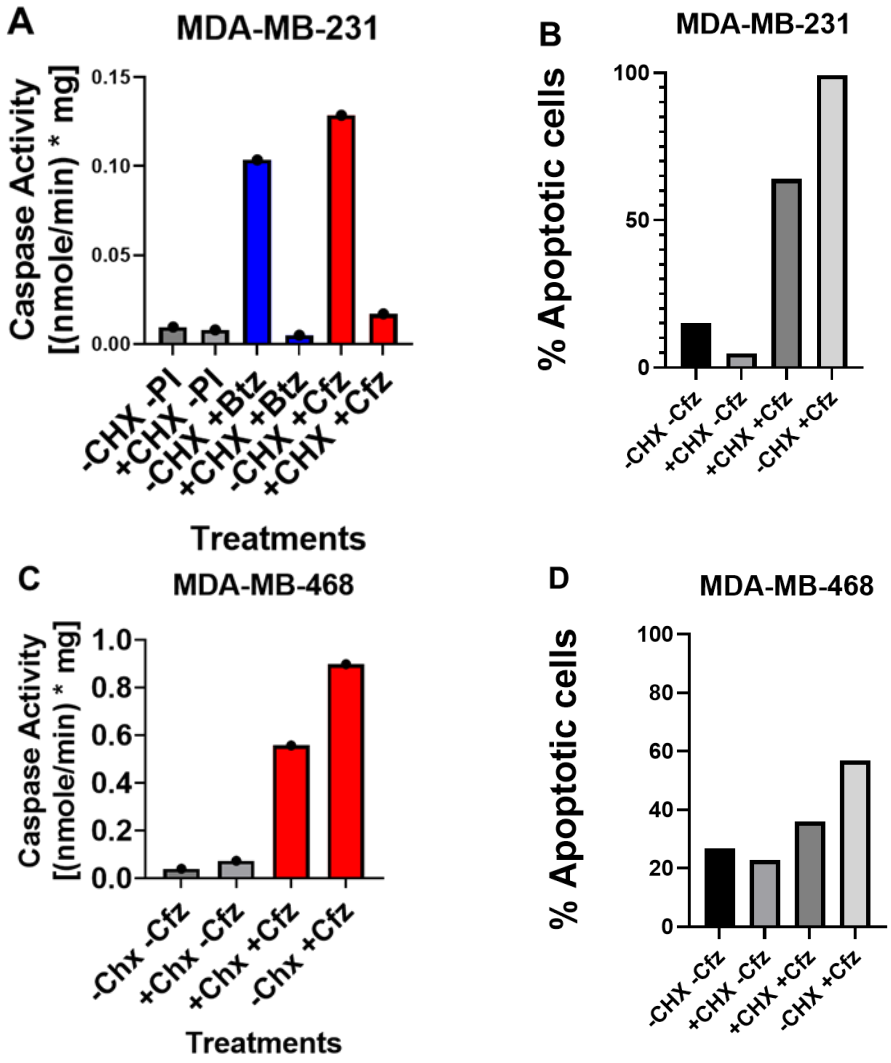


**Figure 3.11 Inhibiting protein synthesis rescues cells from apoptosis.**

A. MDA-MB-231 cells were treated with 0.4µg/ml CHX and Btz/Cfz. n= 1. Caspase activity was measured using caspase activity assay.
B. MDA-MB-231 cells were treated with 0.4µg/ml CHX and Cfz. n= 1. Apoptosis was measured via flow cytometry using caspase-3/7 Green Detection reagent and SYTOX Red dead cells stain.
C. MDA-MB-468 cells were treated with 5µg/ml CHX and Btz/Cfz. n=1. Caspase activity was measured using caspase activity assay.
D. MDA-MB-468 cells were treated with 5µg/ml CHX and Cfz. n= 1. Apoptosis was measured via flow cytometry using caspase-3/7 Green Detection reagent and SYTOX Red dead cells stain.

**Protein Phosphatase 1 complex appears to play a role in mediating PI-induced apoptosis, though not through the regulation of protein synthesis.**

Given the lack of eIF2α phosphorylation, we expected that eIF2α kinases, such as PERK, would not play a role in PI-induced apoptosis. While eIF2α is phosphorylated by eIF2α kinases, the dephosphorylation of eIF2α is mediated by two protein phosphatase PP1 regulatory subunits: CReP and GADD34, which confer eIF2α specificity to the PP1 complex. CReP is the constitutive repressor of eIF2α phosphorylation, while GADD34 is the stress-inducible repressor of eIF2α phosphorylation(169). CReP protein and mRNA levels don't change in response to stress(170). Either one or both proteins could be responsible for the dephosphorylation of p-eIF2α in response to PI. Given that we did not observe a phosphorylation of eIF2α in response to PIs in two of our three cell lines, we believe eIF2α kinases, such as PERK, GCN2, and HRI, are not playing a key role in mediating PI-induced apoptosis. We aimed to investigate how eIF2α phosphatases mediate PI-induced effects and lead to apoptosis in TNBC cells.

We pulse-treated SUM149 cells with 33, 100, or 300nM Cfz, followed by culturing in a drug-free media, and collected the cells 3, 6, and 9 hours after the start of the treatment. We observed a prominent increase in CReP expression at 3 hours for 33, 100, and 300nM Cfz (Figure 3.12A). CReP was upregulated within one hour when treated with 10μM Cfz (Figure 3.12B), and GADD34 was upregulated in response to Cfz as well, although not as rapidly as CReP (Figure 3.12B). This may be due to CReP accumulation resulting from proteasome inhibition, as CREP is expressed constitutively, whereas GADD34 is usually induced transcriptionally upon proteotoxic stress(171). We used 10 μM Cfz for this experiment because it was an extremely toxic dose, and

that would certainly induce PI-mediated apoptosis. Quantification of the western blot is shown below the blot (Figure 3.12B).

We treated MDA-MB-231 cells with 500nM Btz and observed an increase in CReP expression at 8-hour time points (Figure 3.12C- top panel). The increase in CReP expression observed 8 hours correlated with a lack of eIF2α phosphorylation (Figure 3.12C- top panel). We found an increase in GADD34 expression in MDA-MB-231 cells in response to 200nM and 500nM Btz at 8 hours (Figure 3.12C-bottom panel), however p-eIF2α did not appear to correlate with GADD34 expression, as there was an increase in p-eIF2α at 4 hours, while we observed no change in GADD34 expression at that time point.

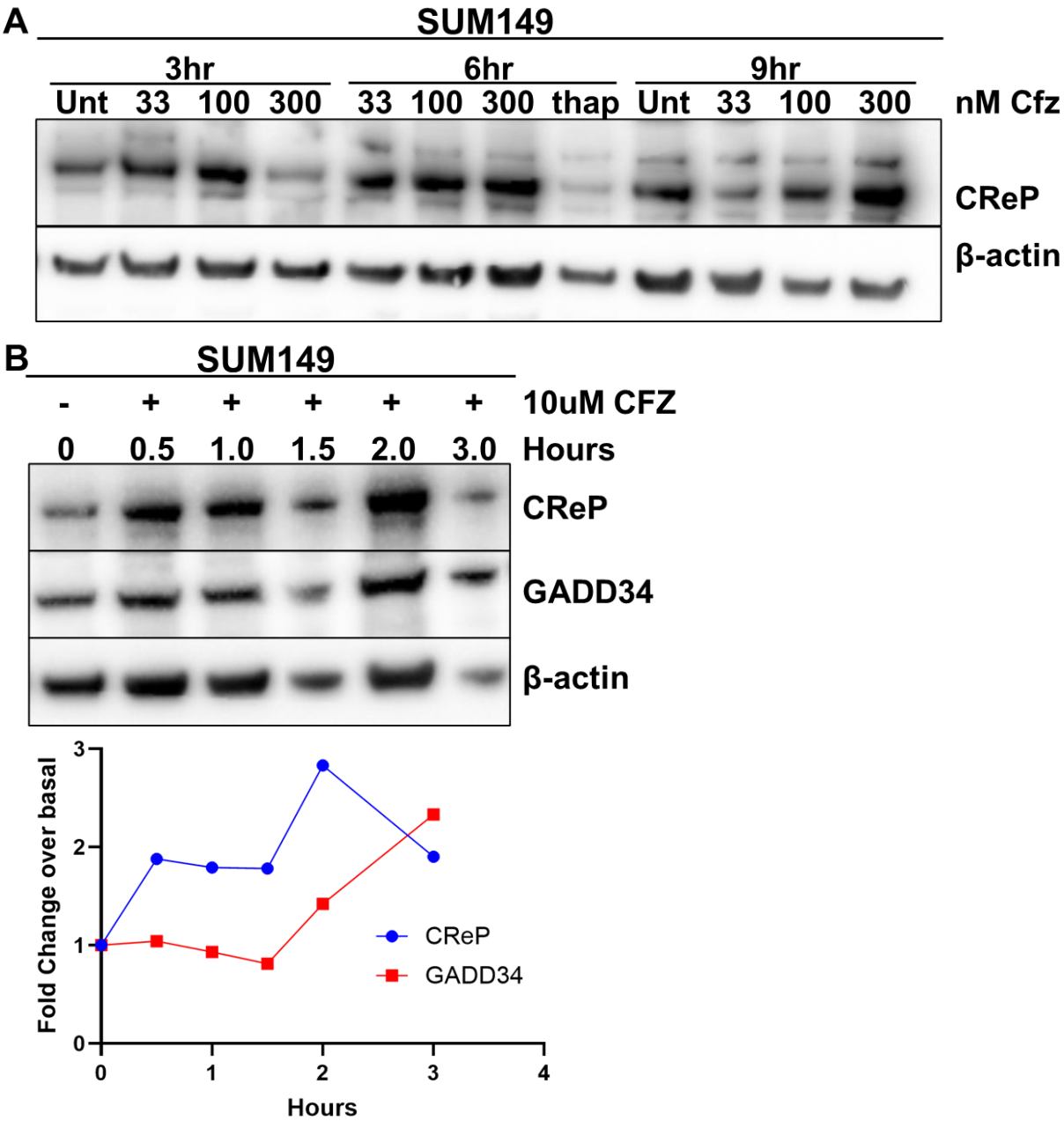
A
SUM149
3hr
6hr
9hr
Unt 33 100 300 33 100 300 thap Unt 33 100 300
nM Cfz
CReP
β-actin
B
SUM149
- + + + + + 10uM CFZ
0 0.5 1.0 1.5 2.0 3.0 Hours
CReP
GADD34
β-actin
Fold Change over basal
0
1
2
3
0
1
2
3
4
Hours
CReP
GADD34

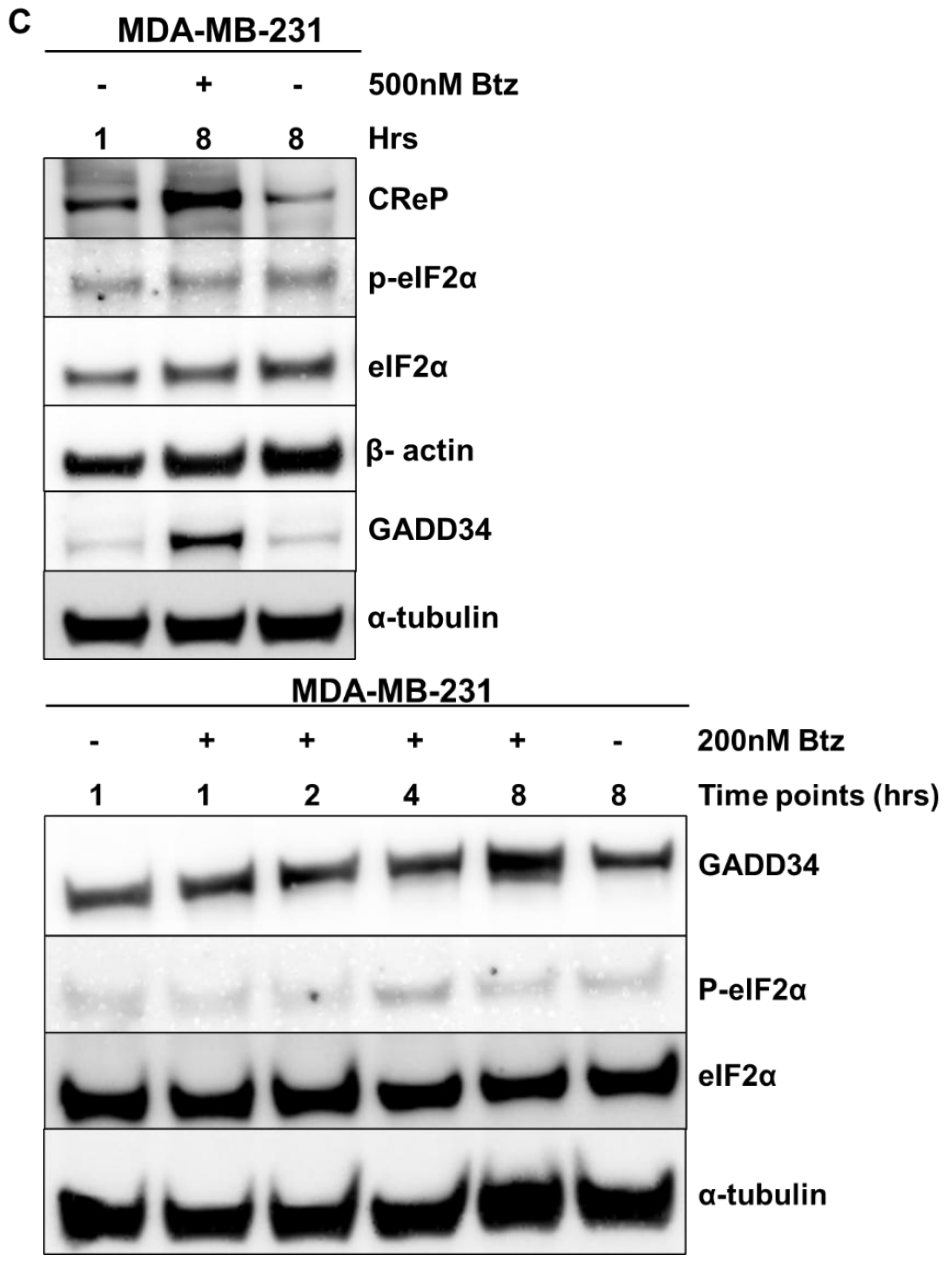


**Figure 3.12 Proteasome inhibition results in the upregulation of CReP and GADD34**

A. SUM149 cells were pulse-treated with 500nM Btz for 1 hour, before being collected at the indicated time point. Western blot shows changes to GADD34 in response to Btz. In a sample denoted as "thap" cells were treated with 10μM Thapsigargin instead of Cfz.
B. SUM149 cells were pulse-treated with 10μM Cfz for 1 hour, before being collected at the indicated time points.
C. MDA-MB-231 cells were pulse-treated with the indicated dose of Btz for 1 hour, before being collected at the indicated time points. Western blot shows changes in p-eIF2α, eIF2α, and CReP in response to Btz.

Despite evidence of the increasing abundance of proteins in the PP1 complex, a lack of activation of the integrated stress response (ISR) could occur via a PP1 complex-independent mechanism. To verify that the lack of eIF2α phosphorylation was happening due to CReP and GADD34 via the PP1 complex, cells were treated with Salubrinal, an inhibitor that is selective for the eIF2α phosphatase complex, in combination with Cfz. We observed that in response to Cfz alone, there was an increase in CReP and GADD34, with a corresponding decrease in phosphorylated eIF2α (Figure 3.13). A combination of Salubrinal and Cfz still resulted in an upregulation of CReP and GADD34 at 9 hours; however, there was no corresponding decrease in p-eIF2α. This suggested to us that the PP1 complex is involved in the dephosphorylation of eIF2α in response to proteasome inhibitors. An upregulation of CReP and GADD34 suggests that either or both could be the primary mediators of eIF2α dephosphorylation under PI-induced stress. Further repeats need to be performed in additional cell lines, and we would like to see the effects at all time points.

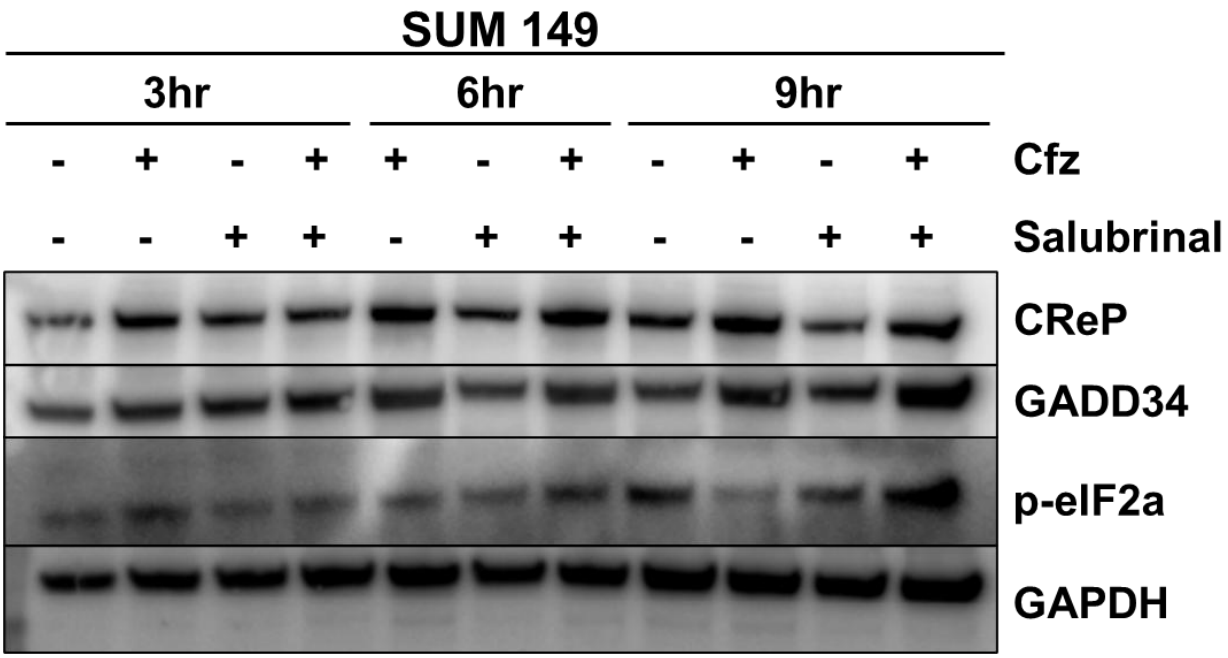


**Figure 3.13 When eIF2α phosphatases are inhibited, Cfz activates ISR**

SUM149 cells were treated with 75μM of Salubrinal for one hour before pulse-treatment with 300nM Cfz. Cells were collected at the indicated time points.

Due to proteasome inhibitors partially inhibiting the proteasomes, a lower rate of protein degradation occurs in the cells. A lower rate of degradation results in a longer half-life of proteins. This could be especially significant for short-lived proteins that can induce their effects in cells for a longer period before being degraded. An increase in CReP and GADD34 in response to proteasome inhibitors could be attributed to an increase in protein half-life or to the production of newly synthesized CReP/GADD34 proteins. CReP has been found to have a short half-life(172)of approximately 45 minutes(173) in HaCaT cells. GADD34 also has a short half-life of less than one hour(174). CReP and GADD34 are both degraded by the proteasome.

We performed a cycloheximide chase experiment to study the half-life of CReP and GADD34. To determine the half-life of the protein at basal conditions, SUM149 cells were treated with cycloheximide only, Cfz only, or a combination of both, and collected every thirty minutes up to 3 hours post-treatment (Figure 3.14A). The cycloheximide-only treatment would enable us to determine the half-life of the protein, and the combination of CHX and Cfz would allow us to investigate how the half-life of the protein changes in response to proteasome inhibition. CReP half-life appeared to be approximately 30 minutes at basal conditions. The half-life of GADD34 at basal conditions appeared to be approximately an hour. SUM149 cells showed an increase in CReP and GADD34 half-lives (Figure 3.14A) in response to Cfz, and an increase in CReP half-life was observed in MDA-MB-231 cells as well (Figure 3.14 B). Quantification of the SUM149 CReP expression western blot is shown below the blot (Figure 3.14A), and quantification of MDA-231-MB CReP expression western blot is shown below the blot (Figure 3.14B).

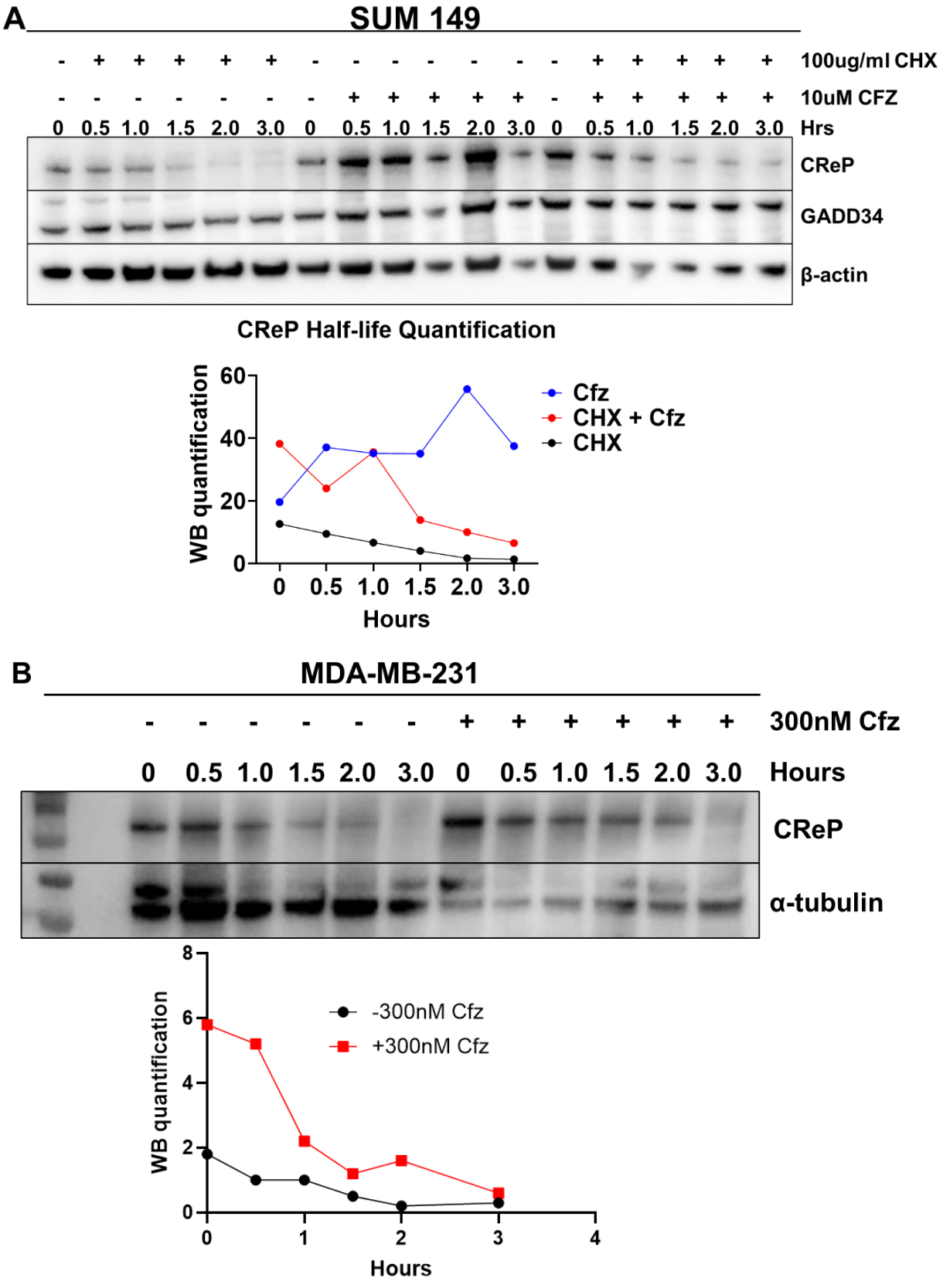
A
SUM 149
100ug/ml CHX
10uM CFZ
Hrs
CReP
GADD34
β-actin
CReP Half-life Quantification
WB quantification
Cfz
CHX + Cfz
CHX
Hours
B
MDA-MB-231
300nM Cfz
Hours
CReP
α-tubulin
WB quantification
-300nM Cfz
+300nM Cfz
Hours

**Figure 3.14 Inhibition of the proteasome causes an increase in the half-life of CReP and GADD34**

A. SUM149 cells were treated with 100µg/ml cycloheximide alone, 10µM Cfz alone, or a combination of 100µg/ml Cycloheximide and 10µM Cfz. Cells were collected at the indicated time points.
B. MDA-MB-231 cells were treated with 100µg/ml Cycloheximide alone, or a combination of Cycloheximide and 300nM Cfz, and collected at the indicated time points.

The longer half-life of the protein could explain the upregulation of CReP and GADD34. With a lack of eIF2α phosphorylation, there would be a continued elevated load on the proteasome, which could lead the cells to undergo apoptosis. Based on this, we aimed to investigate the roles of CReP and GADD34 in PI-induced apoptosis.

We used siRNA to perform knockdown experiments to study the role of CReP and GADD34 in PI-induced apoptosis. To ensure the specificity of siRNA-mediated knockdowns, we used two siRNA molecules for each protein. Additionally, we used a scrambled siRNA as a negative control to ensure that the results of the siRNA transfection process were due to the specificity of the siRNA molecules, rather than an off-target effect of the transfection. We initially tested several different siRNAs and selected the two molecules that showed the strongest reduction of expression of GADD34 and CReP proteins (Figure 3.15A). Of the four siRNA molecules we tested, CReP 07 and CReP 08 produced the best results in untreated SUM149 cells (Figure 3.15A). CReP 07 and CReP 08 siRNA molecules also produced results in untreated MDA-MB-231 cells (Figure 3.15B). After identifying the siRNA molecules that produced the strongest knockdowns, we pulse-treated CReP knockdown SUM149 cells with 33, 100, or 300nM Cfz, and collected at the indicated time points (Figure 3.15C). We observed a lack of CReP expression in the SUM149 cells transfected with the CReP 08 siRNA. Compared to cells without CReP knockdown, CReP KD cells exhibited increased phosphorylated eIF2α expression under both untreated and Cfz-treated conditions. We treated MDA-MB-231 cells with 500nM Btz and observed that CReP siRNA resulted in the expected knockdown of CReP and corresponded to an upregulation of phosphorylated eIF2α at basal conditions (Figure 3.15D).

We tested the effectiveness of four different GADD34 siRNA molecules (GADD34 05, 06, 08, and 18) and found that GADD34 06 and GADD34 08 produced the strongest knockdown effect in MDA-MB-231 cells (Figure 3.15E). We then tested how the knockdown of GADD34 translated to phosphorylation of eIF2α in response to PI. The GADD34 siRNA molecules that produced the strongest knockdown effect resulted in elevated phosphorylated eIF2α levels at basal conditions, but phosphorylation was observed in response to Btz (Figure 3.15F).

However, the promising effects of CReP siRNA on eIF2α phosphorylation have not been reproducible in subsequent experiments. GADD34 knockdown led to no increase in eIF2α in response to PI.

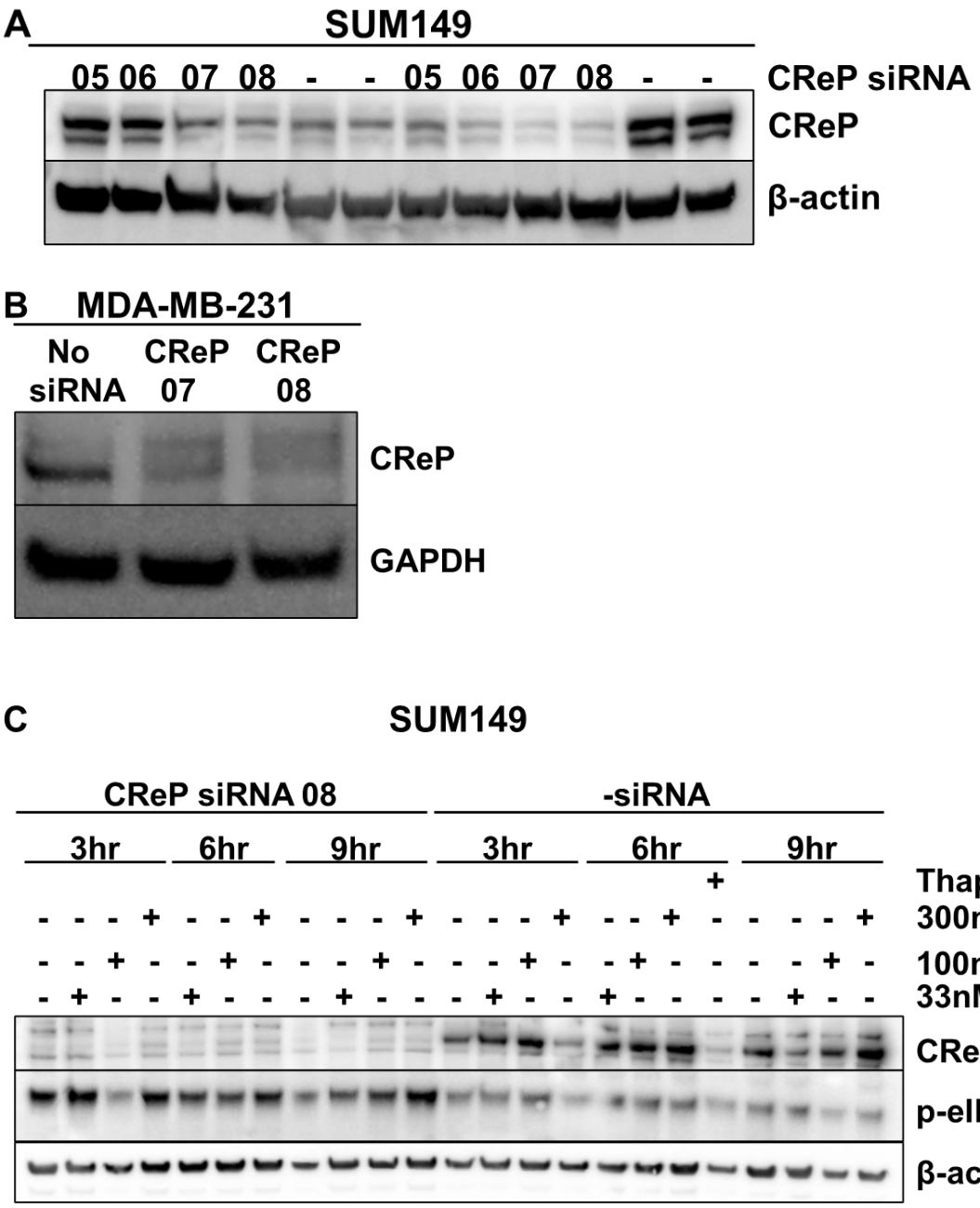
A
SUM149
05 06 07 08 - - 05 06 07 08 - -
CReP siRNA
CReP
β-actin
B
MDA-MB-231
No siRNA
CReP 07
CReP 08
CReP
GAPDH
C
SUM149
CReP siRNA 08
-siRNA
3hr
6hr
9hr
3hr
6hr
9hr
Thapsigargin
300nM Cfz
100nM Cfz
33nM Cfz
CReP
p-eIF2α
β-actin

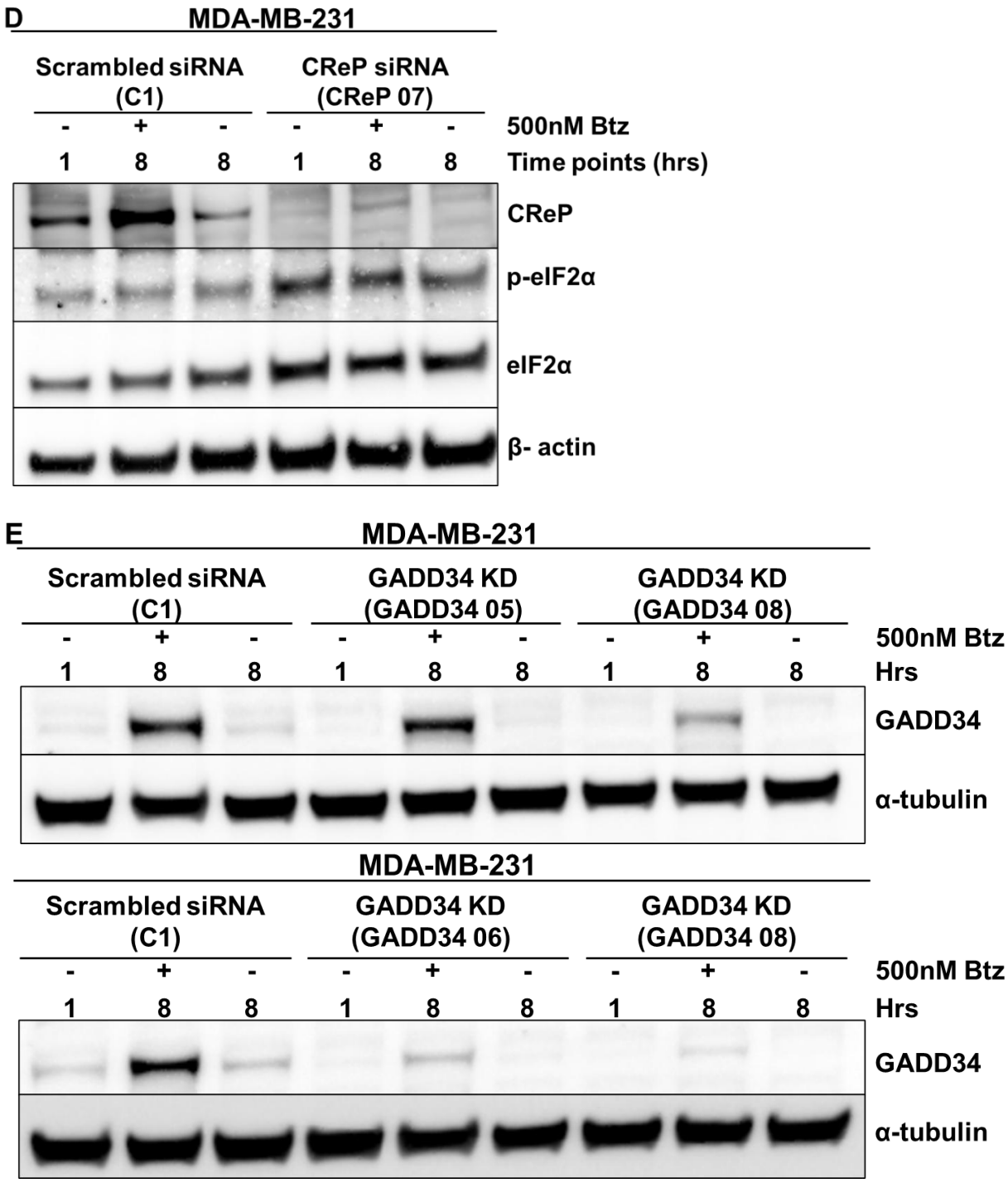
D
MDA-MB-231
Scrambled siRNA (C1)
CReP siRNA (CReP 07)
- + - - + -
500nM Btz
1 8 8 1 8 8
Time points (hrs)
CReP
p-eIF2α
eIF2α
β- actin
E
MDA-MB-231
Scrambled siRNA (C1)
GADD34 KD (GADD34 05)
GADD34 KD (GADD34 08)
- + - - + - - + -
500nM Btz
1 8 8 1 8 8 1 8 8
Hrs
GADD34
α-tubulin
MDA-MB-231
Scrambled siRNA (C1)
GADD34 KD (GADD34 06)
GADD34 KD (GADD34 08)
- + - - + - - + -
500nM Btz
1 8 8 1 8 8 1 8 8
Hrs
GADD34
α-tubulin

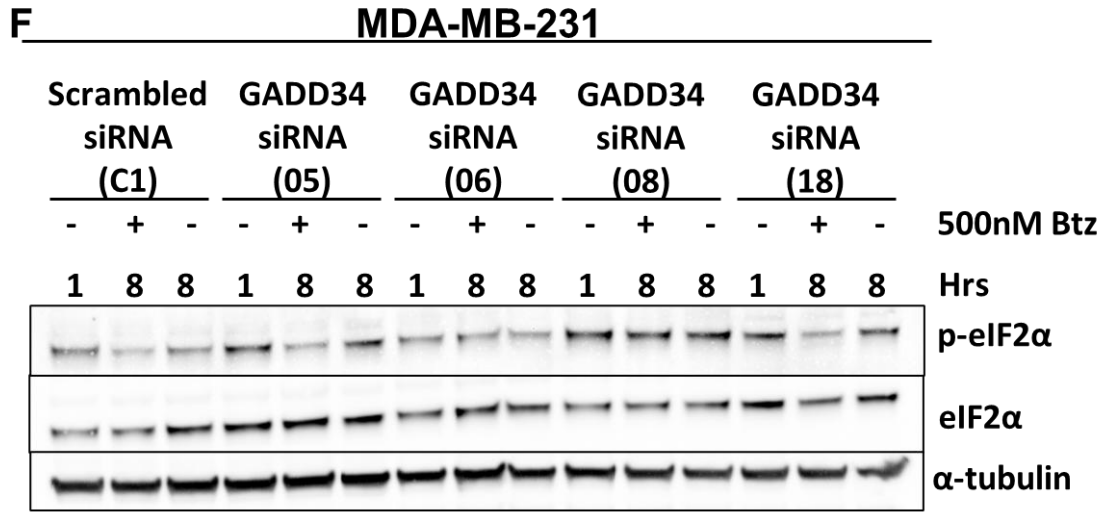


**Figure 3.15 Validation of CReP and GADD34 siRNA knockdown**

A. SUM149 were transfected with four different CReP siRNA molecules for 72 hours. Transfection efficiency was verified by protein expression analysis using western blot.
B. MDA-MB-231 cells were transfected with CReP 07 and CReP 08 siRNA and collected 72 hours after transfection.
C. SUM149 cells were transfected with CReP 08 siRNA for 72 hours. Cells were pulse-treated with various doses of Cfz and collected at the indicated time points.
D. MDA-MB-231 cells were transfected with CReP 07 siRNA for 72 hours. Cells were pulse-treated with 500nM Btz and collected 8 hours after the start of treatment.
E. MDA-MB-231 cells were transfected with scrambled siRNA or GADD34 05, 06, and 08 siRNA molecules for 72 hours. Cells were then pulse-treated with 500nM Btz for one hour and collected 8 hours from the start of treatment.
F. MDA-MB-231 cells were transfected with scrambled siRNA or four different GADD34 siRNA molecules for 72 hours. Cells were then pulse-treated with 500nM Btz for one hour and collected at the indicated time points.

We observed that knockdown of CReP using siRNA did not consistently affect eIF2α phosphorylation, and the knockdown of GADD34 did not affect eIF2α phosphorylation. This suggested to us that CReP and GADD34 either did not play a role in eIF2α phosphorylation, protein synthesis, or PI-induced apoptosis, or did play a role in regulating PI-induced apoptosis through an alternative mechanism. To test CReP and GADD34's role in mediating PI-induced apoptosis, we transfected the cells to knock down CReP or GADD34, treated the cells with proteasome inhibitors, and then measured apoptosis using caspase activity assay or flow cytometry. We hypothesized that the knockdown of CReP and GADD34, and the corresponding increase in phosphorylated eIF2α, would reduce the proteasome load and rescue cells from PI-induced apoptosis. We also hypothesized that if both CReP and GADD34 are playing a role in mediating PI-induced apoptosis, a combination of CReP and GADD34 KD would have a stronger rescue effect than CReP or GADD34 KD would have individually.

We observed an increase in caspase activity in response to 500nM Btz in MDA-MB-231 cells, which was reduced in CReP KD cells at 8 hours (Figure 3.16A). This was observed in response to both CReP siRNA molecules. GADD34 KD also produced a rescue effect in response to 500nM Btz at 8 hours (Figure 3.16B).

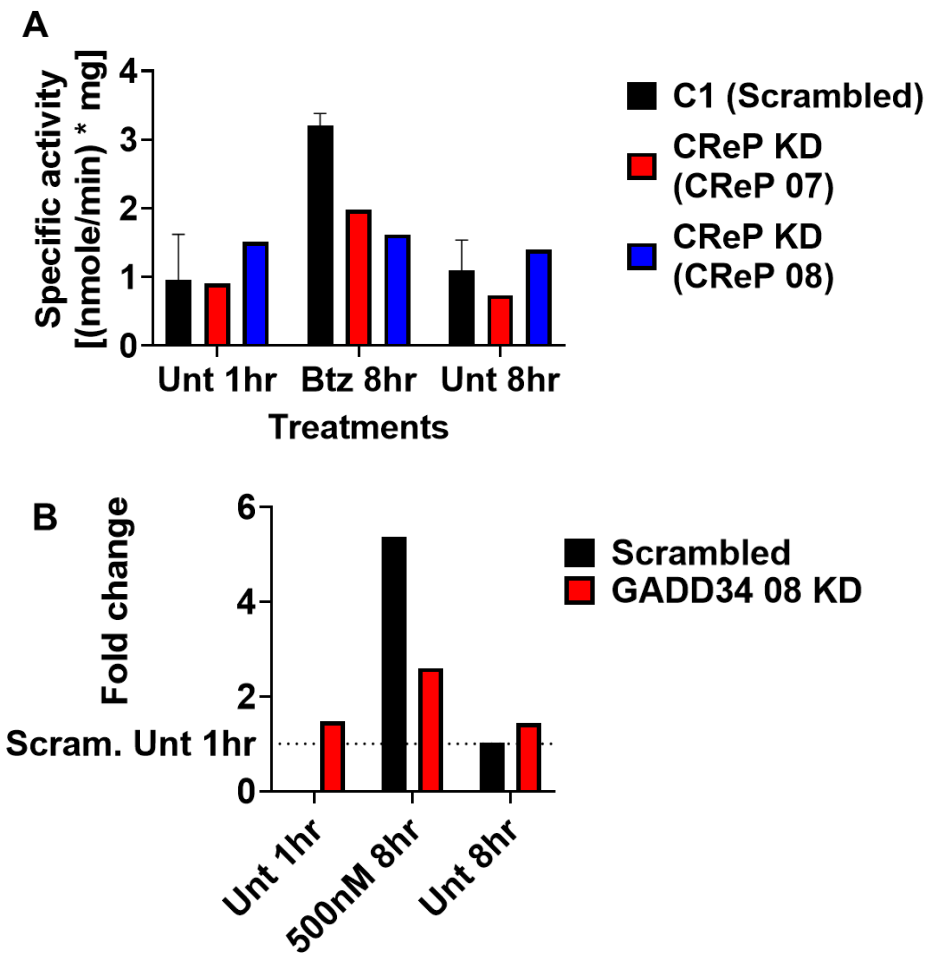


**Figure 3.16 Role of CReP and GADD34 on PI-induced apoptosis**

A. MDA-MB-231 cells were transfected with scrambled siRNA, CReP 07, or CReP 08 siRNA for 72 hours and then pulse-treated with 500nM Btz for one hour. Cells were collected 8 hours from the start of treatment. Caspase activity was measured using caspase activity assay.

B. MDA-MB-231 cells were transfected with scrambled siRNA or GADD34 08 siRNA for 72 hours and then pulse-treated with 500nM Btz for one hour. Cells were collected 8 hours from the start of treatment. Caspase activity was measured using caspase activity assay.

The results of our knockdown studies confirmed that knockdown of CReP and GADD34 rescues cells from apoptosis at 8 hours. Since we hypothesized that the effects are due to their role in mediating protein synthesis, we next looked at the role CReP and GADD34 knockdown had in protein synthesis. We already confirmed that GADD34 knockdown does not affect eIF2α phosphorylation in response to PIs, suggesting that GADD34 siRNA would not have any effect on protein synthesis.

We observed that in response to Btz, MDA-MB-231 cells with CReP KD or GADD34 KD did not have any significant change in protein synthesis (Figure 3.17). This confirmed that GADD34 is not playing a role in regulating protein synthesis. It also showed that CReP does not appear to regulate protein synthesis in response to PIs. Since the rescue effects of CReP and GADD34 knockdown at earlier time points are not due to changes in protein synthesis, this suggests that their effects may be due to a novel mechanism that needs to be further investigated.

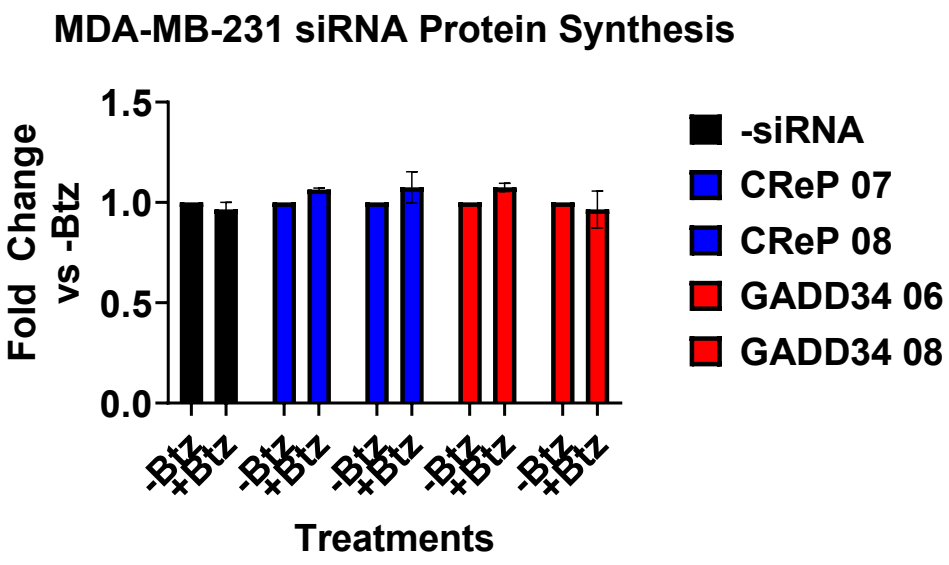


**Figure 3.17 CReP and GADD34 KD's role in regulating protein synthesis**

MDA-MB-231 cells were transfected with scrambled siRNA, CReP 07, or CReP 08 siRNA for 72 hours and then pulse-treated with 500nM Btz for one hour. Cells were collected 6 hours from the start of treatments. Puromycin (2.5 μg/ml and Btz (10 μM) were added at the indicated time points. 20 minutes after puromycin addition, cells were harvested using ice-cold PBS, supplemented with CHX (50 μg/ml). Puromycin incorporation was measured by dot blots. N=2 (A,B) biological replicates.

Quantification of data from experiments performed by other members of the laboratory.

**Discussion**

Proteasome inhibitors are currently approved for the treatment of multiple myeloma and mantle cell lymphoma but have not been shown to work in solid tumors. However, no clinical studies involving their use in TNBC have been performed despite preclinical data suggesting sensitivity. Translating proteasome inhibitors to TNBC is highly relevant because no targeted therapies currently exist, though clinical trials with PD-L1 inhibitors have been conducted(175,176). To explore the potential use of proteasome inhibitors in TNBC, it is necessary to identify the mechanism by which these agents induce apoptosis in TNBC cells. In multiple myeloma, sensitivity to proteasome inhibitors is attributed to elevated protein synthesis and increased endoplasmic reticulum (ER) stress driven by antibody production. TNBC cells do not produce antibodies, yet TNBC cell lines have shown a similar sensitivity profile to PIs as multiple myeloma cell lines.

While there is variability regarding the status of eIF2α phosphorylation, the Boise lab suggested that multiple myeloma cells initiate the unfolded protein response in response to proteasome inhibitors, resulting in rapid induction of PERK, phosphorylation of eIF2α, and downstream activation of ATF4 and CHOP(105). This is not what we observed in our multiple myeloma cell line. We observed a dephosphorylation of eIF2a in response to Btz. One key difference between our lab's and their lab's experiments is that they continuously treated their cells with Btz for 12 or 24 hours. Our method better mimics clinical exposure, but the longer, continuous incubation may activate different pathways by increasing the potential of off-target effects. In addition, we observed a lack of phosphorylation or dephosphorylation in response to PIs in TNBC cells. A lack of phosphorylation or dephosphorylation would result in continued global protein synthesis,

exacerbating proteotoxic stress induced by proteasome inhibitors and placing a greater burden on the proteasome.

Dephosphorylation of eIF2α is regulated by the protein phosphatase 1 (PP1) complex, which has two active subunits, Constitutive repressor of eIF2α phosphorylation (CReP), and GADD34. This work found that CReP and GADD34 are upregulated in response to proteasome inhibitors. Longer half-life of CReP and GADD34 was detected, which could be explained by the partial inhibition of the proteasome due to proteasome inhibitors.

The effect of CReP in regulating eIF2α in response to PIs was not consistent. We could not consistently reproduce the rescue effects of CReP knockdown on eIF2α phosphorylation. The knockdown of GADD34 did not play a role in regulating eIF2α phosphorylation. However, the knockdown of neither protein resulted in a change in protein synthesis. This would suggest that CReP nor GADD34 are potentially playing a role in mediating PI-induced apoptosis. Confusingly, caspase activity data indicated that CReP and GADD34 regulate PI-induced apoptosis at 8 hours. All this together suggests that while CReP and GADD34 play a role in PI-induced apoptosis, it is not through the dephosphorylation of eIF2α, but rather through a potentially novel mechanism. It is also possible that our siRNAs had non-specific binding, leading to additional effects beyond the expected knockdown. We tried to address this situation by using two different siRNAs to verify our results, but it is possible that both siRNAs had the same non-specific effect. While this is unlikely, we would need to sequence our RNA after

transfection to verify the specificity of our siRNA, or verify our results using alternative knockdown methods, such as CRISPR-Cas9.

In this chapter, we demonstrated that TNBC cell lines are sensitive to proteasome inhibitors, like multiple myeloma cells. We showed that eIF2α is not phosphorylated in response to PIs, and that CReP and GADD34 levels increased. While we have not been able to consistently link CReP and GADD34 to mediating the phosphorylation status of eIF2α in response to PIs, we did observe that the knockdown of CReP and GADD34 has a rescue effect at earlier time points. Suggesting that CReP and GADD34 may be regulating sensitivity to PIs, potentially through an eIF2α-independent manner.

## Chapter 4: Regulators of NOXA accumulation in response to proteasome inhibitors


### Abstract

Extensive investigations into the mechanisms of apoptosis induced by PIs in multiple myeloma have revealed that NOXA is the primary mediator of cell death. Based on the literature, we expected to see an increase in NOXA expression mediating apoptosis in response to PIs in TNBC as well. Here, we demonstrated that PIs induce NOXA upregulation in TNBC cells, as occurs in MM cells. To elucidate the mechanism regulating this response, we examined pathways upstream of NOXA that could result in NOXA upregulation. We found that the increase in NOXA expression occurred independently of ATF3 and the JNK signaling pathway, and was dependent on c-myc expression. Our results indicate that c-myc-dependent accumulation of NOXA is dependent on translation of new NOXA proteins, though direct transcriptional activation by c-myc cannot be ruled out. These results bypass the oft-debated ATF3-NOXA axis as the inducer of apoptosis and introduce c-myc as a key mediator of PI-induced apoptosis in TNBC cells.


### Introduction

The BCL-2 family of proteins plays a key role in regulating mitochondrial apoptosis(177). The BCL-2 family of proteins can be divided into three groups: anti-apoptotic proteins, pro-apoptotic proteins, and the pore-forming apoptotic proteins. The three groups interact to inhibit or induce apoptosis. The anti-apoptotic proteins include BCL-XL, BCL-2, and MCL-1, while the sensitizing pro-apoptotic proteins include NOXA, PUMA, and BAD. The pore-forming pro-apoptotic proteins include BAX and BAK(178). The pore-forming proteins, when released, form

pores in the mitochondrial outer membrane, leading to caspase activation and apoptosis. BAX and BAK are sequestered and inhibited by MCL-1, which prevents apoptosis. NOXA, a pro-apoptotic BCL-2 protein, has been observed to accumulate in response to proteasome inhibitors in multiple myeloma (179). NOXA functions by being a competitive inhibitor of MCL-1. When NOXA accumulation occurs, it binds to and inhibits MCL-1, freeing BAX and BAK to induce apoptosis.

NOXA has been shown to be activated in response to various cellular stress responses(180). The mechanism by which proteasome inhibitors induce apoptosis in TNBC differs from that in MM; however, NOXA accumulation still appears to play a key role in PI-induced apoptosis in TNBC cells(154). This suggests that, while the pathways upstream of NOXA that are activated in response to PIs are not clearly identified, and may potentially differ from what is observed in multiple myeloma, they still cause NOXA accumulation. Therefore, the proteasome dependence observed in TNBC cells may still be mediated by NOXA(154). We believe that the mechanism of PI-induced apoptosis is a lack of eIF2α phosphorylation, leading to a sustained increase in proteasomal load. Based on this, we wanted to identify the pathway by which the lack of eIF2α phosphorylation and sustained increase in proteasomal load upregulate NOXA. By identifying the mechanism by which NOXA is upregulated, we could potentially identify additional targets for combination therapy.

In multiple myeloma, PIs cause a phosphorylation of eIF2α through the activation of the PERK arm of the UPR(105), which leads to the upregulation of ATF4 and then ATF3(12–14). The

upregulation of ATF3 leads to NOXA accumulation, ultimately driving apoptosis(181,182). Petrocca et al. and others have found that NOXA is upregulated in response to PIs in TNBC cells, and preliminary data from our lab support this finding. As shown in Chapter 3, in TNBC cells, there is a lack of eIF2α phosphorylation, suggesting that an alternative path is causing an accumulation of NOXA in response to PIs in TNBC cells.

NOXA can be upregulated by several different stressors, proteins, and pathways. The pathway that upregulates NOXA in multiple myeloma is the unfolded protein response (UPR)(183). The UPR is activated by an elevated protein load due to the accumulation of misfolded or unfolded proteins in the ER, and functions to reduce the protein load and return cells to a state of protein homeostasis. The UPR has three signaling arms through which it induces its effects: IRE1α, PERK, and ATF6. If the UPR is unable to reduce the elevated protein load and resulting ER stress, it will cause the cell to undergo apoptosis. PERK functions to reduce protein synthesis through the phosphorylation of eIF2α. Phosphorylation of eIF2α results in an inhibition of global protein synthesis. The phosphorylation of eIF2α also upregulates the transcription factor ATF4. ATF4 dimerizes with ATF3, leading to the upregulation of NOXA(181,182,184). This is the mechanism by which proteasome inhibitors are thought to induce apoptosis in multiple myeloma.

The UPR can also upregulate NOXA through the IRE1α arm. IRE1α, when activated, leads to the splicing of XBP1. The spliced form of XBP1, XBP1s, results in upregulation of specific UPR genes and ER chaperones that promote increased efficiency and capacity of folding proteins. In

cases of continued ER stress, the IRE1α arm of the UPR can activate JNK signaling(185). JNK activation can induce apoptosis through ATF3. As discussed with PERK, ATF3 can upregulate NOXA.

Another known regulator of NOXA is c-Myc. In normal cells, the role of c-myc is associated with the cell cycle and metabolism and is tightly regulated. Additionally, c-myc is a well-known oncogene that has been found to play a crucial role in the transformation and proliferation of various cancers and is believed to be dysregulated in many cancers(186). While all breast cancer subtypes express c-Myc, it is expressed higher in TNBC cells(187). MYC has been found to bind to NOXA promoter sites and could directly upregulate NOXA(188). In pancreatic cancer cell lines, NOXA was found to play a significant role in MYC-driven sensitivity to proteasome inhibition(189).

Given the support for NOXA-mediated apoptosis in TNBC cells and MM, we wanted to verify that NOXA accumulation was occurring and identify the mechanism that regulates it in response to PIs.

## Results

### NOXA accumulates in response to proteasome inhibitors in TNBC cells

We initially wanted to confirm that NOXA is upregulated in response to proteasome inhibitors in our cell lines. Using INA6, a multiple myeloma cell line, pulse-treated with Btz and Cfz, as a positive control, we observed an increase in NOXA expression in response to both proteasome inhibitors as early as 4 hours (Fig. 4.1A). After confirming NOXA accumulation in a multiple myeloma cell line, we next wanted to observe NOXA expression in response to PIs in TNBC cell lines. The sensitivity graphs of these TNBC cell lines to PIs are shown earlier (Fig. 3.1). MDA-MB-231 cells were pulse-treated with 200nM Btz for one hour and collected 1, 2, 4, 6, or 8 hours from the start of treatment (Fig. 4.2B), and NOXA accumulation was observed as early as four hours from the start of treatment, with the most accumulation occurring at 8 hours. NOXA expression was quantified and graphed below the blot. Next, MDA-MB-231 cells were pulse-treated with 1000, 500, 250, 125, or 62.5 nM Cfz or Btz for one hour and collected 8 hours from the start of treatment (Fig. 4.1C). We observed NOXA accumulation occurring in doses as low as 62.5nM. SUM149 cells showed NOXA accumulation at 12 hours at 200nM and 1μM Cfz (Fig. 4.1D). MDA-MB-468 cells also showed NOXA accumulation in response to Cfz (Fig. 4.1E).

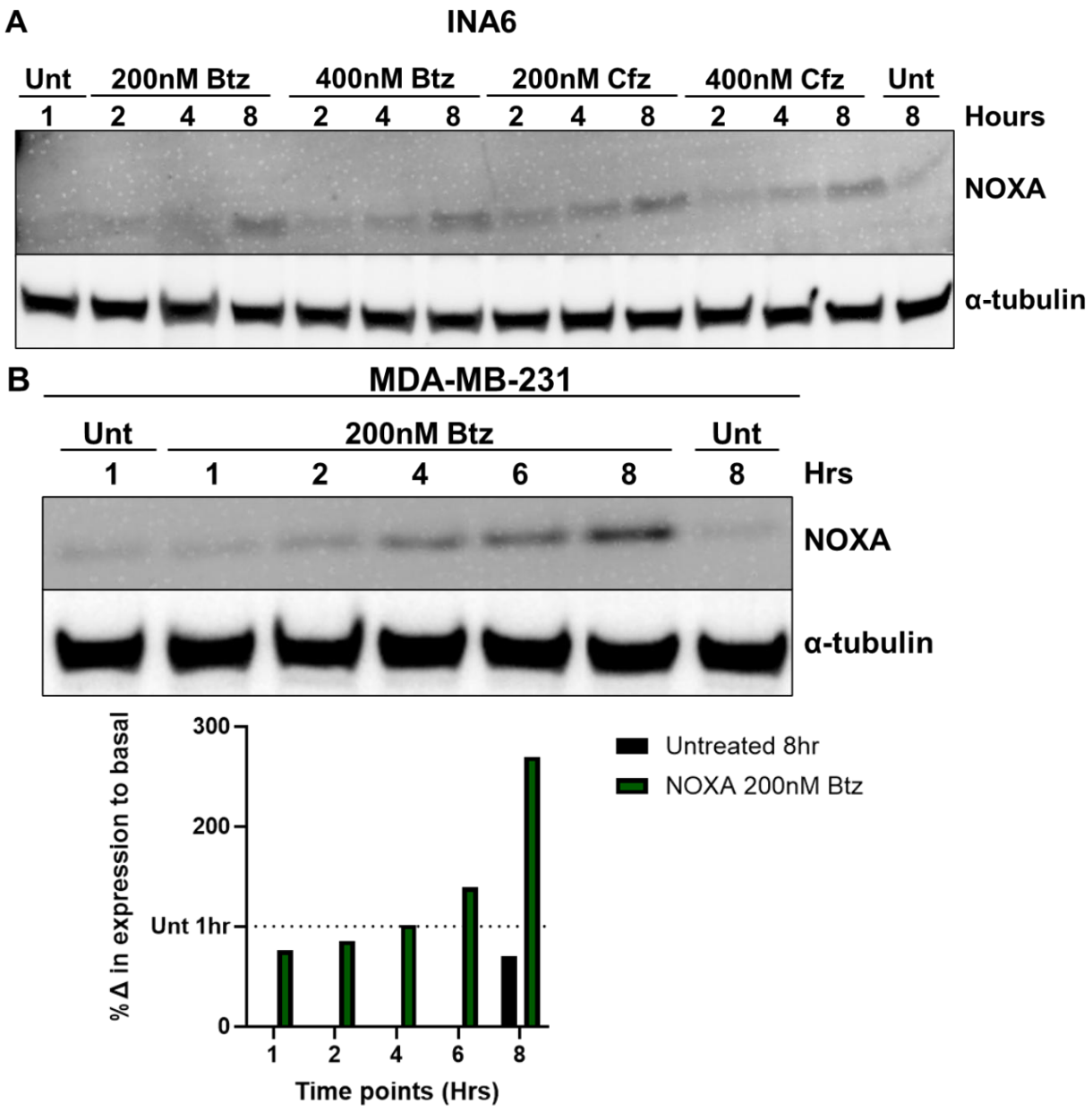
A
INA6
Unt
200nM Btz
400nM Btz
200nM Cfz
400nM Cfz
Unt
1 2 4 8 2 4 8 2 4 8 2 4 8 8
Hours
NOXA
α-tubulin
B
MDA-MB-231
Unt
200nM Btz
Unt
1 1 2 4 6 8 8
Hrs
NOXA
α-tubulin
% Δ In expression to basal
300
200
Unt 1hr
0
1 2 4 6 8
Time points (Hrs)
Untreated 8hr
NOXA 200nM Btz
C
MDA-MB-231
Carfilzomib
Bortezomib
Unt 1000 500 250 125 62.5 1000 500 250 125 62.5 Unt
[nM]
1 8 8 8 8 8 8 8 8 8 8 8
Time points (hrs)
NOXA
α-tubulin

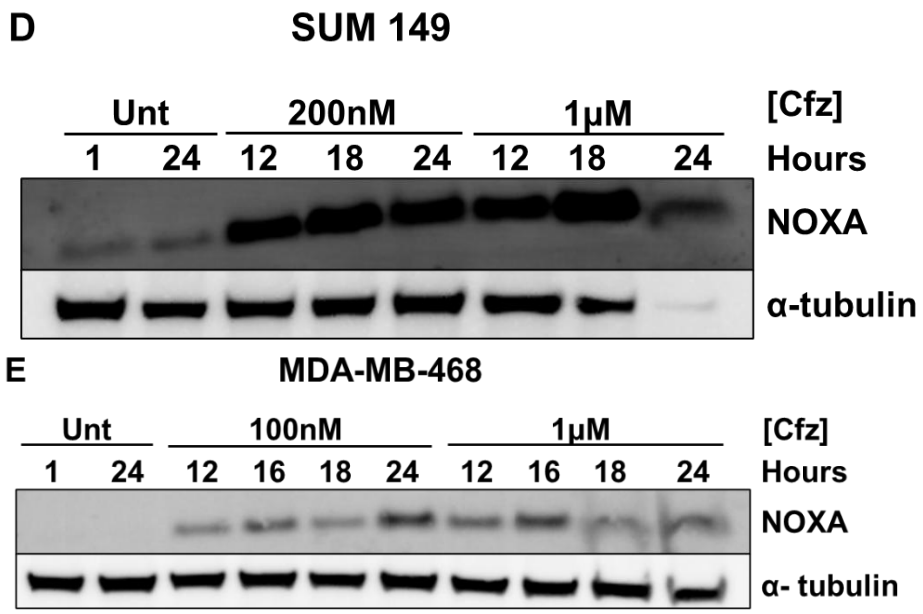


**Figure 4.1 TNBC cell lines' sensitivity to Proteasome inhibition**

A. INA6 cells were pulse-treated with the indicated dose of Btz or Cfz for one hour. Cells were then incubated in fresh media and collected at 2, 4, and 8 hours from the start of the treatments. NOXA expression was measured using western blotting.
B. MDA-MB-231 cells were pulse-treated with 200nM Btz for one hour and collected at the indicated hours. Quantification of the western blot is graphed.
C. MDA-MB-231 cells were pulse-treated with decreasing doses of Cfz or Btz and collected 8 hours from the start of treatment.
D. SUM149 cells were pulse-treated with 200nM or 1μM Cfz for one hour and incubated in fresh media till collection time. Cells were collected 12, 18, and 24 hours after the start of treatments.
E. MDA-MB-468 cells were pulse-treated with 100nM or 1μM Cfz for one hour and incubated in fresh media till collection time. Cells were collected 12, 16, 18, and 24 hours after the start of treatments.

Similar to what was expected and observed in multiple myeloma, the TNBC cell lines also showed NOXA accumulation occurring in response to Cfz and Btz. However, NOXA accumulation does not directly indicate that NOXA mediates apoptosis in response to PI. Apoptosis may occur in an NOXA-independent manner, or NOXA may not be the primary regulator. To determine the role NOXA plays in PI-induced apoptosis, we used siRNA to knock down NOXA expression and measured the change in caspase activity in response to PIs. TNBC cells were transfected with siRNA in fresh media the day after they were plated. Cells were then treated with PIs 72 hours after transfection. We typically use two different siRNAs for each knockdown to verify the validity of the siRNA; however, we were only able to use one NOXA siRNA for our experiments, as only one was able to effectively knock down NOXA expression.

Because NOXA accumulation is associated with apoptosis, we did not expect to find significant NOXA expression under basal conditions. We therefore treated the transfected MDA-MB-231 cells with 1 μM Cfz for one hour and then collected them 18 hours from the start of the treatment (Fig. 4.2A). Cells transfected with scrambled siRNA had NOXA expression in response to 1 μM Cfz, which was rescued in cells with NOXA knocked down (Fig. 4.2A). We next verified the effectiveness of our NOXA siRNA in MDA-MB-468 cells (Fig. 4.2B). MDA-MB-468 cells were either transfected with no siRNA or transfected with NOXA siRNA for 72 hours. Following transfection, the cells were treated with either 300 nM Btz or 300 nM Cfz for 1 hour and then collected 6 hours after the start of treatment. We observed that in response to NOXA siRNA, NOXA accumulation was rescued in response to both Cfz and Btz, resulting in a decrease in apoptosis, compared to cells transfected with scrambled siRNA, as measured by PARP/Cl-PARP using western blotting (Fig. 4.2B). Additionally, MDA-MB-231 cells were transfected with

scrambled siRNA (C1) or NOXA siRNA and treated with increasing doses of Cfz for 1 hour. Afterward, they were collected 18 hours after the start of treatment (Fig. 4.2C). We observed that the knockdown of NOXA expression reduced the percentage of apoptotic cells at all doses of Cfz. To build on this, we wanted to see the rescue effect NOXA KD would have at an earlier time point in response to Btz and Cfz. We treated MDA-MB-231 cells that were transfected with scrambled siRNA or NOXA KD siRNA, with 200nM Btz or 400nM Cfz and collected the cells 9 hours after the start of treatments (Fig. 4.2D). We observed a significant rescue in apoptotic cells in cells with NOXA KD, compared to cells transfected with scrambled siRNA.

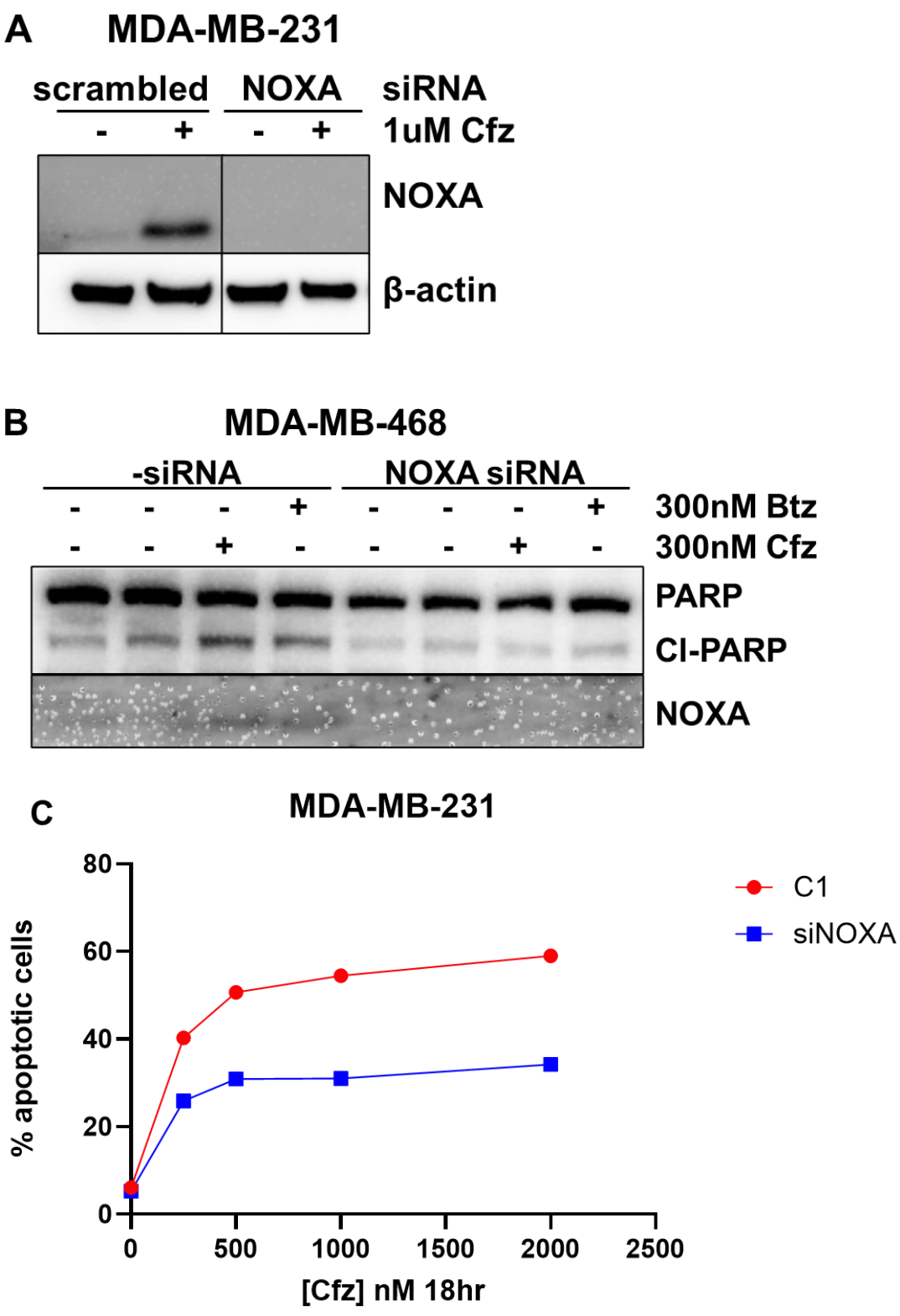
A
MDA-MB-231
scrambled
NOXA
siRNA
- + - +
1uM Cfz
NOXA
β-actin
B
MDA-MB-468
-siRNA
NOXA siRNA
- - - + - - - +
300nM Btz
- - + - - - + -
300nM Cfz
PARP
Cl-PARP
NOXA
C
MDA-MB-231
% apoptotic cells
80
60
40
20
0
0
500
1000
1500
2000
2500
[Cfz] nM 18hr
C1
siNOXA

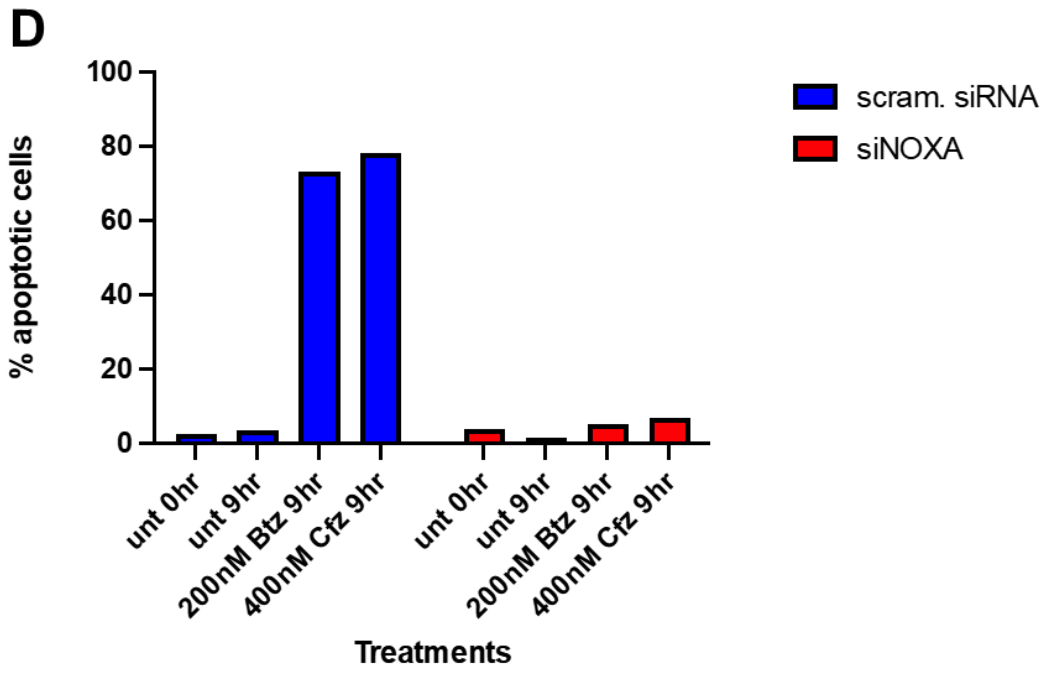


**Figure 4.2 NOXA upregulation occurs in response to proteasome inhibition. This upregulation is seen with cell death occurring.**

A. MDA-MB-231 cells were transfected with scrambled siRNA or NOXA KD siRNA and pulse-treated with 1 μM Cfz. Cells were collected 18 hours after the start of the treatment.
B. MDA-MB-468 cells were either transfected with NOXA KD siRNA or no siRNA. Cells were pulse-treated with 300 nM Btz and Cfz and collected 6 hours after the start of the treatment. NOXA and PARP/Cl-PARP expression was measured using western blotting.
C. MDA-MB-231 cells were transfected with scrambled siRNA or NOXA KD siRNA. Cells were then pulse-treated with the indicated dose of Cfz. Cells were then collected 18 hours after the start of the treatments, and apoptosis was measured using flow cytometry. n=1.
D. MDA-MB-231 cells were transfected with scrambled siRNA or NOXA KD siRNA. Cells were pulse-treated with 200 nM Btz or 400 nM Cfz for one hour and collected 9 hours from the start of treatment. Apoptosis was measured using flow cytometry. n=1.

We were able to confirm that the knockdown of NOXA resulted in a rescue from apoptosis in response to PIs. While knockdown of NOXA did not completely rescue cells from PI-induced apoptosis (Fig. 4.2B), there was a large reduction in the cytotoxic effects of proteasome inhibitors, suggesting that NOXA plays a key role in mediating PI-induced apoptosis. Since we have verified that NOXA plays a significant role, we next aimed to identify the pathways mediating NOXA upregulation.

**Regulators of NOXA accumulation**

NOXA has been found to be upregulated by different proteins in response to various stressors. In multiple myeloma, proteasome inhibitors are believed to induce NOXA accumulation through the ATF4/ATF3 pathway(183,184), which is downstream of eIF2α, a component of the unfolded protein response. In addition to ATF4/ATF3, NOXA upregulation can occur through activation of JNK, which is part of the MAPK signaling cascade, or through c-myc. C-myc has been found to upregulate NOXA either through direct upregulation of NOXA or through signaling cascades.

We wanted to investigate each potential mechanism to find which is responsible for NOXA accumulation in response to PIs. We investigated the dephosphorylation of eIF2α and the changes in downstream signaling in Chapter 3. In this Chapter, we examine the role of ATF3 in NOXA signaling. In addition, we study JNK activation and the role it plays in NOXA accumulation, and how c-myc affects NOXA upregulation in response to PIs in TNBC cells.

**Transcription factors downstream of eIF2α do not regulate NOXA accumulation**

While we did not observe eIF2α phosphorylation in response to PIs, we wanted to see if the downstream pathway was still responsible for NOXA upregulation. In multiple myeloma cells, ATF3 is thought to upregulate NOXA expression(184). ATF3, which is downstream of ATF4, can be upregulated by p-eIF2α. ATF3 is upregulated by ATF4, which is directly upregulated by eIF2α phosphorylation. While we showed that eIF2α is not phosphorylated in the previous chapter, ATF3 can be activated through other eIF2α-independent pathways(190,191). First, we wanted to confirm that ATF3 is upregulated by PIs. If so, we wanted to confirm ATF3's role in regulating NOXA's expression and, if ATF3 is key to regulating NOXA, identify which factor activated ATF3. To test the role of ATF3 in regulating NOXA, we used siRNA to knock down ATF3 and assessed whether it rescued cells from NOXA accumulation.

Since ATF3 transcription factor directly upregulates NOXA transcription in multiple myeloma cells(184,192,193), we first wanted to confirm that ATF3 is upregulated in response to PIs (Fig. 4.3A). MDA-MB-231 cells were pulse-treated with 100nM Cfz and collected 6 hours from the start of treatments. We observed an increase in ATF3 in response to Cfz. After confirming that PIs induce ATF3 upregulation, we next wanted to study whether ATF3 upregulates NOXA. While we typically use two different siRNAs for each knockdown to verify the validity of the siRNA, we were only able to use one ATF3 siRNA molecule, as one of the molecules tested had a strong knockdown effect on ATF3. This molecule was previously used by our lab.

MDA-MB-231 cells were transfected with scrambled siRNA or siRNA to knock down ATF3 or NOXA (Fig. 4.3B). We observed that ATF3 was knocked down in cells transfected with ATF3 KD siRNA. In response to 300nM Btz or 300nM Cfz, MDA-MB-231 cells with ATF3 KD did not express ATF3 but still had NOXA expression (Fig. 4.3B). We then tested this in MDA-MB-468 cells. In response to 500 nM Cfz, MDA-MB-468 cells treated with ATF3 siRNA did not express ATF3, but still upregulated NOXA. MDA-MB-468 cells transfected with NOXA KD did not have any NOXA expression in response to Cfz (Fig. 4.3C). Apoptosis was measured in MDA-MB-231 cells with scrambled siRNA, or ATF3 or NOXA KD (Fig. 4.3D). We did not observe a rescue in apoptosis in cells with ATF3 KD, but there was a rescue effect in cells with NOXA KD (Fig. 4.3D). This data together suggests that ATF3 is not p-eIF2α-dependent and ATF3 does not mediate NOXA accumulation in response to PIs. Based on this, we wanted to investigate other pathways that could be upregulating NOXA in response to PIs.

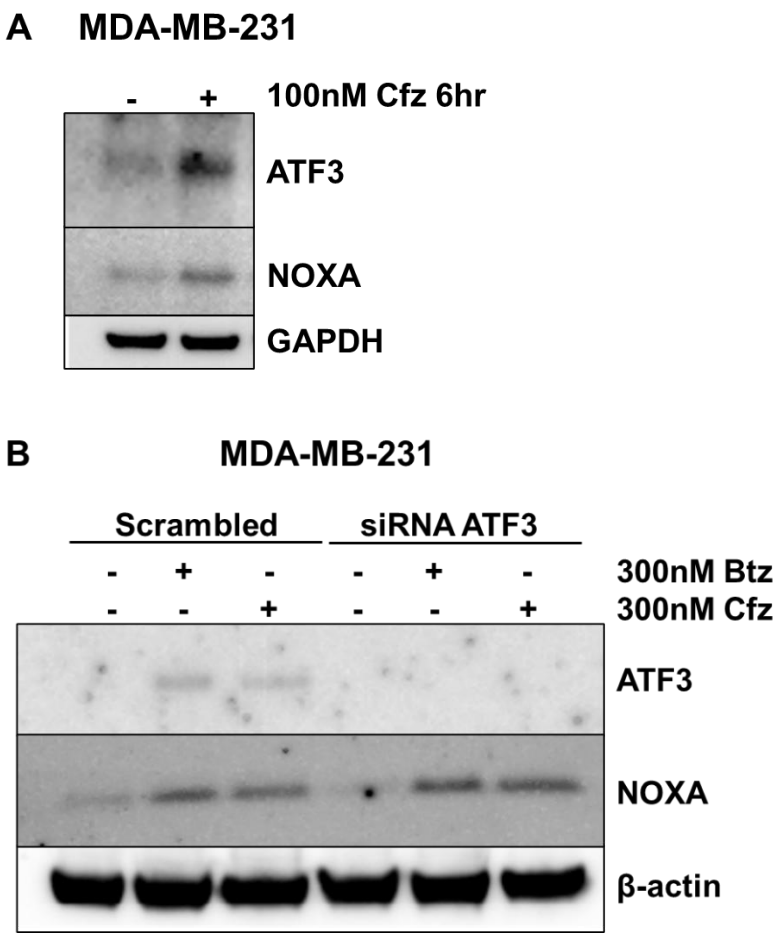
A
MDA-MB-231
- +
100nM Cfz 6hr
ATF3
NOXA
GAPDH
B
MDA-MB-231
Scrambled
siRNA ATF3
- + - - + -
300nM Btz
- - + - - +
300nM Cfz
ATF3
NOXA
β-actin
C
MDA-MB-468
Scrambled
ATF3 KD
NOXA KD
- + - + - +
500nM Cfz
ATF3
NOXA

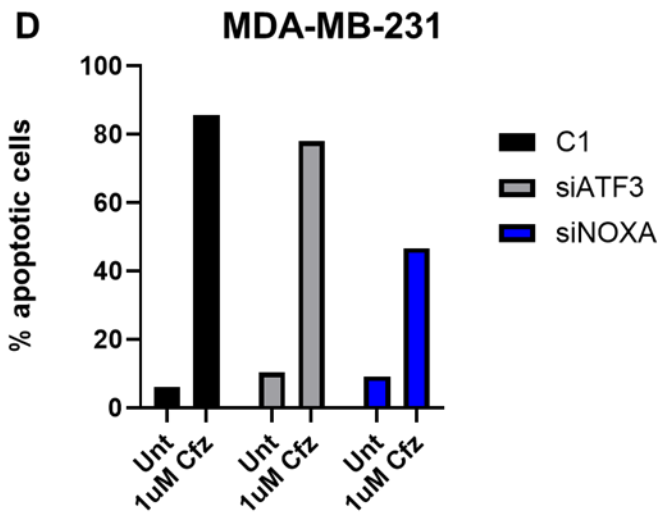


**Figure 4.3 Lack of Rescue effect in ATF3 knocked down cells**

A. Cells were pulse-treated with 100nM Cfz and collected 6 hours after the start of treatment.
B. MDA-MB-231 cells were transfected with siRNA to knock down ATF3, NOXA, or scrambled siRNA for 72 hours. Cells were then pulse-treated with 1 μM Cfz for one hour and collected 18 hours after the start of treatment.
C. MDA-MB-468 cells were transfected with scrambled siRNA or siRNA to knock down ATF3 or NOXA for 72 hours. Cells were then pulse-treated with 500 nM Cfz and collected.
D. MDA-MB-231 cells were transfected with the indicated siRNA for 72 hours. Cells were then pulse-treated with 1μM Cfz and collected 18 hours from the start of treatments. n=1.

**JNK activation does not mediate NOXA accumulation in response to PIs**

We have ruled out that ATF3 is not playing a key role in NOXA regulation, suggesting that an alternative mechanism is regulating NOXA accumulation, such as JNK or c-myc. The JNK pathway has been shown to play a major role in apoptosis in response to different stressors. C-jun N-terminal kinase (JNK) is part of the MAPK signaling cascade pathways. The MAPK signaling pathway is one of the major signaling systems in cells, playing a role in a diverse range of cellular processes, including cell survival/death and development. TNF-α, NF-κB, JSAP1 JIP, and β-arrestin have been found to regulate JNK activity. TNF-α is a proinflammatory cytokine that can upregulate JNK signaling. On the other hand, NF-κB has been found to inhibit JNK signaling, though it is downstream of TNF-α. NK-κB is a transcription factor that has been found to have anti-apoptotic properties and to regulate apoptosis, cell proliferation, and differentiation(194). However, NF-κB has been found not to be the major factor mediating sensitivity to PIs(85). JNK has been found to upregulate ATF3, which in turn upregulates NOXA. JNK activity can be measured through the phosphorylation of its substrate, c-Jun, using Western blot imaging. To determine the role of JNK in proteasome inhibitor-induced apoptosis, we measured NOXA expression and c-Jun phosphorylation levels. In addition, phosphorylation activates JNK, which can drive NOXA expression(195,196). Therefore, we evaluated NOXA expression in cells co-treated with a JNK inhibitor and Cfz.

We observed (Figure 4.4) that Cfz activates JNK, as measured by p-c-jun, and an increase in NOXA expression. In response to the JNK inhibitor alone, there was no NOXA accumulation, showing that the inhibitor by itself was not toxic to the cells. In cells treated with the JNK inhibitor and Cfz, there was a lack of -c-jun phosphorylation, meaning that the JNK pathway was

inhibited; however, we continued to observe NOXA accumulation. This suggests that while JNK activation does occur in response to proteasome inhibitors, it is not responsible for the PI-induced upregulation of NOXA. This suggests that an alternative pathway is responsible for the accumulation of NOXA.

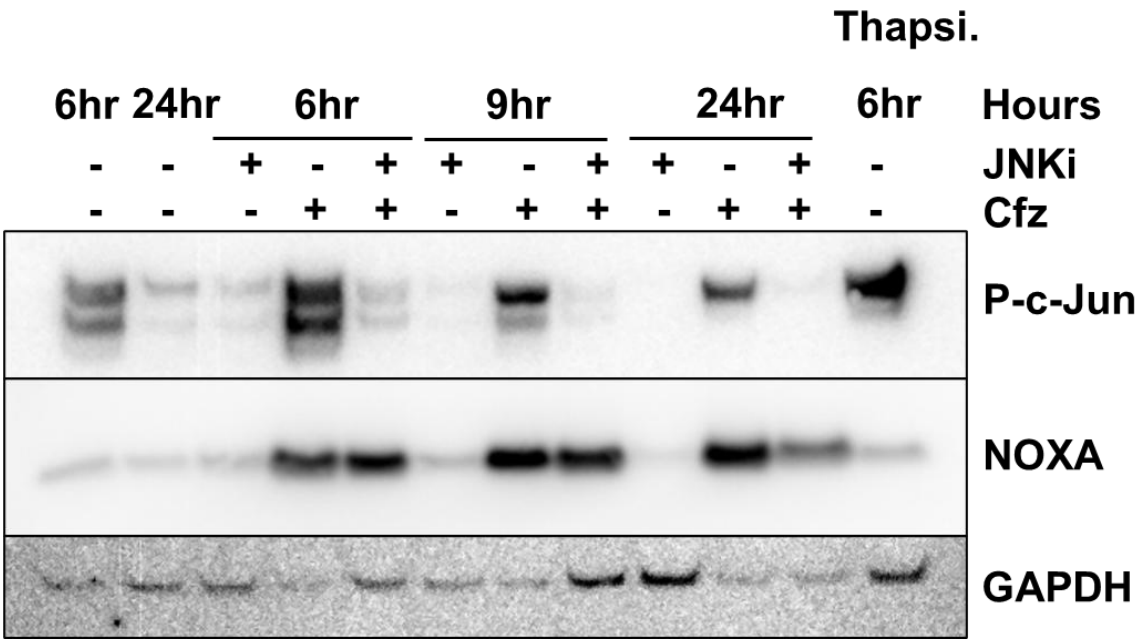


**Figure 4.4 Inhibiting JNK signaling does not rescue cells from NOXA accumulation**

SUM149 cells were treated with 10 μM JNK inhibitor VIII, 300 nM Cfz, or a combination of both for one hour and collected at the indicated time points. JNK signaling activation was measured through p-c-jun expression. Thapsigargin was used as a positive control because it is a known activator of JNK.

**C-myc regulates NOXA accumulation and sensitivity of TNBC cells to PIs**

C-myc can also upregulate NOXA expression in response to proteasome inhibitors(44,131). C-myc is an oncogene referred to as a "master regulator" due to its role in controlling various aspects of cellular growth and metabolism. C-myc has been found to upregulate NOXA through several different mechanisms.

C-myc can directly upregulate NOXA(44) or through signaling cascades downstream(131). To determine the mechanism by which c-myc plays a role in mediating the sensitivity of proteasome inhibitors in TNBC cells, we first investigated whether c-myc is upregulated in response to PIs, and verified if our c-myc siRNAs were knocking down c-myc expression (Fig. 4.5A). We transfected SUM 149 cells with no siRNA or one of our c-myc siRNAs and then pulse-treated the cells with 100nM Cfz (Fig. 4.5A). We observed an increase in c-myc expression in response to 100nM Cfz in the non-transfected cells, while there was a lack of c-myc expression in the cells transfected with c-myc siRNA (Fig. 4.5A).

We transfected MDA-MB-231 cells with c-myc siRNA and treated them with 100nM Cfz, then collected them at 3, 6, and 9 hours after treatment. We measured c-myc and NOXA expression via Western blot. We observed (Fig. 4.5B) that in response to Cfz, there is an increase in c-myc expression, which was accompanied by NOXA accumulation.

To measure the effect of c-myc on NOXA accumulation, we knocked down c-myc expression using siRNA. We observed that in response to 100nM Cfz, cells with c-myc knocked down did not upregulate c-myc, verifying that our transfection was successful in MDA-MB-231 cells, in

addition to SUM 149 cells (Fig. 4.5B). Corresponding to a lack of c-myc upregulation, we observed no NOXA accumulation in response to PIs (Fig. 4.5B). Our results were verified by using flow cytometry to measure apoptosis. We observed that c-myc knockdown significantly rescued cells from Btz and Cfz (Fig. 4.5C).

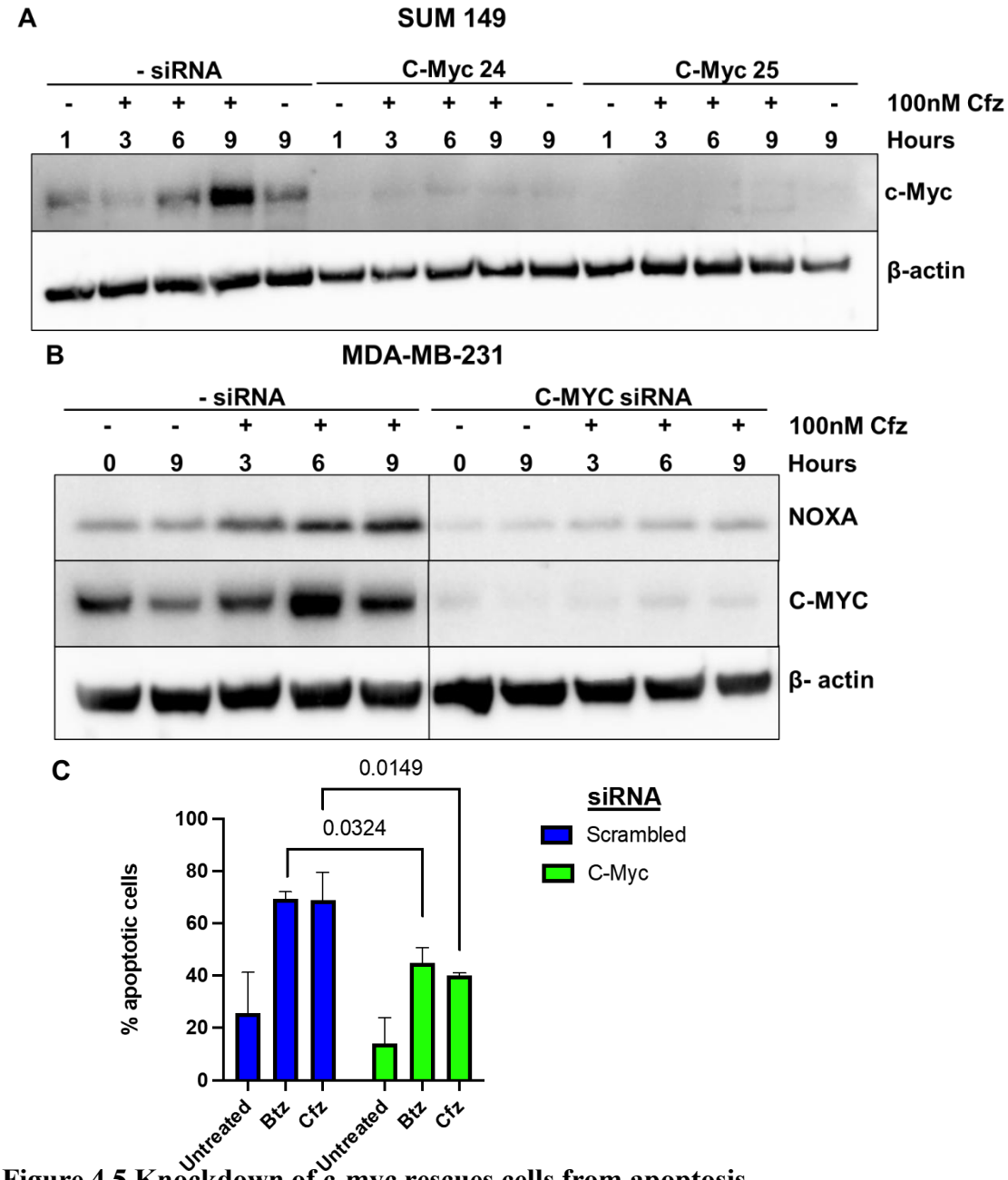


**Figure 4.5 Knockdown of c-myc rescues cells from apoptosis**

A. SUM 149 cells were transfected with no siRNA, or one of the c-myc siRNAs 72 hours prior to treatments. Cells were then pulse-treated with 100nM Cfz and collected at the indicated time points

B. MDA-MB-231 cells were transfected with scrambled siRNA or c-myc siRNA 72 hours prior to treatment and collected at the indicated time points.

C. MDA-MB-231 cells were transfected with scrambled siRNA or c-myc siRNA 72 hours prior to 1-hour pulse-treatment with either Btz or Cfz. Cells were collected 18 hours from the start of treatments and apoptosis was measured using flow cytometry. n = 2

Based on the rescue effect knocking down c-myc had on TNBC cells, we wanted to identify the mechanism by which c-myc was regulating PI-induced apoptosis.

C-myc has been found to regulate NOXA directly and through signaling cascades. Additionally, c-myc has been found to affect protein synthesis. We aimed to determine whether c-myc affects protein synthesis in TNBC cells and whether this mechanism is responsible for its upregulation of NOXA.

In Figure 4.6, cells were treated with a combination of Cfz and CHX, resulting in a rescue in NOXA accumulation. This suggests that c-myc induction of newly synthesized NOXA is dependent on protein synthesis, but this does not rule out direct activation of NOXA by c-myc.

In the future, we will want to directly study the effects of c-myc on protein synthesis in TNBC cells. We will use siRNA to knock down c-myc and measure basal protein synthesis using puromycin incorporation. While we did perform this experiment in the past, the results were inconsistent and so further repeats need to be performed.

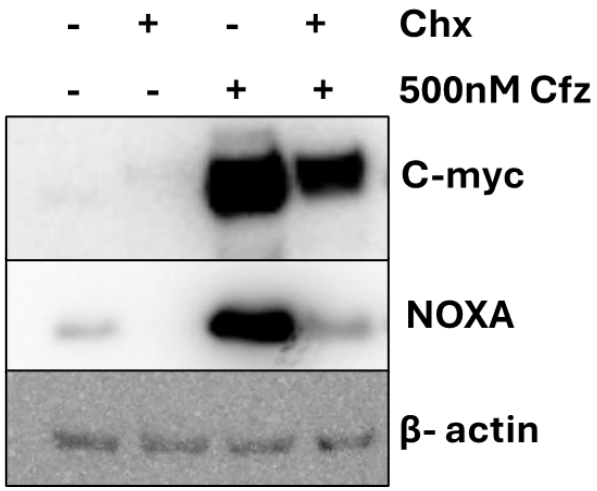


**Figure 4.6 The effect of c-myc on basal protein synthesis**

MDA-MB-468 cells were pulse-treated with 500nM Cfz and then treated with 100 ng/ml Chx. Cells were collected 18 hours after the start of treatments.

Given the changes observed in basal protein synthesis rates and their potential role in sensitizing TNBC cells to PIs, we sought to investigate other factors that c-myc may regulate to sensitize TNBC cells. We considered the possibility that c-myc may be affecting proteasome activity, either by downregulating the number of proteasomes in the cell or affecting their activity.

We measured β5 activity to see how it changes in basal conditions in response to c-myc knockdown. We used β5 as a measurement for proteasome activity because that is the primary active site on the proteasome responsible for protein breakdown and is the primary target for most proteasome inhibitors. We observed a large reduction in β5 activity in response to c-myc knockdown in basal conditions (Figure 4.7). The result suggests that c-myc upregulates proteasome activity. This result is further validated in the literature in various other tumors(197,198), though they did not directly show the upregulation of protein synthesis.

We observed that cells with c-myc knocked down had a decrease in β5 activity (Fig. 4.7), which may be attributed to the decreased basal protein synthesis rate observed in these cells (Fig. 4.6A).

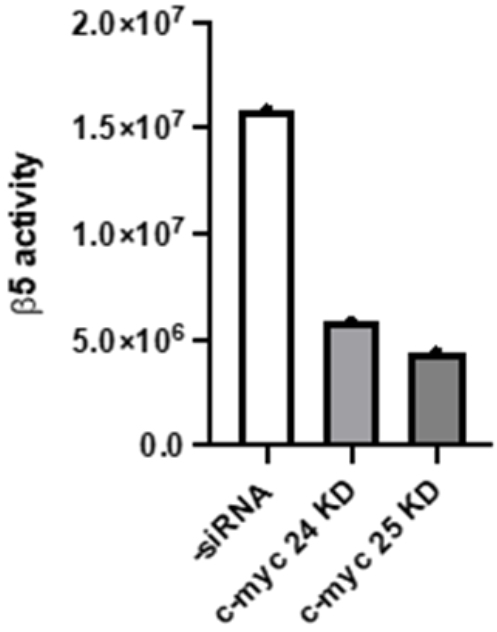


**Figure 4.7 Decrease in β5 activity in c-myc knocked down cells**

β5 activity was measured in MDA-MB-231 cells by the detection of cleaved β5 substrate LLVY-AMC. Cells were transfected with two different siRNA molecules 72 hours prior to collection. n=1.

**Discussion**

Given that we found in Chapter 3 that the pathway by which proteasome inhibitors induce apoptosis was not through the phosphorylation of eIF2α as we thought, we wanted to identify the apoptotic protein responsible for inducing apoptosis. It was previously proposed that NOXA is the pro-apoptotic protein that induces apoptosis in MM cells in response to PI, and while the pathway upstream appears to vary from what we initially expected, NOXA continued to be upregulated in MM and TNBC cells in response to PIs. To verify the significance of NOXA, we performed knockdown studies and found that the knockdown of NOXA led to rescuing cells from PI-induced apoptosis, though it was not a complete rescue, suggesting an alternative mechanism may also be contributing to PI-induced apoptosis, though it is not as significant as NOXA. Further work is needed to identify the other pro-apoptotic protein that may play a role. Based on literature searches(122,199,200), I believe it could be the pro-apoptotic protein BIM. BIM is a pro-apoptotic protein, like NOXA, that has been found to be upregulated in response to Btz(199). BIM has also been associated with regulating MYC-induced apoptosis, unlike other pro-apoptotic proteins such as PUMA(200).

We next sought to identify the mechanism regulating NOXA accumulation in response to PIs and found that c-myc plays a key role in regulating NOXA accumulation in response to PIs in TNBC cells. C-myc is a common oncoprotein that is upregulated in several types of cancer and can upregulate NOXA through multiple mechanisms. Here we have established that c-myc is a key regulator of NOXA accumulation in TNBC cells in response to PIs and it is through this mechanism that PIs induce apoptosis. Future directions of this work will involve identifying the exact mechanism by which c-myc upregulates NOXA in TNBC cells. One potential mechanism

by which c-myc could upregulate NOXA is by directly interacting with NOXA's promoter(44). To further validate c-myc's role in inducing NOXA accumulation in TNBC cell lines, we will select TNBC cell lines that do not have c-myc expression and measure their sensitivity to PIs. Linking c-myc expression and NOXA upregulation in response to PIs in TNBC cells is significant because it could open a therapeutic window for using PIs in TNBC patients with high c-myc expression.

In this chapter, I demonstrated that NOXA accumulation occurs in response to PIs in an eIF2α-independent manner. NOXA upregulation appears to be associated with c-myc expression, and the knockdown of c-myc results in a rescue from NOXA accumulation. C-myc's effect on NOXA accumulation appears to be regulated through protein synthesis, but this does not rule out the possibility of c-myc upregulating NOXA directly through the promoter for NOXA. This possibility will be further investigated by our lab.

## Chapter 5: Conclusions and future directions

### A lack of eIF2α phosphorylation in response to proteasome inhibition in TNBC cells

Proteasome inhibitors, such as Btz and Cfz, are currently approved for the treatment of multiple myeloma and mantle cell lymphoma. While they are effective in those cancers, studies have shown they are effective in other cancers and cell lines as well. Studies conducted by Petrocca et al(154) and our lab confirmed that TNBC cell lines are sensitive to proteasome inhibitors. Multiple myeloma cells produce antibodies, which increase the load on the proteasome, which sensitizes them to proteasome inhibitors. However, TNBC cells do not produce antibodies, suggesting that the mechanism sensitizing them to proteasome inhibitors differs, and the pathway by which PIs induce apoptosis in TNBC cells may vary, too. While eIF2α is expected to be phosphorylated in MM cells in response to PIs, we observed a lack of eIF2α phosphorylation, and in some cases, we even observed dephosphorylation in TNBC cells. The phosphorylation of eIF2α results in an inhibition of global protein synthesis. A lack of eIF2α phosphorylation would suggest that protein synthesis is not being inhibited, and therefore, the proteasome is under elevated stress. This inability to reduce protein synthesis could be a mechanism by which TNBC cells are sensitized to PIs.

While we could not detect eIF2α phosphorylation, we wanted to verify the activation of the other UPR arms, other than PERK. We measured IRE1α/XBP1 activation and ATF6 activation in response to proteasome inhibitors. If any of the eIF2α kinases are being activated, but eIF2α is not being phosphorylated, it would suggest that something was preventing the kinases from

inducing their effects on eIF2α. XBP1 activation can be measured by comparing the XBP1 unspliced variant expression to the spliced variant. We observed a lack of XBP1 spliced variant in response to 500nM and 1μM Cfz (Fig. 5.1A). We observed that IRE1α phosphorylates in response to 500 nM and 1μM Cfz, but at 9 hours and 18 hours (Fig. 5.1B), which does not correlate with phosphorylation of eIF2α. In addition, we observed processed ATF6 at 18 hours in response to 500nM Cfz (Fig. 5.1C), which also did not translate to eIF2α phosphorylation. The time points where ATF6 and IRE1α activation were observed occurred later than when apoptosis was observed in chapters 3 and 4. This suggests that the IRE1α and ATF6 activation do not play a role in PI-induced apoptosis.

Another factor that could be causing a lack of eIF2α phosphorylation is eIF2B, a guanine exchange factor. eIF2B functions to reload the eIF2 complex with GTP, allowing it to engage in a new round of translation initiation(201). The phosphorylation of eIF2α converts the eIF2 complex from a substrate into a competitive inhibitor of eIF2B(201,202). The eIF2B complex is limited in cells and is present in lower abundance than eIF2 in cells(201). In cases where eIF2B is elevated, eIF2B would be able to outcompete p-eIF2α and prevent more of the eIF2 complex from becoming phosphorylated. eIF2B could be upregulated at baseline in TNBC cells, which could partially explain why TNBC cells are sensitive to PIs, or PIs could prevent eIF2B degradation, leading to its accumulation.

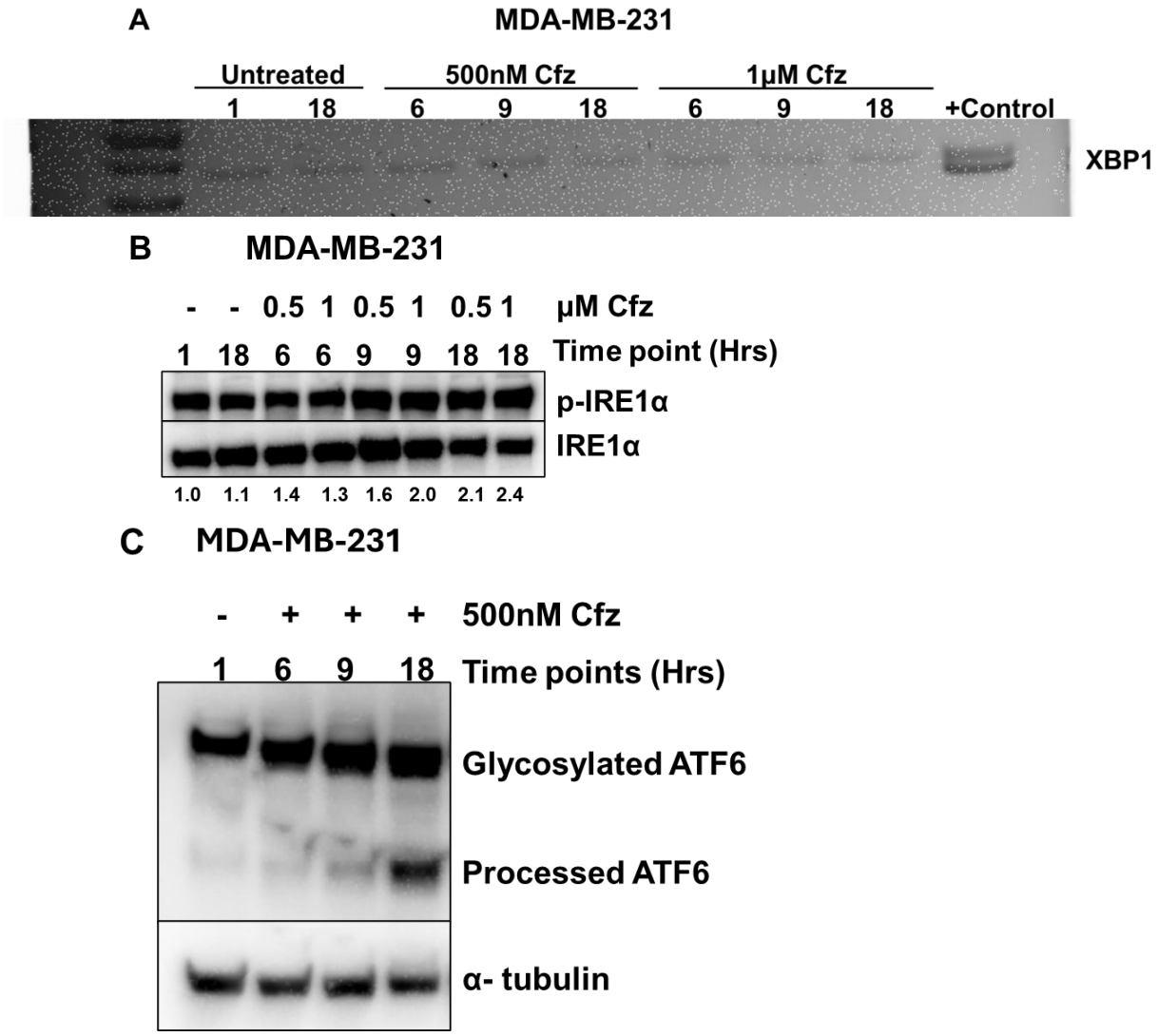


**Figure 5.1 Activation of the UPR arms**

A. MDA-MB-231 cells were pulse-treated with 500nM or 1μM Cfz and collected at the indicated time points. XBP1 splicing was imaged on a 3.5% gel.
B. MDA-MB-231 cells were pulse-treated with 500nM or 1μM Cfz and collected at the indicated time points. Proteins were imaged using western blotting. Quantification of the blot standardized to change from untreated 1 hour is shown below the blot.
C. MDA-MB-231 cells were pulse-treated with 500nM Cfz and collected at the indicated time points. Proteins were imaged using western blotting.

**Lack of protein synthesis in response to proteasome inhibition**

This work found that CReP and GADD34 are upregulated in response to proteasome inhibitors. The effect of CReP on eIF2α dephosphorylation was not consistently reproducible, and GADD34 was found not to play a role in mediating eIF2α phosphorylation status. However, both proteins were found to mediate PI-induced apoptosis at 8 hours. In this work, longer half-lives of CReP and GADD34 were observed, which could be explained by partial proteasome inhibition induced by proteasome inhibitors. The longer half-lives observed could be how CReP and GADD34 induce their effects. Additionally, GADD34 is regulated transcriptionally; therefore, studies are needed to determine if there is transcriptional upregulation. This could potentially be achieved by using a combination of proteasome inhibitors and transcriptional inhibitors, such as actinomycin D, to see the effect on GADD34 expression.

NOXA accumulation has been observed in MM cells in response to PIs and is considered to play a key role in mediating PI-induced apoptosis. NOXA accumulation was believed to occur downstream of eIF2α phosphorylation-dependent upregulation of ATF4. While we observed a lack of eIF2α phosphorylation, we did observe increases in ATF4 and ATF3; however, knockdown studies of both transcription factors led us to believe that neither plays a role in upregulating NOXA in response to PIs in TNBC cells.

We found that c-MYC plays a key role in mediating NOXA in TNBC cells in response to PIs in Chapter 4. Knockdown of c-MYC rescued cells from NOXA accumulation and PI-induced apoptosis. Knockdown of c-MYC also affected protein synthesis and β5 activity (a proteasomal

catalytic site). c-MYC can upregulate NOXA expression through multiple mechanisms, including direct binding to the NOXA promoter. This is a question that we will be looking to answer in future studies. In addition, we want to investigate the mechanism by which c-MYC regulates β5 activity. Given the lack of eIF2α phosphorylation and our finding that c-MYC affects protein synthesis, we also want to investigate how these two mechanisms potentially interact. Figure 5.2 illustrates the pathways investigated in this dissertation.

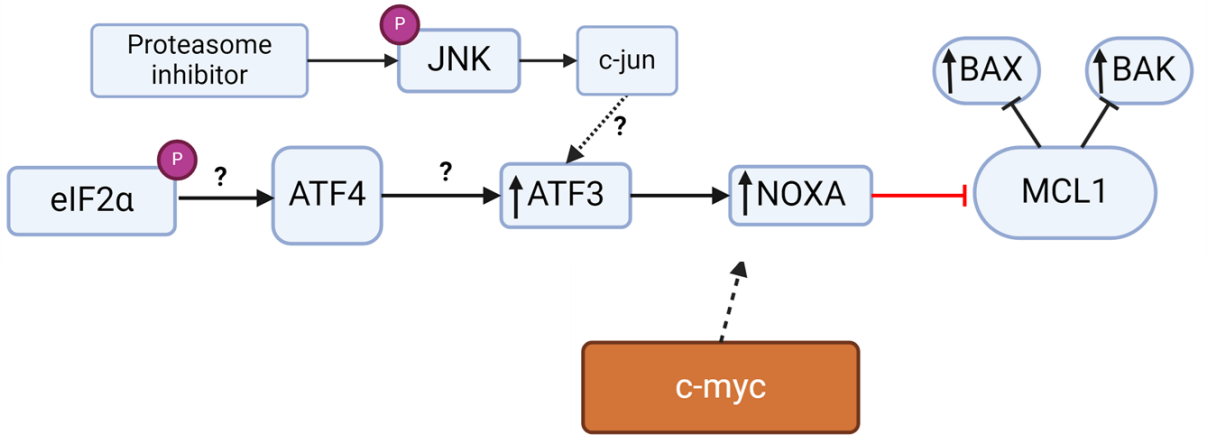


**Figure 5.2 The regulators of NOXA investigated in this dissertation**

In this study, we use the puromycin incorporation assay to measure protein synthesis. As described in Chapter 3, the rate of puromycin incorporation is proportional to the rate of protein synthesis. However, polypeptides, including those with puromycin incorporated, are constantly synthesized and degraded until the rates of synthesis and degradation reach an equilibrium. We are then able to visualize the rate of protein synthesis via western blotting. While this method is effective, it can pose challenges when studying changes in protein synthesis rate in response to proteasome inhibitors. Because proteasome inhibitors impair the proteasome from breaking down proteins, it will lead to an increase in puromycin incorporation readout, but we would not be able to distinguish whether the increase in puromycin incorporation caused by PIs is due to an increase in protein synthesis or due to an impairment in protein breakdown. To overcome this challenge, we used the THRONCAT method to directly assess whether proteasome inhibition increases protein synthesis. THRONCAT is a metabolic labeling method based on Threonine-derived non-canonical amino acid tagging. This method uses a bioorthogonal threonine analog, β-ethynylserine (βES), incorporated into nascent proteins(203). Existing labeling methods, such as bioorthogonal methionine analogs, azidohomoalanine (AHA) and homopropargylglycine (HPG), and puromycin analog O-propargyl-puromycin (OPP), can be used to study changes in the rate of protein synthesis; however, each method has flaws. OPP can label newly synthesized proteins quickly and in complete growth media(203). Still, OPP is toxic to cells and can lead to truncated proteins that are unstable and proteolytically degraded within an hour(203). Labeling with AHA and HPG is less toxic but poorly incorporated into proteins and treating cells in media depleted of intracellular methionine pools requires treatment(203). THRONCAT, a method developed by the Bonger lab, is a novel labeling method allowing fast, efficient, and non-toxic incorporation of amino acid analogs. At the same time, cells are grown in complete media(203).

We treated cells with βES or puromycin following treatments with PIs. After harvesting, the incorporated βES was conjugated with Cy-5-azide fluorophore via click chemistry. The rate of newly synthesized proteins using βES was then measured using in-gel fluorescence, while cells treated with puromycin were imaged via western blotting.

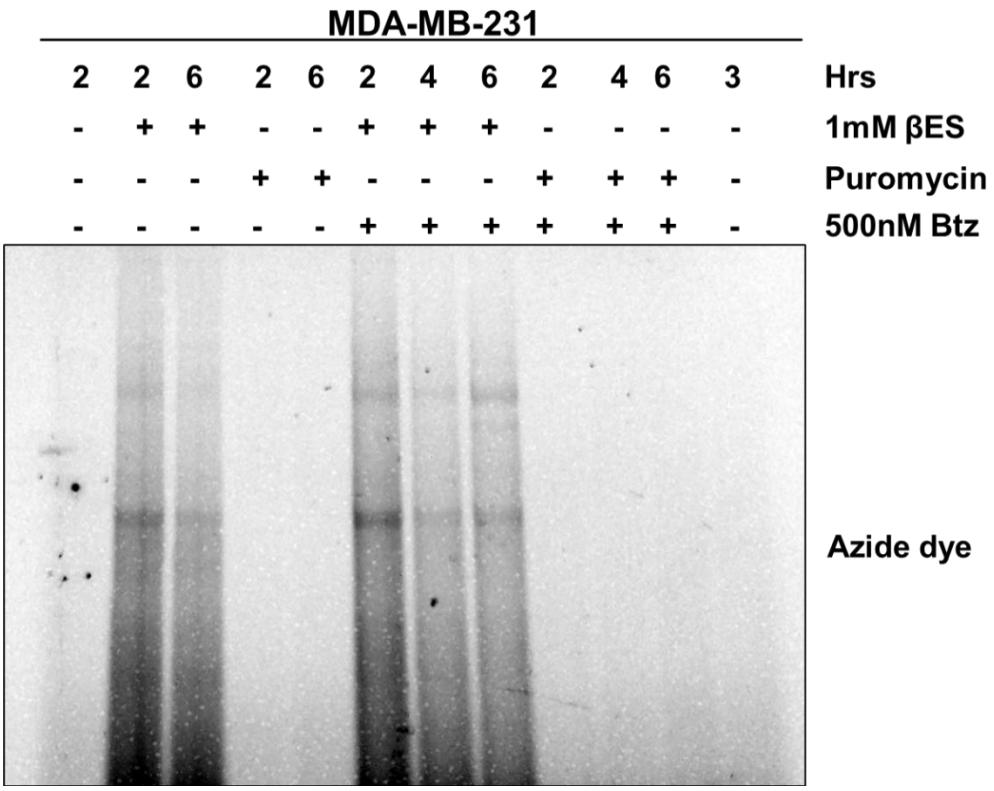


**Figure 5.3 Proteasome inhibition did not cause an increase in newly synthesized proteins**

MDA-MB-231 cells were treated with 500nM Btz for an hour before being collected at the indicated time. Samples containing 1mM βES were treated with βES 1 hour before collection time. Cells treated with puromycin were treated with puromycin 30 minutes prior to collection time.

We found that in response to PIs, there was no increase in newly synthesized proteins (Fig. 5.2); however, this experiment was conducted only once, and we could not perform more repeats because we did not have enough reagents for this study, which are not commercially available. Our results from puromycin incorporation suggested that there was no increase in protein synthesis in response to PIs in SUM149 cells. In MDA-MB-231 cells, there was a decrease in protein synthesis at two hours, after which it stayed steady (Figure 3.7). Taken together, the puromycin incorporation data and the THRONCAT data show no increase in newly synthesized proteins.

CReP and GADD34's role in mediating PI-induced apoptosis was believed to be through the dephosphorylation of eIF2α. However, the data suggests that CReP and GADD34 do play a role in mediating the effects of PI-induced apoptosis (Figure 3.16), but the lack of dephosphorylation of eIF2α and a lack of increase in protein synthesis in response to PIs leads us to believe that CReP and GADD34 may be playing a role in mediating PI-induced apoptosis through a novel mechanism. This will be further investigated by our lab in the future.

**PTEN's role in sensitizing TNBC cells to proteasome inhibitors**

Other factors may be mediating PI-induced apoptosis. As discussed in Chapter 1, PTEN status in cells has been found to affect sensitivity to proteasome inhibitors. PTEN functions by blocking the activation of AKT and mTOR. PTEN deficiency was found to increase proteasome proteolytic activity and facilitate the effect of proteasome inhibitors in cholangiocarcinoma(43). This has also been observed in other types of cancer(40,43,51,93). PTEN deficiency may explain

why TNBC cells are sensitive to PIs. A study found that 35% of TNBC tumors contained a PTEN deficiency(204,205). A future direction for this study will be to identify the status of PTEN expression in the TNBC cell lines used. We would like to categorize multiple TNBC cell lines based on their PTEN expression status. We would then perform sensitivity experiments to determine if PTEN expression status affects sensitivity to PIs in triple-negative breast cancer cells. If cells with PTEN deficiency are found to be more sensitive to PIs than cells with PTEN expression, we would overexpress PTEN in the sensitive cells and study whether it leads to a loss of sensitivity. Additionally, we would knock down PTEN in cells containing PTEN expression and study whether that sensitizes those cells to PIs.

**Summary**

The work presented in this dissertation indicates that TNBC cells are sensitive to PIs and that NOXA is the primary pro-apoptotic protein driving apoptosis. This sensitivity is mediated by CReP and GADD34 through potentially novel mechanisms, as evidenced by the lack of eIF2α phosphorylation. In addition, c-myc appears to play a critical role in mediating PI-induced apoptosis by regulating NOXA. Further investigation into the mechanism by which c-myc upregulates NOXA in TNBC cells is recommended.

**References**


1. Finley D. Recognition and Processing of Ubiquitin-Protein Conjugates by the Proteasome. Annu Rev Biochem. 2009;78:477–513. doi:10.1146/ANNUREV.BIOCHEM.78.081507.101607 PubMed PMID: 19489727.

2. Hershko A, Ciechanover A. The ubiquitin system. Annu Rev Biochem. 1998 Jul 1;67(Volume 67):425–79. doi:10.1146/ANNUREV.BIOCHEM.67.1.425/CITE/REFWORKS PubMed PMID: 9759494.

3. Suraweera A, Münch C, Hanssum A, Bertolotti A. Failure of Amino Acid Homeostasis Causes Cell Death following Proteasome Inhibition. Mol Cell. 2012 Oct 10;48(2):242–53. doi:10.1016/J.MOLCEL.2012.08.003 PubMed PMID: 22959274.

4. Kisselev AF, Akopian TN, Castillo V, Goldberg AL. Proteasome active sites allosterically regulate each other, suggesting a cyclical bite-chew mechanism for protein breakdown. Mol Cell. 1999 Sep 1;4(3):395–402. doi:10.1016/S1097-2765(00)80341-X PubMed PMID: 10518220.

5. Lü S, Wang J. The resistance mechanisms of proteasome inhibitor bortezomib. Biomark Res. 2013 Mar 1;1(1):13. doi:10.1186/2050-7771-1-13 PubMed PMID: 24252210.

6. Kisselev AF, Callard A, Goldberg AL. Importance of the different proteolytic sites of the proteasome and the efficacy of inhibitors varies with the protein substrate. Journal of Biological Chemistry. 2006 Mar 31;281(13):8582–90. doi:10.1074/jbc.M509043200 PubMed PMID: 16455650.

7. Hwang J, Qi L. Quality Control in the Endoplasmic Reticulum: Crosstalk between ERAD and UPR pathways. Trends Biochem Sci. 2018 Aug 1;43(8):593–605. doi:10.1016/J.TIBS.2018.06.005/ASSET/E204B364-AD06-4B23-982D-B0B0798C11D4/MAIN.ASSETS/GR3.JPG PubMed PMID: 30056836.

8. Hetz C. The unfolded protein response: controlling cell fate decisions under ER stress and beyond. Nat Rev Mol Cell Biol. 2012 Jan 18;13(2):89–102. doi:10.1038/nrm3270 PubMed PMID: 22251901.

9. Werner ED, Brodsky JL, McCracken AA. Proteasome-dependent endoplasmic reticulum-associated protein degradation: An unconventional route to a familiar fate. Proc Natl Acad Sci U S A. 1996 Nov 26;93(24):13797–801. doi:10.1073/PNAS.93.24.13797 PubMed PMID: 8943015.

10. Krshnan L, van de Weijer ML, Carvalho P. Endoplasmic Reticulum–Associated Protein Degradation. Cold Spring Harb Perspect Biol. 2022;14(12):a041247. doi:10.1101/CSHPERSPECT.A041247 PubMed PMID: 35940909.

11. Bagratuni T, Patseas D, Mavrianou-koutsoukou N, Liacos CI, Sklirou AD, Rousakis P, et al. Characterization of a PERK Kinase Inhibitor with Anti-Myeloma Activity. Cancers (Basel). 2020 Oct 1;12(10):2864. doi:10.3390/CANCERS12102864 PubMed PMID: 33028016.

12. Le HT, Yu J, Ahn HS, Kim MJ, Chae IG, Cho HN, et al. eIF2α phosphorylation-ATF4 axis-mediated transcriptional reprogramming mitigates mitochondrial impairment during ER stress. Mol Cells. 2025 Feb 1;48(2):100176. doi:10.1016/J.MOCELL.2024.100176 PubMed PMID: 39756584.

13. B'Chir W, Maurin AC, Carraro V, Averous J, Jousse C, Muranishi Y, et al. The eIF2α/ATF4 pathway is essential for stress-induced autophagy gene expression. Nucleic Acids Res. 2013 Sep;41(16):7683–99. doi:10.1093/NAR/GKT563 PubMed PMID: 23804767.

14. Jiang HY, Wek SA, McGrath BC, Lu D, Hai T, Harding HP, et al. Activating Transcription Factor 3 Is Integral to the Eukaryotic Initiation Factor 2 Kinase Stress Response. Mol Cell Biol. 2004 Feb 1;24(3):1365–77. doi:10.1128/MCB.24.3.1365-1377.2004 PubMed PMID: 14729979.

15. Ploner C, Kofler R, Villunger A. Noxa: at the tip of the balance between life and death. Oncogene. 2008;27(Suppl 1):S84-92. doi:10.1038/ONC.2009.46 PubMed PMID: 19641509.

16. Lei Y, Yu H, Ding S, Liu H, Liu C, Fu R. Molecular mechanism of ATF6 in unfolded protein response and its role in disease. Heliyon. 2024 Mar 15;10(5):e25937. doi:10.1016/J.HELIYON.2024.E25937 PubMed PMID: 38434326.

17. Siwecka N, Rozpędek-Kamińska W, Wawrzynkiewicz A, Pytel D, Diehl JA, Majsterek I. The Structure, Activation and Signaling of IRE1 and Its Role in Determining Cell Fate. Biomedicines. 2021 Feb 1;9(2):156. doi:10.3390/BIOMEDICINES9020156 PubMed PMID: 33562589.

18. Brown M, Strudwick N, Suwara M, Sutcliffe LK, Mihai AD, Ali AA, et al. An initial phase of JNK activation inhibits cell death early in the endoplasmic reticulum stress response. J Cell Sci. 2016 Jun 15;129(12):2317–28. doi:10.1242/JCS.179127 PubMed PMID: 27122189.

19. Zeke A, Misheva M, Reményi A, Bogoyevitch MA. JNK Signaling: Regulation and Functions Based on Complex Protein-Protein Partnerships. Microbiol Mol Biol Rev. 2016 Sep;80(3):793–835. doi:10.1128/MMBR.00043-14 PubMed PMID: 27466283.

20. Lin JH, Li H, Yasumura D, Cohen HR, Zhang C, Panning B, et al. IRE1 Signaling Affects Cell Fate During the Unfolded Protein Response. Science. 2007 Nov 2;318(5852):944–9. doi:10.1126/SCIENCE.1146361 PubMed PMID: 17991856.

21. Rastogi N, Mishra DP. Therapeutic targeting of cancer cell cycle using proteasome inhibitors. Cell Div. 2012 Dec 26;7:26. doi:10.1186/1747-1028-7-26 PubMed PMID: 23268747.

22. Zhang M, Zhang L, Hei R, Li X, Cai H, Wu X, et al. CDK inhibitors in cancer therapy, an overview of recent development. Am J Cancer Res. 2021;11(5):1913–35. PubMed PMID: 34094661.

23. Karimian A, Ahmadi Y, Yousefi B. Multiple functions of p21 in cell cycle, apoptosis and transcriptional regulation after DNA damage. DNA Repair (Amst). 2016 Jun 1;42:63–71. doi:10.1016/J.DNAREP.2016.04.008 PubMed PMID: 27156098.

24. Pakjoo M, Ahmadi SE, Zahedi M, Jaafari N, Khademi R, Amini A, et al. Interplay between proteasome inhibitors and NF-κB pathway in leukemia and lymphoma: a comprehensive review on challenges ahead of proteasome inhibitors. Cell Communication and Signaling. 2024 Feb 8;22(1):105. doi:10.1186/S12964-023-01433-5 PubMed PMID: 38331801.

25. Liu T, Zhang L, Joo D, Sun SC. NF-κB signaling in inflammation. Signal Transduction and Targeted Therapy 2017 2:1. 2017 Jul 14;2(1):17023. doi:10.1038/sigtrans.2017.23 PubMed PMID: 29158945.

26. Georgiopoulos G, Makris N, Laina A, Theodorakakou F, Briasoulis A, Trougakos IP, et al. Cardiovascular Toxicity of Proteasome Inhibitors: Underlying Mechanisms and Management Strategies: JACC: CardioOncology State-of-the-Art Review. JACC CardioOncol. 2023 Feb 1;5(1):1–21. doi:10.1016/J.JACCAO.2022.12.005 PubMed PMID: 36875897.

27. Dimopoulos MA, Moreau P, Palumbo A, Joshua D, Pour L, Hájek R, et al. Carfilzomib and dexamethasone versus bortezomib and dexamethasone for patients with relapsed or refractory multiple myeloma (ENDEAVOR): And randomised, phase 3, open-label, multicentre study. Lancet Oncol. 2016 Jan 1;17(1):27–38. doi:10.1016/S1470-2045(15)00464-7 PubMed PMID: 26671818.

28. Sogbein O, Paul P, Umar M, Chaari A, Batuman V, Upadhyay R. Bortezomib in cancer therapy: Mechanisms, side effects, and future proteasome inhibitors. Life Sci. 2024 Dec 1;358:123125. doi:10.1016/J.LFS.2024.123125 PubMed PMID: 39413903.

29. Study Details | NCT03345095 | A Phase III Trial of With Marizomib in Patients With Newly Diagnosed Glioblastoma | ClinicalTrials.gov. [cited 2025 Dec 28]. Available from: https://clinicaltrials.gov/study/NCT03345095

30. Roth P, Gorlia T, Reijneveld JC, de Vos F, Idbaih A, Frenel JS, et al. Marizomib for patients with newly diagnosed glioblastoma: A randomized phase 3 trial. Neuro Oncol. 2024 Sep 1;26(9):1670–82. doi:10.1093/NEUONC/NOAE053 PubMed PMID: 38502052.

31. Study Details | NCT01348919 | Delanzomib (CEP-18770) in Combination With Lenalidomide and Dexamethasone in Relapsed or Refractory Multiple Myeloma | ClinicalTrials.gov [Internet]. [cited 2025 Dec 28]. Available from: https://www.clinicaltrials.gov/study/NCT01348919

32. Vogl DT, Martin TG, Vij R, Hari P, Mikhael JR, Siegel D, et al. Phase I/II study of the novel proteasome inhibitor delanzomib (CEP-18770) for relapsed and refractory multiple myeloma. Leuk Lymphoma. 2017 Aug 3;58(8):1872–9. doi:10.1080/10428194.2016.1263842 PubMed PMID: 28140719.

33. Nagaraj NS, Singh O V., Merchant NB. Proteomics: a strategy to understand the novel targets in protein misfolding and cancer therapy. Expert Rev Proteomics. 2010 Aug;7(4):613–23. doi:10.1586/EPR.10.70 PubMed PMID: 20653514.

34. Aronson LI, Davies FE. DangER: protein ovERload. Targeting protein degradation to treat myeloma. Haematologica. 2012 Aug 1;97(8):1119–30. doi:10.3324/HAEMATOL.2012.064923 PubMed PMID: 22580998.

35. Ito S. Proteasome Inhibitors for the Treatment of Multiple Myeloma. Cancers (Basel). 2020 Feb 1;12(2):265. doi:10.3390/CANCERS12020265 PubMed PMID: 31979059.

36. Zhang L, Wu M, Su R, Zhang D, Yang G. The Efficacy and Mechanism of Proteasome Inhibitors in Solid Tumor Treatment. Recent Pat Anticancer Drug Discov. 2022 Dec 3;17(3):268–83. doi:10.2174/1574892816666211202154536 PubMed PMID: 34856915.

37. Weyburne ES, Wilkins OM, Sha Z, Williams DA, Pletnev AA, de Bruin G, et al. Inhibition of the proteasome β2 site sensitizes triple-negative breast cancer cells to β5 inhibitors through a mechanism involving Nrf1 suppression. Cell Chem Biol. 2017 Feb 16;24(2):218–30. doi:10.1016/J.CHEMBIOL.2016.12.016 PubMed PMID: 28132893.

38. Roeten MSF, Cloos J, Jansen G. Positioning of proteasome inhibitors in therapy of solid malignancies. Cancer Chemother Pharmacol. 2017 Feb 1;81(2):227–43. doi:10.1007/S00280-017-3489-0 PubMed PMID: 29184971.

39. Asano S, Fukuda Y, Beck F, Aufderheide A, Förster F, Danev R, et al. A molecular census of 26S proteasomes in intact neurons. Science. 2015 Jan 23;347(6220):439–42.

40. Chui MH, Doodnauth SA, Erdmann N, Tiedemann RE, Sircoulomb F, Drapkin R, et al. Chromosomal instability and mTORC1 activation through PTEN loss contribute to proteotoxic stress in ovarian carcinoma. Cancer Res. 2019 Nov 1;79(21):5536–49. doi:10.1158/0008-5472.CAN-18-3029 PubMed PMID: 31530568.

41. Fraunhoffer NA, Abuelafia AM, Bigonnet M, Gayet O, Roques J, Telle E, et al. Evidencing a pancreatic ductal adenocarcinoma subpopulation sensitive to the proteasome inhibitor carfilzomib. Clinical Cancer Research. 2020 Oct 15;26(20):5506–19. doi:10.1158/1078-0432.CCR-20-1232 PubMed PMID: 32669378.

42. Cerruti F, Jocollè G, Salio C, Oliva L, Paglietti L, Alessandria B, et al. Proteasome stress sensitizes malignant pleural mesothelioma cells to bortezomib-induced apoptosis. Sci Rep. 2017 Dec 1;7(1). doi:10.1038/s41598-017-17977-9 PubMed PMID: 29247244.

43. Jiang TY, Pan YF, Wan ZH, Lin YK, Zhu B, Yuan ZG, et al. PTEN status determines chemosensitivity to proteasome inhibition in cholangiocarcinoma. Sci Transl Med. 2020 Sep 23;12(562). doi:10.1126/scitranslmed.aay0152 PubMed PMID: 32967970.

44. Busacca S, Chacko AD, Klabatsa A, Arthur K, Sheaff M, Gunasekharan VK, et al. BAK and NOXA Are Critical Determinants of Mitochondrial Apoptosis Induced by Bortezomib in Mesothelioma. PLoS One. 2013 Jun 7;8(6). doi:10.1371/journal.pone.0065489 PubMed PMID: 23762382.

45. Selimovic D, Porzig BBOW, El-Khattouti A, Badura HE, Ahmad M, Ghanjati F, et al. Bortezomib/proteasome inhibitor triggers both apoptosis and autophagy-dependent pathways in melanoma cells. Cell Signal. 2013;25(1):308–18. doi:10.1016/j.cellsig.2012.10.004 PubMed PMID: 23079083.

46. Nawrocki ST, Mcconkey DJ. The proteasome inhibitor bortezomib inhibits tumor cell growth and induces apoptosis by activating the cJUN NH2-terminal kinase (JNK) pathway in pancreatic cancer. Cancer Res. 2004 Apr 1;64(7):4005.

47. Herrmann JL, Briones F, Brisbay S, Logothetis CJ, Mcdonnell TJ. Prostate carcinoma cell death resulting from inhibition of proteasome activity is independent of functional Bcl-2 and p53. Oncogene [Internet]. 1998 Dec 7 [cited 2026 Apr 16];17(22):2889–99. Available from: https://pubmed.ncbi.nlm.nih.gov/9879995/

48. Fribley A, Zeng Q, Wang CY. Proteasome Inhibitor PS-341 Induces Apoptosis through Induction of Endoplasmic Reticulum Stress-Reactive Oxygen Species in Head and Neck Squamous Cell Carcinoma Cells. Mol Cell Biol. 2004 Nov 1;24(22):9695–704. doi:10.1128/mcb.24.22.9695-9704.2004 PubMed PMID: 15509775.

49. Zanotto-Filho A, Braganhol E, Oliveira Battastini AM, Fonseca Moreira JC. Proteasome inhibitor MG132 induces selective apoptosis in glioblastoma cells through inhibition of PI3K/Akt and NFkappaB pathways, mitochondrial dysfunction, and activation of p38-JNK1/2 signaling. Invest New Drugs. 2012 Dec 28;30(6):2252–62. doi:10.1007/S10637-012-9804-Z/FIGURES/7 PubMed PMID: 22367315.

50. Yin D, Zhou H, Kumagai T, Liu G, Ong JM, Black KL, et al. Proteasome inhibitor PS-341 causes cell growth arrest and apoptosis in human glioblastoma multiforme (GBM).

Oncogene 2005 24:3. 2004 Nov 8;24(3):344–54. doi:10.1038/sj.onc.1208225 PubMed PMID: 15531918.

51. Benitez JA, Finlay D, Castanza A, Parisian AD, Ma J, Longobardi C, et al. PTEN deficiency leads to proteasome addiction: a novel vulnerability in glioblastoma. Neuro Oncol. 2021 Jul 1;23(7):1072–86. doi:10.1093/NEUONC/NOAB001 PubMed PMID: 33428749.

52. Di K, Lloyd GK, Abraham V, Maclaren A, Burrows FJ, Desjardins A, et al. Marizomib activity as a single agent in malignant gliomas: ability to cross the blood-brain barrier. Neuro Oncol. 2015 Jun 10;18(6):840–8. doi:10.1093/NEUONC/NOV299 PubMed PMID: 26681765.

53. Zhang X, Li W, Wang C, Leng X, Lian S, Feng J, et al. Inhibition of autophagy enhances apoptosis induced by proteasome inhibitor bortezomib in human glioblastoma U87 and U251 cells. Mol Cell Biochem. 2013 Jan;385(1):265–75. doi:10.1007/S11010-013-1835-Z PubMed PMID: 24104452.

54. Manton CA, Johnson B, Singh M, Bailey CP, Bouchier-Hayes L, Chandra J. Induction of cell death by the novel proteasome inhibitor marizomib in glioblastoma in vitro and in vivo. Sci Rep. 2016 Jan 25;6:18953. doi:10.1038/SREP18953 PubMed PMID: 26804704.

55. Yoo YD, Lee D, Cha-Molstad H, Kim H, Mun SR, Ji C, et al. Glioma-derived cancer stem cells are hypersensitive to proteasomal inhibition. EMBO Rep. 2016 Jan;18(1):150–68. doi:10.15252/EMBR.201642360 PubMed PMID: 27993939.

56. Hoerig CM, Plant-Fox AS, Pulley MD, Di K, Bota DA. Exploring the role and clinical implications of proteasome inhibition in medulloblastoma. Pediatr Blood Cancer. 2021 Oct 1;68(10):e29168. doi:10.1002/PBC.29168 PubMed PMID: 34114315.

57. Shi Y, Bieerkehazhi S, Ma H. Next-generation proteasome inhibitor oprozomib enhances sensitivity to doxorubicin in triple-negative breast cancer cells. Int J Clin Exp Pathol. 2018;11(5):2347–55. PubMed PMID: 31938346.

58. Larsson P, Pettersson D, Olsson M, Sarathchandra S, Abramsson A, Zetterberg H, et al. Repurposing proteasome inhibitors for improved treatment of triple-negative breast cancer. Cell Death Discovery 2024 10:1. 2024 Jan 29;10(1):1–15. doi:10.1038/s41420-024-01819-5

59. Chua ADW, Thaarun T, Yang H, Lee ARY Bin. Proteasome inhibitors in the treatment of nonsmall cell lung cancer: A systematic review of clinical evidence. Health Sci Rep. 2023 Nov 1;6(11):e1443. doi:10.1002/HSR2.1443 PubMed PMID: 38028684.

60. Rao R, Nalluri S, Fiskus W, Savoie A, Buckley KM, Ha K, et al. Role of C/EBP homologous protein (CHOP) in Panobinostat-mediated potentiation of Bortezomib-

induced lethal ER stress in Mantle Cell Lymphoma cells. Clin Cancer Res. 2010 Oct 10;16(19):4742. doi:10.1158/1078-0432.CCR-10-0529 PubMed PMID: 20647473.

61. Pérez-Galán P, Roue G, Villamor N, Montserrat E, Campo E, Colomer D. The proteasome inhibitor bortezomib induces apoptosis in mantle-cell lymphoma through generation of ROS and Noxa activation independent of p53 status. Blood. 2006 Jan 1;107(1):257–64. doi:10.1182/BLOOD-2005-05-2091 PubMed PMID: 16166592.

62. Dunleavy K, Pittaluga S, Czuczman MS, Dave SS, Wright G, Grant N, et al. Differential efficacy of bortezomib plus chemotherapy within molecular subtypes of diffuse large B-cell lymphoma. Blood. 2009 Jun 6;113(24):6069–76. doi:10.1182/BLOOD-2009-01-199679 PubMed PMID: 19380866.

63. Ling YH, Liebes L, Zou Y, Perez-Soler R. Reactive oxygen species generation and mitochondrial dysfunction in the apoptotic response to Bortezomib, a novel proteasome inhibitor, in human H460 non-small cell lung cancer cells. J Biol Chem. 2003 Sep 5;278(36):33714–23. doi:10.1074/JBC.M302559200 PubMed PMID: 12821677.

64. O'Connor OA, Wright J, Moskowitz C, Muzzy J, MacGregor-Cortelli B, Stubblefield M, et al. Phase II clinical experience with the novel proteasome inhibitor bortezomib in patients with indolent non-Hodgkin's lymphoma and mantle cell lymphoma. J Clin Oncol. 2005;23(4):676–84. doi:10.1200/JCO.2005.02.050 PubMed PMID: 15613699.

65. Goy A, Younes A, McLaughlin P, Pro B, Romaguera JE, Hagemeister F, et al. Phase II study of proteasome inhibitor bortezomib in relapsed or refractory B-cell non-Hodgkin's lymphoma. J Clin Oncol. 2005;23(4):667–75. doi:10.1200/JCO.2005.03.108 PubMed PMID: 15613697.

66. Evens AM, Smith MR, Lossos IS, Helenowski I, Millenson M, Winter JN, et al. Frontline bortezomib and rituximab for the treatment of newly diagnosed high tumour burden indolent non-Hodgkin lymphoma: A multicentre phase II study. Br J Haematol. 2014;166(4):514–20. doi:10.1111/BJH.12915 PubMed PMID: 24761968.

67. Boccellato C, Kolbe E, Peters N, Juric V, Fullstone G, Verreault M, et al. Marizomib sensitizes primary glioma cells to apoptosis induced by a latest-generation TRAIL receptor agonist. Cell Death & Disease 2021 12:7. 2021 Jun 24;12(7):1–11. doi:10.1038/s41419-021-03927-x PubMed PMID: 34168123.

68. Nath Varma S, Ye S, Ferlin S, Comer C, Cotton K, Niklison-Chirou MV. The Proteasome Inhibitor CEP-18770 Induces Cell Death in Medulloblastoma. Pharmaceutics. 2024 May 1;16(5):672. doi:10.3390/PHARMACEUTICS16050672 PubMed PMID: 38794334.

69. Bianchi G, Oliva L, Cascio P, Pengo N, Fontana F, Cerruti F, et al. The proteasome load versus capacity balance determines apoptotic sensitivity of multiple myeloma cells to

proteasome inhibition. Blood. 2009 Mar 26;113(13):3040–9. doi:10.1182/BLOOD-2008-08-172734 PubMed PMID: 19164601.

70. Deshaies RJ. Proteotoxic crisis, the ubiquitin-proteasome system, and cancer therapy. BMC Biol. 2014;12(1):94. doi:10.1186/S12915-014-0094-0 PubMed PMID: 25385277.

71. Xu Y, Fulciniti M, Samur MK, Ho M, Deng S, Liu L, et al. YWHAE/14-3-3e expression impacts the protein load, contributing to proteasome inhibitor sensitivity in multiple myeloma. Blood. 2020 Jul 1;136(4):468–79. doi:10.1182/BLOOD.2019004147 PubMed PMID: 32187357.

72. Cenci S, Oliva L, Cerruti F, Milan E, Bianchi G, Raule M, et al. Pivotal Advance: Protein synthesis modulates responsiveness of differentiating and malignant plasma cells to proteasome inhibitors. J Leukoc Biol. 2012 Nov 1;92(5):921–31. doi:10.1189/jlb.1011497 PubMed PMID: 22685320.

73. Cenci S, Mezghrani A, Cascio P, Bianchi G, Cerruti F, Fra A, et al. Progressively impaired proteasomal capacity during terminal plasma cell differentiation. EMBO Journal. 2006 Mar 8;25(5):1104–13. doi:10.1038/SJ.EMBOJ.7601009/FIGURES/7 PubMed PMID: 16498407.

74. Misiewicz-Krzeminska I, de Ramón C, Corchete LA, Krzeminski P, Rojas EA, Isidro I, et al. Quantitative expression of Ikaros, IRF4, and PSMD10 proteins predicts survival in VRD-treated patients with multiple myeloma. Blood Adv. 2020 Dec 8;4(23):6023–33. doi:10.1182/bloodadvances.2020002711 PubMed PMID: 33284947.

75. Dantuma NP, Lindsten K, Glas R, Jellne M, Masucci MG. Short-lived green fluorescent proteins for quantifying ubiquitin/proteasome-dependent proteolysis in living cells. Nat Biotechnol. 2000 May;18(5):538–43. doi:10.1038/75406 PubMed PMID: 10802622.

76. Huang Z, Wu Y, Zhou X, Xu J, Zhu W, Shu Y, et al. Efficacy of therapy with bortezomib in solid tumors: a review based on 32 clinical trials. Future Oncol. 2014 Aug 1;10(10):1795–807. doi:10.2217/FON.14.30 PubMed PMID: 25303058.

77. Alwahsh M, Farhat J, Talhouni S, Hamadneh L, Hergenröder R. Bortezomib advanced mechanisms of action in multiple myeloma, solid and liquid tumors along with its novel therapeutic applications. EXCLI J. 2023;22:146–68. doi:10.17179/EXCLI2022-5653 PubMed PMID: 36998701.

78. Zhou W, Hu J, Tang H, Wang D, Huang X, He C, et al. Small interfering RNA targeting mcl-1 enhances proteasome inhibitor-induced apoptosis in various solid malignant tumors. BMC Cancer. 2011 Nov 14;11:485. doi:10.1186/1471-2407-11-485 PubMed PMID: 22078414.

79. Papandreou CN, Daliani DD, Nix D, Yang H, Madden T, Wang X, et al. Phase I trial of the proteasome inhibitor bortezomib in patients with advanced solid tumors with observations in androgen-independent prostate cancer. J Clin Oncol. 2004;22(11):2108–21. doi:10.1200/JCO.2004.02.106 PubMed PMID: 15169797.

80. Aviner R. The science of puromycin: From studies of ribosome function to applications in biotechnology. Comput Struct Biotechnol J. 2020 Jan 1;18:1074. doi:10.1016/J.CSBJ.2020.04.014 PubMed PMID: 32435426.

81. Laplante M, Sabatini DM. mTOR signaling at a glance. J Cell Sci. 2009 Oct 15;122(20):3589–94. doi:10.1242/JCS.051011 PubMed PMID: 19812304.

82. Panwar V, Singh A, Bhatt M, Tonk RK, Azizov S, Raza AS, et al. Multifaceted role of mTOR (mammalian target of rapamycin) signaling pathway in human health and disease. Signal Transduction and Targeted Therapy 2023. 2023 Oct 2;8(1):375. doi:10.1038/s41392-023-01608-z PubMed PMID: 37779156.

83. Decaux O, Clément M, Magrangeas F, Gouraud W, Charbonnel C, Campion L, et al. Inhibition of mTORC1 activity by REDD1 induction in myeloma cells resistant to bortezomib cytotoxicity. Cancer Sci. 2010 Apr;101(4):889–97. doi:10.1111/j.1349-7006.2009.01467.x PubMed PMID: 20100206.

84. Kim JY, Kwon YG, Kim YM. The stress-responsive protein REDD1 and its pathophysiological functions. Exp Mol Med. 2023 Sep 1;55(9):1933–44. doi:10.1038/S12276-023-01056-3 PubMed PMID: 37653030.

85. Meister S, Schubert U, Neubert K, Herrmann K, Burger R, Gramatzki M, et al. Extensive immunoglobulin production sensitizes myeloma cells for proteasome inhibition. Cancer Res. 2007 Feb 15;67(4):1783–92. doi:10.1158/0008-5472.CAN-06-2258 PubMed PMID: 17308121.

86. Ip CKM, Wong AST. p70 S6 kinase and actin dynamics: A perspective. Spermatogenesis. 2012 Jan;2(1):44–52. doi:10.4161/SPMG.19413 PubMed PMID: 22553489.

87. Wang T, Edgar BA. TOR Signaling and Cell Death. Enzymes (Essen). 2010 Jan 1;28(C):217–44. doi:10.1016/S1874-6047(10)28011-3

88. Fumarola C, La Monica S, Alfieri RR, Borra E, Guidotti GG. Cell size reduction induced by inhibition of the mTOR/S6K-signaling pathway protects Jurkat cells from apoptosis. Cell Death & Differentiation 2005 12:10. 2005 May 20;12(10):1344–57. doi:10.1038/sj.cdd.4401660 PubMed PMID: 15905878.

89. Hopkins BD, Hodakoski C, Barrows D, Mense SM, Parsons RE. PTEN function, the long and the short of it. Trends Biochem Sci. 2014;39(4):183–90. doi:10.1016/J.TIBS.2014.02.006 PubMed PMID: 24656806.

90. Molinari F, Frattini M. Functions and regulation of the PTEN gene in colorectal cancer. Front Oncol. 2014 Jan 15;3:326. doi:10.3389/FONC.2013.00326/BIBTEX

91. Dibble CC, Cantley LC. Regulation of mTORC1 by PI3K Signaling. Trends Cell Biol. 2015 Sep 1;25(9):545–55. doi:10.1016/J.TCB.2015.06.002 PubMed PMID: 26159692.

92. Li H, Prever L, Hirsch E, Gulluni F. Targeting pi3k/akt/mtor signaling pathway in breast cancer. Cancers (Basel). 2021 Jul 2;13(14):3517. doi:10.3390/CANCERS13143517/S1

93. Jiang TY, Feng XF, Fang Z, Cui XW, Lin YK, Pan YF, et al. PTEN deficiency facilitates the therapeutic vulnerability to proteasome inhibitor bortezomib in gallbladder cancer. Cancer Lett. 2021 Mar 31;501:187–99. doi:10.1016/J.CANLET.2020.11.016 PubMed PMID: 33220333.

94. Oromendia AB, Dodgson SE, Amon A. Aneuploidy causes proteotoxic stress in yeast. Genes Dev. 2012;26(24):2696–708. doi:10.1101/GAD.207407.112 PubMed PMID: 23222101.

95. Santaguida S, Amon A. Short- and long-term effects of chromosome mis-segregation and aneuploidy. Nature Reviews Molecular Cell Biology 2015 16:8. 2015 Jul 23;16(8):473–85. doi:10.1038/nrm4025 PubMed PMID: 26204159.

96. Santaguida S, Vasile E, White E, Amon A. Aneuploidy-induced cellular stresses limit autophagic degradation. Genes Dev. 2015 Oct 1;29(19):2010–21. doi:10.1101/GAD.269118.115 PubMed PMID: 26404941.

97. HSPA5 - Endoplasmic reticulum chaperone BiP - Homo sapiens (Human) | UniProtKB | UniProt [Internet]. [cited 2026 Jan 15]. Available from: https://www.uniprot.org/uniprotkb/P11021/entry

98. Pobre KFR, Poet GJ, Hendershot LM. The endoplasmic reticulum (ER) chaperone BiP is a master regulator of ER functions: Getting by with a little help from ERdj friends. J Biol Chem. 2018 Feb 8;294(6):2098–108. doi:10.1074/JBC.REV118.002804 PubMed PMID: 30563838.

99. Núñez-Vázquez S, Sánchez-Vera I, Saura-Esteller J, Cosialls AM, Noisier AFM, Albericio F, et al. NOXA upregulation by the prohibitin-binding compound fluorizoline is transcriptionally regulated by integrated stress response-induced ATF3 and ATF4. FEBS J. 2021 Feb 1;288(4):1271–85. doi:10.1111/FEBS.15480 PubMed PMID: 32648994.

100. Rosebeck S, Sudini K, Chen T, Leaman DW. Involvement of Noxa in mediating cellular ER stress responses to lytic virus infection. Virology. 2011 Sep 1;417(2):293–303. doi:10.1016/J.VIROL.2011.06.010 PubMed PMID: 21742363.

101. Neill G, Masson GR. A stay of execution: ATF4 regulation and potential outcomes for the integrated stress response. Front Mol Neurosci. 2023 Feb 7;16:1112253. doi:10.3389/FNMOL.2023.1112253/XML

102. Zheng X, Han C, Ge K, Li Z, Wu P, Yu X, et al. Regulation of the PERK pathway attenuates hypoxia-induced apoptosis in a 661W photoreceptor cell model. Exp Eye Res. 2025 Dec 1;261:110667. doi:10.1016/J.EXER.2025.110667 PubMed PMID: 41043499.

103. Abdel-Nour M, Carneiro LAM, Downey J, Tsalikis J, Outlioua A, Prescott D, et al. The heme-regulated inhibitor is a cytosolic sensor of protein misfolding that controls innate immune signaling. Science (1979). 2019;364(6448):eaaw4144. doi:10.1126/science.aaw4144 PubMed PMID: 31273097.

104. Pakos-Zebrucka K, Koryga I, Mnich K, Ljujic M, Samali A, Gorman AM. The integrated stress response. EMBO Rep. 2016 Oct;17(10):1374–95. doi:10.15252/EMBR.201642195 PubMed PMID: 27629041.

105. Obeng EA, Carlson LM, Gutman DM, Harrington WJ, Lee KP, Boise LH. Proteasome inhibitors induce a terminal unfolded protein response in multiple myeloma cells. Blood. 2006 Jun 15;107(12):4907–16. doi:10.1182/BLOOD-2005-08-3531 PubMed PMID: 16507771.

106. Schewe DM, Aguirre-Ghiso JA. Inhibition of eIF2α Dephosphorylation Maximizes Bortezomib Efficiency and Eliminates Quiescent Multiple Myeloma Cells Surviving Proteasome Inhibitor Therapy. Cancer Res. 2009 Feb 15;69(4):1545–52. doi:10.1158/0008-5472.CAN-08-3858 PubMed PMID: 19190324.

107. Vandewynckel YP, Coucke C, Laukens D, Devisscher L, Paridaens A, Bogaerts E, et al. Next-generation proteasome inhibitor oprozomib synergizes with modulators of the unfolded protein response to suppress hepatocellular carcinoma. Oncotarget. 2016 May 7;7(23):34988–5000. doi:10.18632/ONCOTARGET.9222 PubMed PMID: 27167000.

108. White MC, Schroeder RD, Zhu K, Xiong K, McConkey DJ. HRI-mediated translational repression reduces proteotoxicity and sensitivity to bortezomib in human pancreatic cancer cells. Oncogene. 2018 Aug 9;37(32):4413–27. doi:10.1038/S41388-018-0227-Y PubMed PMID: 29720726.

109. Nawrocki ST, Carew JS, Dunner K, Boise LH, Chiao PJ, Huang P, et al. Bortezomib Inhibits PKR-Like Endoplasmic Reticulum (ER) Kinase and Induces Apoptosis via ER Stress in Human Pancreatic Cancer Cells. Cancer Res. 2005 Dec 15;65(24):11510–9. doi:10.1158/0008-5472.CAN-05-2394 PubMed PMID: 16357160.

110. Yang Y, Liu L, Naik I, Braunstein Z, Zhong J, Ren B. Transcription Factor C/EBP Homologous Protein in Health and Diseases. Front Immunol. 2017 Nov 27;8(NOV):1612. doi:10.3389/FIMMU.2017.01612 PubMed PMID: 29230213.

111. Jiang HY, Wek RC. Phosphorylation of the α-subunit of the eukaryotic initiation factor-2 (eIF2α) reduces protein synthesis and enhances apoptosis in response to proteasome inhibition. Journal of Biological Chemistry. 2005 Apr 8;280(14):14189–202. doi:10.1074/JBC.M413660200/ASSET/0078378C-EFC2-4B3A-B513-DE3272F77910/MAIN.ASSETS/GR11.JPG PubMed PMID: 15684420.

112. Zhang S, Macias-Garcia A, Ulirsch JC, Velazquez J, Butty VL, Levine SS, et al. HRI coordinates translation necessary for protein homeostasis and mitochondrial function in erythropoiesis. Elife. 2019 Apr 1;8:e46976. doi:10.7554/ELIFE.46976 PubMed PMID: 31033440.

113. Chakrabarty Y, Yang Z, Chen H, Chan DC. The HRI branch of the integrated stress response selectively triggers mitophagy. Mol Cell. 2024 Mar 21;84(6):1090–100. doi:10.1016/J.MOLCEL.2024.01.016 PubMed PMID: 38340717.

114. Chen JJ. HRI protein kinase in cytoplasmic heme sensing and mitochondrial stress response: Relevance to hematological and mitochondrial diseases. Journal of Biological Chemistry. 2025 May 1;301(5):108494. doi:10.1016/J.JBC.2025.108494 PubMed PMID: 40209956.

115. Zhao C, Guo H, Hou Y, Lei T, Wei D, Zhao Y. Multiple Roles of the Stress Sensor GCN2 in Immune Cells. Int J Mol Sci. 2023 Mar 1;24(5):4285. doi:10.3390/IJMS24054285 PubMed PMID: 36901714.

116. Jiang HY, Wek RC. Phosphorylation of the α-Subunit of the Eukaryotic Initiation Factor-2 (eIF2α) Reduces Protein Synthesis and Enhances Apoptosis in Response to Proteasome Inhibition. Journal of Biological Chemistry. 2005 Apr 8;280(14):14189–202. doi:10.1074/JBC.M413660200 PubMed PMID: 15684420.

117. Kale J, Osterlund EJ, Andrews DW. BCL-2 family proteins: changing partners in the dance towards death. Cell Death & Differentiation 2018 25:1. 2017 Nov 17;25(1):65–80. doi:10.1038/cdd.2017.186 PubMed PMID: 29149100.

118. Peña-Blanco A, García-Sáez AJ. Bax, Bak and beyond - mitochondrial performance in apoptosis. FEBS J. 2018 Feb 1;285(3):416–31. doi:10.1111/FEBS.14186 PubMed PMID: 28755482.

119. Renault TT, Chipuk JE. Death upon a kiss: mitochondrial outer membrane composition and organelle communication govern sensitivity to BAK/BAX-dependent apoptosis. Chem Biol. 2013 Jan 16;21(1):114–23. doi:10.1016/J.CHEMBIOL.2013.10.009 PubMed PMID: 24269152.

120. L.Omonosova E, C.Hinnadurai G. BH3-only proteins in apoptosis and beyond: an overview. Oncogene 2009 27:1. 2009 Jul 30;27(1):S2–19. doi:10.1038/onc.2009.39 PubMed PMID: 19641503.

121. Zhu H, Zhang L, Dong F, Guo W, Wu S, Teraishi F, et al. Bik/NBK accumulation correlates with apoptosis-induction by bortezomib (PS-341, Velcade) and other proteasome inhibitors. Oncogene. 2005 Jul 21;24(31):4993–9. doi:10.1038/SJ.ONC.1208683 PubMed PMID: 15824729.

122. Nikrad M, Johnson T, Puthalalath H, Coultas L, Adams J, Kraft AS. The proteasome inhibitor bortezomib sensitizes cells to killing by death receptor ligand TRAIL via BH3-only proteins Bik and Bim. Mol Cancer Ther. 2005 Mar 1;4(3):443–9. doi:10.1158/1535-7163.MCT-04-0260 PubMed PMID: 15767553.

123. Fernández Y, Verhaegen M, Miller TP, Rush JL, Steiner P, Opipari AW, et al. Differential Regulation of Noxa in Normal Melanocytes and Melanoma Cells by Proteasome Inhibition: Therapeutic Implications. Cancer Res [Internet]. 2005 Jul 15;65(14):6294–304. Available from: http://cancerres.aacrjournals.org/

124. Shibue T, Suzuki S, Okamoto H, Yoshida H, Ohba Y, Takaoka A, et al. Differential contribution of Puma and Noxa in dual regulation of p53-mediated apoptotic pathways. EMBO J. 2006 Oct 10;25(20):4952–62. doi:10.1038/SJ.EMBOJ.7601359 PubMed PMID: 17024184.

125. Qin JZ, Ziffra J, Stennett L, Bodner B, Bonish BK, Chaturvedi V, et al. Proteasome Inhibitors Trigger NOXA-Mediated Apoptosis in Melanoma and Myeloma Cells. Cancer Res. 2005 Jul 15;65(14):6282–93. doi:10.1158/0008-5472.CAN-05-0676 PubMed PMID: 16024630.

126. Baou M, Kohlhaas SL, Butterworth M, Vogler M, Dinsdale D, Walewska R, et al. Role of NOXA and its ubiquitination in proteasome inhibitor-induced apoptosis in chronic lymphocytic leukemia cells. Haematologica. 2010 Sep;95(9):1510–8. doi:10.3324/HAEMATOL.2010.022368 PubMed PMID: 20378569.

127. Fribley AM, Evenchik B, Zeng Q, Park BK, Guan JY, Zhang H, et al. Proteasome inhibitor PS-341 induces apoptosis in cisplatin-resistant squamous cell carcinoma cells by induction of Noxa. J Biol Chem. 2006 Oct 20;281(42):31440–7. doi:10.1074/JBC.M604356200 PubMed PMID: 16928686.

128. Qin JZ, Ziffra J, Stennett L, Bodner B, Bonish BK, Chaturvedi V, et al. Proteasome inhibitors trigger NOXA-mediated apoptosis in melanoma and myeloma cells. Cancer Res. 2005 Jul 15;65(14):6282–93. doi:10.1158/0008-5472.CAN-05-0676 PubMed PMID: 16024630.

129. Fernández Y, Verhaegen M, Miller TP, Rush JL, Steiner P, Opipari AW, et al. Differential regulation of noxa in normal melanocytes and melanoma cells by proteasome inhibition: therapeutic implications. Cancer Res. 2005 Jul 15;65(14):6294–304. doi:10.1158/0008-5472.CAN-05-0686 PubMed PMID: 16024631.

130. Besse A, Sedlarikova L, Buechler L, Kraus M, Yang CH, Strakova N, et al. HIV-protease inhibitors potentiate the activity of carfilzomib in triple-negative breast cancer. British Journal of Cancer 2024. 2024 Jul 5;131(5):918–30. doi:10.1038/s41416-024-02774-9 PubMed PMID: 38969867.

131. Lankes K, Hassan Z, Doffo MJ, Schneeweis C, Lier S, Öllinger R, et al. Targeting the ubiquitin-proteasome system in a pancreatic cancer subtype with hyperactive MYC. Mol Oncol. 2020 Dec 1;14(12):3048–64. doi:10.1002/1878-0261.12835 PubMed PMID: 33099868.

132. Pourdehnad M, Truitt ML, Siddiqi IN, Ducker GS, Shokat KM, Ruggero D. Myc and mTOR converge on a common node in protein synthesis control that confers synthetic lethality in Myc-driven cancers. Proc Natl Acad Sci U S A. 2013 Jul 16;110(29):11988–93. doi:10.1073/pnas.1310230110 PubMed PMID: 23803853.

133. Lauricella M, Emanuele S, D'Anneo A, Calvaruso G, Vassallo B, Carlisi D, et al. JNK and AP-1 mediate apoptosis induced by bortezomib in HepG2 cells via FasL/caspase-8 and mitochondria-dependent pathways. Apoptosis. 2006 Mar;11(4):607–25. doi:10.1007/s10495-006-4689-y PubMed PMID: 16528474.

134. Cenci S, van Anken E, Sitia R. Proteostenosis and plasma cell pathophysiology. Current Opinion in Cell Biology. 2011. p. 216–22. doi:10.1016/j.ceb.2010.11.004 PubMed PMID: 21169004.

135. Cascio P, Oliva L, Cerruti F, Mariani E, Pasqualetto E, Cenci S, et al. Dampening Ab responses using proteasome inhibitors following in vivo B cell activation. Eur J Immunol. 2008 Mar 1;38(3):658–67. doi:10.1002/EJI.200737743 PubMed PMID: 18253932.

136. Yu J, Wang Z, Kinzler KW, Vogelstein B, Zhang L. PUMA mediates the apoptotic response to p53 in colorectal cancer cells. Proc Natl Acad Sci U S A. 2003 Feb 18;100(4):1931–6. doi:10.1073/PNAS.2627984100/ASSET/62D191A3-8810-4E5A-AEFC-4B1E836921C6/ASSETS/GRAPHIC/PQ0437984005.JPEG PubMed PMID: 12574499.

137. Nakano K, Vousden KH. PUMA, a Novel Proapoptotic Gene, Is Induced by p53. Mol Cell. 2001 Mar 1;7(3):683–94. doi:10.1016/S1097-2765(01)00214-3 PubMed PMID: 11463392.

138. Ding WX, Ni HM, Chen X, Yu J, Zhang L, Yin XM. A coordinated action of Bax, PUMA, and p53 promotes MG132-induced mitochondria activation and apoptosis in colon cancer cells. Mol Cancer Ther. 2007 Mar 1;6(3):1062–9. doi:10.1158/1535-7163.MCT-06-0541 PubMed PMID: 17363499.

139. Podar K, Raab MS, Tonon G, Sattler M, Barilà D, Zhang J, et al. Up-regulation of c-Jun inhibits proliferation and induces apoptosis via caspase-triggered c-Abl cleavage in human

multiple myeloma. Cancer Res. 2007 Feb 15;67(4):1680–8. doi:10.1158/0008-5472.CAN-06-1863 PubMed PMID: 17308109.

140. Chen J, Ye C, Wan C, Li G, Peng L, Peng Y, et al. The Roles of c-Jun N-Terminal Kinase (JNK) in Infectious Diseases. Int J Mol Sci. 2021 Sep 1;22(17):9640. doi:10.3390/IJMS22179640 PubMed PMID: 34502556.

141. Bogoyevitch MA, Kobe B. Uses for JNK: the Many and Varied Substrates of the c-Jun N-Terminal Kinases. Microbiology and Molecular Biology Reviews. 2006 Dec;70(4):1061–95. doi:10.1128/MMBR.00025-06 PubMed PMID: 17158707.

142. Pietkiewicz S, Sohn D, Piekorz RP, Grether-Beck S, Budach W, Sabapathy K, et al. Oppositional Regulation of Noxa by JNK1 and JNK2 during Apoptosis Induced by Proteasomal Inhibitors. PLoS One. 2013 Apr 11;8(4):e61438. doi:10.1371/journal.pone.0061438 PubMed PMID: 23593480.

143. Nunes AT, Annunziata CM. Proteasome Inhibitors: Structure and Function. Semin Oncol. 2018 Dec 1;44(6):377–80. doi:10.1053/J.SEMINONCOL.2018.01.004 PubMed PMID: 29935898.

144. Lin A. Activation of the JNK signaling pathway: Breaking the brake on apoptosis. BioEssays. 2003 Jan 1;25(1):17–24. doi:10.1002/BIES.10204 PubMed PMID: 12508278.

145. Son Y, Cheong YK, Kim NH, Chung HT, Kang DG, Pae HO. Mitogen-Activated Protein Kinases and Reactive Oxygen Species: How Can ROS Activate MAPK Pathways? J Signal Transduct. 2011 Feb 6;2011:792639. doi:10.1155/2011/792639 PubMed PMID: 21637379.

146. Treatment of Triple-negative Breast Cancer | Treatment of TNBC | American Cancer Society [Internet]. [cited 2026 Jan 18]. Available from: https://www.cancer.org/cancer/types/breast-cancer/treatment/treatment-of-triple-negative.html

147. FDA Approves KEYTRUDA® (pembrolizumab) for Treatment of Patients With High-Risk Early-Stage Triple-Negative Breast Cancer in Combination With Chemotherapy as Neoadjuvant Treatment, Then Continued as Single Agent as Adjuvant Treatment After Surgery - Merck.com [Internet]. [cited 2026 Jan 18]. Available from: https://www.merck.com/news/fda-approves-keytruda-pembrolizumab-for-treatment-of-patients-with-high-risk-early-stage-triple-negative-breast-cancer-in-combination-with-chemotherapy-as-neoadjuvant-treatment-then-continued/

148. Keskinkilic M, Sacks R. Antibody-Drug Conjugates in Triple Negative Breast Cancer. Clin Breast Cancer. 2024 Apr 1;24(3):163–74. doi:10.1016/J.CLBC.2024.01.008 PubMed PMID: 38341370.

149. Izadi A, Naimi A, Amjadi E, Beheshtiparvar D, Soltan M. The Prevalence of PD-L1 Expression in Triple-Negative Breast Cancer Patients and Its Correlation with Survival Rates and Other Prognostic Factors: A Survival Analysis. Adv Biomed Res. 2024 Sep 1;13(1):86. doi:10.4103/ABR.ABR_2_24 PubMed PMID: 39512412.

150. Danziger N, Sokol ES, Graf RP, Hiemenz MC, Maule J, Parimi V, et al. Variable Landscape of PD-L1 Expression in Breast Carcinoma as Detected by the DAKO 22C3 Immunohistochemistry Assay. Oncologist. 2023 Apr 6;28(4):319–26. doi:10.1093/ONCOLO/OYAD025 PubMed PMID: 36866462.

151. PD-L1 expression and survival in triple-negative breast cancer [Internet]. [cited 2026 Jan 18]. Available from: https://stories.universityofgalway.ie/pd-l1-expression-and-survival-in-triple-negative-breast-cancer/index.html

152. Vlajnic T, Baur F, Soysal SD, Weber WP, Piscuoglio S, Muenst S. PD-L1 Expression in Triple-negative Breast Cancer - A Comparative Study of 3 Different Antibodies. Applied Immunohistochemistry and Molecular Morphology. 2022 Nov 1;30(10):726–30. doi:10.1097/PAI.0000000000001062 PubMed PMID: 36165931.

153. Mittendorf EA, Philips A V., Meric-Bernstam F, Qiao N, Wu Y, Harrington S, et al. PD-L1 Expression in Triple Negative Breast Cancer. Cancer Immunol Res. 2014 Apr 1;2(4):361–70. doi:10.1158/2326-6066.CIR-13-0127 PubMed PMID: 24764583.

154. Petrocca F, Altschuler G, Tan SM, Mendillo ML, Yan H, Jerry DJ, et al. A Genome-wide siRNA Screen Identifies Proteasome Addiction as a Vulnerability of Basal-like Triple-Negative Breast Cancer Cells. Cancer Cell. 2013 Aug 12;24(2):182–96. doi:10.1016/J.CCR.2013.07.008 PubMed PMID: 23948298.

155. Britton M, Lucas MM, Downey SL, Screen M, Pletnev AA, Verdoes M, et al. Selective inhibitor of proteasome's caspase-like sites sensitizes cells to specific inhibition of chymotrypsin-like sites. Chem Biol. 2009 Dec 24;16(12):1278–89. doi:10.1016/J.CHEMBIOL.2009.11.015 PubMed PMID: 20064438.

156. Hetz C, Papa FR. The Unfolded Protein Response and Cell Fate Control. Mol Cell. 2018 Jan 18;69(2):169–81. doi:10.1016/J.MOLCEL.2017.06.017 PubMed PMID: 29107536.

157. McGrath EP, Logue SE, Mnich K, Deegan S, Jäger R, Gorman AM, et al. The Unfolded Protein Response in Breast Cancer. Cancers (Basel). 2018 Oct 1;10(10):344. doi:10.3390/CANCERS10100344 PubMed PMID: 30248920.

158. Hetz C, Zhang K, Kaufman RJ. Mechanism, regulation and functions of the unfolded protein response. Nat Rev Mol Cell Biol. 2020 Aug 1;21(8):421–38. doi:10.1038/S41580-020-0250-Z PubMed PMID: 32457508.

159. Read A, Schröder M. The Unfolded Protein Response: An Overview. Biology (Basel). 2021 May 1;10(5):384. doi:10.3390/BIOLOGY10050384 PubMed PMID: 33946669.

160. Weyburne ES, Wilkins OM, Sha Z, Williams DA, Pletnev AA, de Bruin G, et al. Inhibition of the proteasome β2 site sensitizes triple-negative breast cancer cells to β5 inhibitors through a mechanism involving Nrf1 suppression. Cell Chem Biol. 2017 Feb 16;24(2):218. doi:10.1016/J.CHEMBIOL.2016.12.016 PubMed PMID: 28132893.

161. Shabaneh TB, Downey SL, Goddard AL, Screen M, Lucas MM, Eastman A, et al. Molecular Basis of Differential Sensitivity of Myeloma Cells to Clinically Relevant Bolus Treatment with Bortezomib. PLoS One. 2013 Feb 27;8(2):e56132. doi:10.1371/JOURNAL.PONE.0056132 PubMed PMID: 23460792.

162. Taniuchi S, Miyake M, Tsugawa K, Oyadomari M, Oyadomari S. Integrated stress response of vertebrates is regulated by four eIF2α kinases. Scientific Reports 2016 6:1. 2016 Sep 16;6(1):32886. doi:10.1038/srep32886 PubMed PMID: 27633668.

163. Koumenis C, Naczki C, Koritzinsky M, Rastani S, Diehl A, Sonenberg N, et al. Regulation of Protein Synthesis by Hypoxia via Activation of the Endoplasmic Reticulum Kinase PERK and Phosphorylation of the Translation Initiation Factor eIF2α. Mol Cell Biol. 2002 Nov 1;22(21):7405–16. doi:10.1128/MCB.22.21.7405-7416.2002 PubMed PMID: 12370288.

164. Roiuk M, Neff M, Teleman AA. Human eIF2A has a minimal role in translation initiation and in uORF-mediated translational control in HeLa cells. Elife. 2025 Jul 2;14. doi:10.7554/ELIFE.105311

165. Tian RD, Chen YQ, He YH, Tang YJ, Chen GM, Yang FW, et al. Phosphorylation of eIF2α mitigates endoplasmic reticulum stress and hepatocyte necroptosis in acute liver injury. Ann Hepatol. 2020 Jan 1;19(1):79–87. doi:10.1016/J.AOHEP.2019.05.008 PubMed PMID: 31548168.

166. Aviner R. The science of puromycin: From studies of ribosome function to applications in biotechnology. Comput Struct Biotechnol J. 2020 Jan 1;18:1074–83. doi:10.1016/J.CSBJ.2020.04.014 PubMed PMID: 32435426.

167. Dot Blot: A Quick and Easy Method for Separation-Free Protein Detection [Internet]. [cited 2026 Mar 15]. Available from: https://www.jacksonimmuno.com/secondary-antibody-resource/immuno-techniques/dot-blotting-for-quick-detection/

168. Mishra V. Dot-blotting: A quick method for expression analysis of recombinant proteins. Curr Protoc. 2022 Sep 1;2(9):e546. doi:10.1002/CPZ1.546 PubMed PMID: 36094175.

169. Krzyzosiak A, Sigurdardottir A, Luh L, Carrara M, Das I, Schneider K, et al. Target-Based Discovery of an Inhibitor of the Regulatory Phosphatase PPP1R15B. Cell. 2018 Aug 23;174(5):1216-1228.e19. doi:10.1016/J.CELL.2018.06.030 PubMed PMID: 30057111.

170. Reid DW, Tay ASL, Sundaram JR, Lee ICJ, Chen Q, George SE, et al. Complementary Roles of GADD34- and CReP-Containing Eukaryotic Initiation Factor 2α Phosphatases during the Unfolded Protein Response. Mol Cell Biol. 2016 Jul 1;36(13):1868–80. doi:10.1128/MCB.00190-16 PubMed PMID: 27161320.

171. Oliveira MM, Mohamed M, Elder MK, Banegas-Morales K, Mamcarz M, Lu EH, et al. The integrated stress response effector GADD34 is repurposed by neurons to promote stimulus-induced translation. Cell Rep. 2024 Feb 27;43(2):113670. doi:10.1016/J.CELREP.2023.113670 PubMed PMID: 38219147.

172. Kloft N, Neukirch C, Von Hoven G, Bobkiewicz W, Weis S, Boller K, et al. A Subunit of Eukaryotic Translation Initiation Factor 2α-Phosphatase (CreP/PPP1R15B) Regulates Membrane Traffic. Journal of Biological Chemistry. 2012 Oct 12;287(42):35299–317. doi:10.1074/JBC.M112.379883 PubMed PMID: 22915583.

173. Hicks D. Characterization of the roles of PPP1R15A (GADD34) and Characterization of the roles of PPP1R15A (GADD34) and PPP1R15B (CReP) in ER stress-induced apoptosis in vivo PPP1R15B (CReP) in ER stress-induced apoptosis in vivo [Internet]. University of The Pacific; [cited 2025 Dec 8]. Available from: https://scholarlycommons.pacific.edu/

174. Choy MS, Yusoff P, Lee IC, Newton JC, Goh CW, Page R, et al. Structural and functional analysis of the GADD34:PP1 eIF2α phosphatase. Cell Rep. 2015 Jun 30;11(12):1885–91. doi:10.1016/J.CELREP.2015.05.043 PubMed PMID: 26095357.

175. Cortes J, Rugo HS, Cescon DW, Im SA, Yusof MM, Gallardo C, et al. Pembrolizumab plus Chemotherapy in Advanced Triple-Negative Breast Cancer. New England Journal of Medicine. 2022 Jul 21;387(3):217–26. doi:10.1056/NEJMOA2202809/SUPPL_FILE/NEJMOA2202809_DATA-SHARING.PDF PubMed PMID: 35857659.

176. Riaz F, Gruber JJ, Telli ML. New Treatment Approaches for Triple-Negative Breast Cancer. American Society of Clinical Oncology Educational Book. 2025 Jun;45(3). doi:10.1200/EDBK-25-481154

177. Albert MC, Brinkmann K, Kashkar H. Noxa and cancer therapy. Mol Cell Oncol. 2014 Jan 1;1(1):e29906. doi:10.4161/MCO.29906

178. Kale J, Osterlund EJ, Andrews DW. BCL-2 family proteins: changing partners in the dance towards death. Cell Death & Differentiation 2018 25:1. 2017 Nov 17;25(1):65–80. doi:10.1038/cdd.2017.186 PubMed PMID: 29149100.

179. Qin JZ, Ziffra J, Stennett L, Bodner B, Bonish BK, Chaturvedi V, et al. Proteasome Inhibitors Trigger NOXA-Mediated Apoptosis in Melanoma and Myeloma Cells. Cancer Res. 2005 Jul 15;65(14):6282–93. doi:10.1158/0008-5472.CAN-05-0676 PubMed PMID: 16024630.

180. Ploner C, Kofler R, Villunger A. Noxa: at the tip of the balance between life and death. Oncogene. 2008;27(Suppl 1):S84. doi:10.1038/ONC.2009.46 PubMed PMID: 19641509.

181. Sharma K, Vu TT, Cook W, Naseri M, Zhan K, Nakajima W, et al. p53-independent Noxa induction by cisplatin is regulated by ATF3/ATF4 in head and neck squamous cell carcinoma cells. Mol Oncol. 2018 Jun 1;12(6):788–98. doi:10.1002/1878-0261.12172 PubMed PMID: 29352505.

182. Núñez-Vázquez S, Sánchez-Vera I, Saura-Esteller J, Cosialls AM, Noisier AFM, Albericio F, et al. NOXA upregulation by the prohibitin-binding compound fluorizoline is transcriptionally regulated by integrated stress response-induced ATF3 and ATF4. FEBS J. 2021 Feb 1;288(4):1271–85. doi:10.1111/FEBS.15480 PubMed PMID: 32648994.

183. Sha Z, Goldberg AL. Multiple myeloma cells are exceptionally sensitive to heat shock, which overwhelms their proteostasis network and induces apoptosis. Proc Natl Acad Sci U S A. 2020 Sep 1;117(35):21588–97. doi:10.1073/PNAS.2001323117/SUPPL_FILE/PNAS.2001323117.SAPP.PDF PubMed PMID: 32817432.

184. Lai X, Huang C, Nie X, Chen Q, Tang Y, Fu X, et al. Bortezomib Inhibits Multiple Myeloma Cells by Transactivating ATF3 to Trigger miR-135a-5p- Dependent Apoptosis. Front Oncol. 2021 Sep 22;11:720261. doi:10.3389/FONC.2021.720261/FULL

185. Adams CJ, Kopp MC, Larburu N, Nowak PR, Ali MMU. Structure and molecular mechanism of ER stress signaling by the unfolded protein response signal activator IRE1. Front Mol Biosci. 2019 Mar 12;6(MAR):439177. doi:10.3389/FMOLB.2019.00011/BIBTEX PubMed PMID: 30931312.

186. Dang C V. A Time for MYC: Metabolism and Therapy. Cold Spring Harb Symp Quant Biol. 2016;81(1):79–83. doi:10.1101/SQB.2016.81.031153 PubMed PMID: 28174256.

187. Stipp MC, Acco A. c-Myc-targeted therapy in breast cancer: A review of fundamentals and pharmacological Insights. Gene. 2025 Mar 15;941:149209. doi:10.1016/J.GENE.2024.149209 PubMed PMID: 39755262.

188. Nikiforov MA, Riblett M, Tang WH, Gratchouck V, Zhuang D, Fernandez Y, et al. Tumor cell-selective regulation of NOXA by c-MYC in response to proteasome inhibition. Proc Natl Acad Sci U S A. 2007 Dec 12;104(49):19488–93. doi:10.1073/PNAS.0708380104 PubMed PMID: 18042711.

189. Nawrocki ST, Carew JS, Maclean KH, Courage JF, Huang P, Houghton JA, et al. Myc regulates aggresome formation, the induction of Noxa, and apoptosis in response to the combination of bortezomib and SAHA. Blood. 2008 Oct 1;112(7):2917–26. doi:10.1182/BLOOD-2007-12-130823 PubMed PMID: 18641367.

190. Thompson MR, Xu D, Williams BRG. ATF3 transcription factor and its emerging roles in immunity and cancer. J Mol Med. 2009 Nov 25;87(11):1053–60. doi:10.1007/S00109-009-0520-X/TABLES/1 PubMed PMID: 19705082.

191. Ku HC, Cheng CF. Master Regulator Activating Transcription Factor 3 (ATF3) in Metabolic Homeostasis and Cancer. Front Endocrinol (Lausanne). 2020 Aug 14;11:552603. doi:10.3389/FENDO.2020.00556/XML PubMed PMID: 32922364.

192. Narita T, Ri M, Masaki A, Mori F, Ito A, Kusumoto S, et al. Lower expression of activating transcription factors 3 and 4 correlates with shorter progression-free survival in multiple myeloma patients receiving bortezomib plus dexamethasone therapy. Blood Cancer J. 2015 Dec 4;5(12):e373–e373. doi:10.1038/bcj.2015.98 PubMed PMID: 26636288.

193. Wang Q, Mora-Jensen H, Weniger MA, Perez-Galan P, Wolford C, Hai T, et al. ERAD inhibitors integrate ER stress with an epigenetic mechanism to activate BH3-only protein NOXA in cancer cells. Proc Natl Acad Sci U S A. 2009 Feb 17;106(7):2200–5. doi:10.1073/PNAS.0807611106/SUPPL_FILE/0807611106SI.PDF PubMed PMID: 19164757.

194. Pakjoo M, Ahmadi SE, Zahedi M, Jaafari N, Khademi R, Amini A, et al. Interplay between proteasome inhibitors and NF-κB pathway in leukemia and lymphoma: a comprehensive review on challenges ahead of proteasome inhibitors. Cell Communication and Signaling 2024 Feb 8;22(1):105. doi:10.1186/S12964-023-01433-5 PubMed PMID: 38331801.

195. Wang P, Yu W, Hu Z, Jia L, Iyer VR, Sanders BG, et al. Involvement of JNK/p73/NOXA in vitamin E analog-induced apoptosis of human breast cancer cells. Mol Carcinog. 2008 Jun;47(6):436–45. doi:10.1002/MC.20400 PubMed PMID: 18058804.

196. Jedariforoughi A, Burke R, Chesak A, Gonzalez Hernandez JL, Hanson RL. JNK activation dynamics drive distinct gene expression patterns over time mediated by mRNA stability. NPJ Syst Biol Appl. 2025 Oct 21;11(1):117. doi:10.1038/s41540-025-00590-2 PubMed PMID: 41120288.

197. Tran HM, Wu KS, Sung SY, Changou CA, Hsieh TH, Liu YR, et al. Upregulation of Protein Synthesis and Proteasome Degradation Confers Sensitivity to Proteasome Inhibitor Bortezomib in Myc-Atypical Teratoid/Rhabdoid Tumors. Cancers (Basel). 2020 Mar 22;12(3):752. doi:10.3390/CANCERS12030752

198. Kunder R, Velyunskiy M, Dunne SF, Cho BK, Kanojia D, Begg L, et al. Synergistic PIM kinase and proteasome inhibition as a therapeutic strategy for MYC-overexpressing triple-negative breast cancer. Cell Chem Biol. 2022 Mar 17;29(3):358-372.e5. doi:10.1016/J.CHEMBIOL.2021.08.011 PubMed PMID: 34525344.

199. Fennell DA, Chacko A, Mutti L. BCL-2 family regulation by the 20S proteasome inhibitor bortezomib. Oncogene. 2008 Feb 21;27(9):1189–97. doi:10.1038/SJ.ONC.1210744 PubMed PMID: 17828309.

200. Muthalagu N, Junttila MR, Wiese KE, Wolf E, Morton J, Bauer B, et al. BIM is the primary mediator of MYC-induced apoptosis in multiple solid tissues. Cell Rep. 2014;8(5):1347–53. doi:10.1016/J.CELREP.2014.07.057 PubMed PMID: 25176652.

201. Sidrauski C, McGeachy AM, Ingolia NT, Walter P. The small molecule ISRIB reverses the effects of eIF2α phosphorylation on translation and stress granule assembly. Elife. 2015 Feb 26;4(4):e05033. doi:10.7554/ELIFE.05033 PubMed PMID: 25719440.

202. Hanson FM, Hodgson RE, Ribeiro de Oliveira MI, Allen KE, Campbell SG. Regulation and function of elF2B in neurological and metabolic disorders. Biosci Rep. 2022 Jun 1;42(6):BSR20211699. doi:10.1042/BSR20211699 PubMed PMID: 35579296.

203. Ignacio BJ, Dijkstra J, Mora N, Slot EFJ, van Weijsten MJ, Storkebaum E, et al. THRONCAT: metabolic labeling of newly synthesized proteins using a bioorthogonal threonine analog. Nat Commun. 2023 Jun 8;14(1):1–15. doi:10.1038/s41467-023-39063-7 PubMed PMID: 37291115.

204. Gasparyan M, Lo MC, Jiang H, Lin CC, Sun D. Combined p53- and PTEN-deficiency activates expression of mesenchyme homeobox 1 (MEOX1) required for growth of triple-negative breast cancer. Journal of Biological Chemistry. 2020 Aug 21;295(34):12188–202. doi:10.1074/JBC.RA119.010710 PubMed PMID: 32467227.

205. Koboldt DC, Fulton RS, McLellan MD, Schmidt H, Kalicki-Veizer J, McMichael JF, et al. Comprehensive molecular portraits of human breast tumours. Nature. 2012 Sep 23;490(7418):61–70. doi:10.1038/nature11412 PubMed PMID: 23000897.